

**Immune Proteins in Neurons –
Towards an Understanding of the Neuronal Role of
the Immune Protein CD3 ζ in NMDA Receptor
Signaling and Cytoskeleton Remodeling**

Dissertation

zur Erlangung des akademischen Grades

doctor rerum naturalium

(Dr. rer. nat.)

genehmigt durch

die Fakultät für Naturwissenschaften

der Otto-von-Guericke-Universität Magdeburg

von Diplom-Neurowiss. Anne-Christin Lehmann

geb. am 22. November 1983 in Burg (b. Magdeburg)

Gutachter

Prof. Dr. D. C. Dieterich

Prof. Dr. Dr. Sven Meuth

Eingereicht am 26. Oktober 2015

Verteidigt am 31. Mai 2016

Acknowledgements

This thesis is the result of five years of dedicated work at the Leibniz-Institute for Neurobiology in Magdeburg, which would not have been possible without the help and support of many friends and colleagues.

First of all, I would like to thank my supervisors Prof. Dr. Daniela C. Dieterich and Dr. Karl-Heinz “Carlitos” Smalla for giving me the opportunity to work on a topic that when it first appeared was rather new for all of us. I am very grateful for the continuous trust they bestowed on me to bring this thesis to a successful end. Furthermore, I thank them for their support, constructive discussions, and valuable suggestions.

I wholeheartedly thank Dr. Rodrigo Herrera-Molina not only for being a wonderful and supportive husband and friend, but also for his help with the image analysis, trend-setting ideas, and never-ending encouragements.

Many thanks to Prof. Dr. Eckart D. Gundelfinger for constructive discussions and valuable comments on the progress of the thesis.

I would also like to thank Kathrin Pohlmann for her valuable technical assistance, supportive attitude, and especially for getting a fridge for our office ☺

Many thanks also to all colleagues and friends from the Special Lab for Molecular Biological Techniques, the Neurochemistry department, and the Institute for Pharmacology and Toxicology for their friendship and help. I especially want to mention Peter Landgraf for his suggestions and for teaching me the art of molecular biology, Anke Müller for introducing me to S2 lab work, and Anika Dirks for being my “drug dealer”, i.e. for her help with all the inhibitors.

Thanks a lot to the lunch bunch Anika, Marie, Sophie and Stefan - you literally made my day! Just talking about “normal” life made everything so much more enjoyable.

Most importantly, I would like to thank my family for their unyielding support throughout the years. I am very grateful for all the encouragements my parents and grandmother have given me to pursue my dreams. All my achievements would not have been possible without their help and love.

Table of Contents

List of Figures.....	IV
Abstract.....	V
Zusammenfassung	VI
1 Introduction.....	1
1.1 Immune Proteins in Neurons	2
1.1.1 CD3 ζ – Structure and Function in T-cells	4
1.1.2 CD3 ζ in Neurons.....	5
1.2 NMDA Receptors	6
1.3 Molecular Mechanisms of Cytoskeleton Reorganization	9
1.4 Objectives	12
2 Material and Methods	13
2.1 Material	13
2.1.1 Chemicals.....	13
2.1.2 Antibodies	13
2.1.2.1 Primary Antibodies	13
2.1.2.2 Secondary Antibodies.....	14
2.1.3 Bacterial Strains and Culture Media.....	14
2.1.4 Animals.....	14
2.2 Methods.....	15
2.2.1 Molecular Biological Methods.....	15
2.2.1.1 PolyA ⁺ -RNA Preparation and Reverse Transcription	15
2.2.1.2 Polymerase Chain Reaction (PCR).....	15
2.2.1.3 Site-directed Mutagenesis	15
2.2.1.4 DNA Restriction	16
2.2.1.5 Agarose Gel Electrophoresis and DNA Extraction from Agarose Gels ..	16
2.2.1.6 Cloning of DNA Fragments into Plasmid Vectors	16
2.2.1.7 Transformation of Chemically Competent Bacteria	17
2.2.1.8 Preparation of Plasmid DNA (mini and midi preparations)	17
2.2.1.9 Generation of Expression Constructs.....	17
2.2.1.10 Sequencing and Sequence Analysis.....	18
2.2.2 Biochemical Methods.....	18
2.2.2.1 Subcellular Fractionation of Tissues	18
2.2.2.2 Determination of Protein Concentrations.....	19

2.2.2.3 Protein precipitation	20
2.2.2.4 Sodium Dodecyl Sulfate Polyacrylamide Gel Electrophoresis (SDS-PAGE)	20
2.2.2.5 Coomassie blue staining of SDS-PAGE gels	20
2.2.2.6 Western Blotting and Immunodetection of Proteins	21
2.2.2.7 Expression and Purification of Tandem-Affinity-Purification-Tagged CD3 ζ (CD3 ζ -TAP)	21
2.2.2.8 Antibody Generation and Affinity Purification of Polyclonal Antisera ..	22
2.2.2.9 Co-Immunoprecipitation using Magnetic anti-GFP Microbeads	23
2.2.2.10 Co-Immunoprecipitation using Protein G magnetic beads	23
2.2.2.11 Biotin-labeling and Isolation of Cell Surface Proteins.....	23
2.2.3 Cell Culture.....	24
2.2.3.1 Cultivation and Transfection of Mammalian Cell Lines	24
2.2.3.2 Cultivation and Transfection of Hippocampal Primary Cells.....	25
2.2.3.3 Generation of Lentiviruses	26
2.2.3.4 Stimulation of Cultured Hippocampal Neurons	26
2.2.3.5 Immunocytochemistry.....	28
2.2.3.6 Image Acquisition and Analysis.....	28
3 Results	31
3.1 A Comparative Study of Immune and Neuronal Signaling Pathways.....	31
T-cell surface glycoprotein CD3 delta/epsilon chain dimer	36
Phosphorylated T-cell surface glycoprotein CD3 delta/epsilon chain dimer	36
T-cell surface glycoprotein CD3 zeta chain dimer	36
3.2 Characterization of CD3ζ in the Brain.....	37
3.2.1 CD3 ζ mRNA is found in Hippocampus and Cortex of Young and Adult Rats	37
3.2.2 CD3 ζ Localization at Different Developmental Stages of Hippocampal Neurons	37
3.2.3 CD3 ζ is Abundant in Rat Brain Fractions.....	39
3.3 Generation of Tools to Characterize CD3ζ in Neurons	40
3.3.1 Generation of Antisera against CD3 ζ	40
3.3.2 Generation and Characterization of Two CD3 ζ Mutants	43
3.3.3 CD3 ζ Fusion Protein and its Mutants Form Dimers	44
3.3.4 Phosphorylation of CD3 ζ -D36A-GFP is Reduced Compared to CD3 ζ GFP	45
3.3.5 CD3 ζ Wildtype and its Mutants Localize Differently in COS7Ccells and in Neurons	47
3.3.6 Cell Surface Expression of CD3 ζ GFP and its Mutants	49
3.3.7 CD3 ζ GFP Overexpression Reduces Dendrite Complexity.....	50

3.3.8	Involvement of CD3 ζ in Actin and Microtubule Regulation	53
3.3.9	Effect of CD3 ζ and its Mutants on Mature Hippocampal Neurons	54
3.4	The CD3ζ-NMDA Receptor Complex.....	57
3.4.1	CD3 ζ and NR2B Form a Complex.....	58
3.4.2	CD3 ζ Affects Expression Levels of NR2B in Hippocampal Neurons	59
3.4.3	NMDA Receptor Activity is needed for CD3 ζ Phosphorylation	62
3.4.4	Influence of CD3 ζ on NR2B Expression Levels in Developing Hippocampal Neurons	63
3.5	CD3ζ Activation Leads to Reorganization of the Actin Cytoskeleton	64
3.5.1	NMDA Receptor Activation is Crucial for CD3 ζ Signaling to the Cytoskeleton	65
3.5.2	Src Kinases are Required for CD3 ζ -dependent Cytoskeletal Remodeling in Developing Neurons.....	69
3.5.3	Downstream Signaling of CD3 ζ is Mediated by ZAP70 Kinase Leading to the Activation of the RhoA/ROCK Pathway	73
4	Discussion.....	76
4.1	A Comparative Study of Immune and Neuronal Signaling	76
4.2	Characterization of CD3 ζ in the Rat Brain	78
4.3	Characterization of Two CD3 ζ Loss-of-Function Mutants.....	80
4.4	Linking CD3 ζ to the NR2B Subunit of the NMDAR.....	83
4.5	CD3 ζ Mediates NR2B-dependent Regulation of the Neuronal Cytoskeleton ...	84
4.6	Conclusion and Outlook.....	87
5	Literature.....	89
6	Appendix.....	101
6.1	Abbreviations.....	101
6.2	Vectors and cDNA Expression Constructs	103
	Information regarding the base pair (bp) positions refer to the cDNA sequence BC097933.1 of CD247 rat.....	103
6.3	Applied Primers	104
6.4	Proteins of the TCR Signaling Network.....	105
6.5	Literature TCR Signaling Network.....	114
Lebenslauf.....		132
Name	Anne-Christin Lehmann.....	132
Geburtstag	22. November 1983.....	132
Geburtsort	Burg (b. Magdeburg).....	132
Staatsangehörigkeit	deutsch.....	132
List of Publications		133
Erklärung		134

List of Figures

Figure 1: Structure of the TCR complex (A) and CD3 ζ (B).....	3
Figure 2: CD3 ζ Signaling in T-cells.....	4
Figure 3: Structure of the postsynaptic density (PSD).....	7
Figure 4: Regulation of the actin cytoskeleton by NMDARs.	11
Figure 5: Scheme of TCR signaling components and their expression in neurons	33
Figure 6: Detailed view of TCR complex signaling.....	36
Figure 7: CD3 ζ transcripts in rat brain.	37
Figure 8: Localization of CD3 ζ in hippocampal neurons at different developmental stages.	38
Figure 9: Postsynaptic localization of CD3 ζ in mature hippocampal neurons.....	39
Figure 10: Subcellular fractionation of adult rat forebrain.....	40
Figure 11: Overview over the antigen epitopes and the names of the corresponding CD3 ζ antisera	42
Figure 12: Characterization and specificity of antisera	43
Figure 13: Overview over both CD3 ζ mutants	44
Figure 14: Dimerization of CD3 ζ mutants compared to wt CD3 ζ	45
Figure 15: Phosphorylation of overexpressed CD3 ζ wt and mutants.....	46
Figure 16: Localization of CD3 ζ and its mutants in COS7 cells	47
Figure 17: Distinct localization pattern of CD3 ζ GFP and its mutants in hippocampal neurons	49
Figure 18: Cell surface expression of CD3 ζ GFP and its mutants in hippocampal neurons.....	50
Figure 19: Overexpression of CD3 ζ GFP reduces dendritic complexity in DIV8 hippocampal neurons ..	51
Figure 20: Efficacy of shRNAs	52
Figure 21: Knockdown of endogenous CD3 ζ increases dendrite complexity	53
Figure 22: Influence of CD3 ζ on neuronal cytoskeleton	54
Figure 23: CD3 ζ -6YF-GFP increases dendrite complexity in mature hippocampal neurons	55
Figure 24: Influence of CD3 ζ on synaptic structures in hippocampal neurons.....	56
Figure 25: CD3 ζ and NR2B form a complex.....	59
Figure 26: Expression levels of NR2B before and after NMDA receptor stimulation	60
Figure 27: Immunofluorescent staining of surface NR2B	61
Figure 28: NMDA receptor activity is crucial for CD3 ζ phosphorylation.....	63
Figure 29: Effect of CD3 ζ on NR2B expression levels in DIV8 hippocampal neurons	64
Figure 30: NMDA receptor blocker APV reverses CD3 ζ effect on dendrite complexity	66
Figure 31: NR2B subunit inhibitor ifenprodil reverses CD3 ζ effect on dendrite complexity	67
Figure 32: AMPA receptor inhibitor CNQX does not rescue the CD3 ζ overexpression phenotype	68
Figure 33: NMDA and AMPA receptor activity has an impact on CD3 ζ phosphorylation in developing neurons.....	69
Figure 34: The general src kinase inhibitor PP2 reverses the effect of CD3 ζ on dendrite complexity	70
Figure 35: Lck inhibitor damnacanthol rescues the CD3 ζ overexpression phenotype.....	71
Figure 36: The PI3K blocker wortmannin rescues the CD3 ζ overexpression phenotype)	72
Figure 37: CD3 ζ phosphorylation is mediated by a src kinase in developing neurons.....	73
Figure 38: ZAP70 inhibitor piceatannol reverses CD3 ζ effect on dendrite complexit	74
Figure 39: ROCK inhibitor Y-27632 reverses CD3 ζ effect on dendrite complexity	75
Figure 40: Proposed model of CD3 ζ signaling in developing hippocampal neurons.....	88

Abstract

All cells of an organism develop from a single cell and, therefore, share an identical genetic repertoire. While differentially regulated gene expression results in individual sets of molecules providing unique and distinct cellular features, comparative studies have revealed striking similarities between the proteomes of different cell types allowing complementary functions on the one side and necessary communication between different organic systems on the other side. Among those, the central nervous system (CNS) had long been seen as a secluded area maintained by the blood-brain barrier shielding the brain from certain external influences such as pathogens and the subsequent immune response. However, the concept of an immune-privileged brain has been revised over the past few decades. For one thing, it was shown that the immune and the central nervous system communicate with each other using chemical transmitters that find their corresponding receptors in cells of both systems. But even more astonishing was the fact to find proteins in neurons thought to be exclusively expressed by immune cells and vice versa.

The present work gives an overview about T cell receptor (TCR) signaling molecules expressed in neurons of the rat, mouse or human brain. Data were collected using several databases and screening published literature. Indeed, 84 out of 95 proteins belonging to the TCR signaling network were found to be expressed in neurons of the CNS. Among these molecules, we discovered the crucial signaling subunit of the TCR complex CD3 ζ , but not the T cell receptor itself. As CD3 ζ only comprises a very short ectodomain unable to bind ligands, it needs an associated receptor to receive extracellular information. This thesis, therefore, evolved around the questions of the receptor-dependency of CD3 ζ in neurons and of its neuronal functions.

Our experiments show that CD3 ζ negatively regulates dendrite outgrowth in DIV8 hippocampal neurons through the RhoA/ROCK pathway. The proposed pathway also includes the immune kinase ZAP70, whose neuronal functions were so far elusive. Importantly, the reorganization of the actin cytoskeleton by CD3 ζ depends on NR2B-containing NMDA receptors implying a novel function for NR2B in hippocampal neurons prior to synaptogenesis.

Apart from presenting novel functions for CD3 ζ and NR2B-containing NMDA receptors, this thesis shows how many parallels can be found between two systems so different at first sight. Therefore, taking a look at immune signaling will be the key towards a better understanding of the functions of CD3 ζ and other immune proteins in neurons.

Zusammenfassung

Die Gesamtheit aller Zellen eines Organismus entwickelt sich aus einer einzigen Zelle und trägt daher das identische genetische Material. Aufgrund der unterschiedlich regulierten Expression von Genen befinden sich in jeder Zelle individuelle Proteinrepertoires, die ihr einzigartige und ihrer Funktion entsprechende Eigenschaften verleihen. Dennoch haben vergleichende Studien erstaunliche Ähnlichkeiten zwischen den Proteomen verschiedener Zelltypen festgestellt, die einerseits komplementäre Funktionen und andererseits die notwendige Kommunikation zwischen verschiedenen Organsystemen ermöglichen. Unter den Systemen wurde das zentrale Nervensystem lange Zeit als isolierte Region betrachtet, die durch die Blut-Hirn-Schranke vor äußeren Einflüssen, wie zum Beispiel vor Pathogenen und der darauffolgenden Immunantwort, geschützt wird. In den letzten Jahrzehnten wurde das Konzept des immunprivilegierten Gehirns jedoch gründlich überarbeitet. Zum einen konnte gezeigt werden, dass das zentrale Nervensystem und das Immunsystem durch chemische Botenstoffe miteinander kommunizieren, die in beiden Systemen entsprechende Rezeptoren finden. Zum anderen wurden erstaunlich viele Proteine in Neuronen gefunden, die zunächst als ausschließlich immun exprimiert beschrieben wurden, bzw. konnten auch neuronale Proteine bereits in T-Zellen nachgewiesen werden.

Die vorliegende Arbeit gibt einen Überblick über Signalmoleküle der T-Zell-Rezeptor-Signaltransduktion, die in Nervenzellen des Gehirns von Ratten, Mäusen oder Menschen exprimiert werden. Die Daten wurden durch die Nutzung verschiedener Datenbanken sowie mittels Literaturrecherche zusammengetragen. Von 95 zum T-Zell-Rezeptor-Signalnetzwerk gehörenden Proteinen konnten 84 in Neuronen des zentralen Nervensystems identifiziert werden. Zu diesen Molekülen zählt auch die essenzielle Signaluntereinheit des T-Zell-Rezeptorkomplexes CD3 ζ , jedoch nicht der Rezeptor selbst. Da CD3 ζ nur eine sehr kurze Ektodomäne besitzt, die nicht in der Lage ist Liganden zu binden, benötigt das Protein einen assoziierten Rezeptor, um extrazelluläre Informationen zu empfangen. Diese Arbeit beschäftigt sich daher mit der Suche nach einem möglichen neuronalen Rezeptor für CD3 ζ und der Beschreibung von CD3 ζ -Funktionen in Neuronen.

Unsere Experimente zeigen, dass CD3 ζ das Dendritenwachstum in sich entwickelnden hippocampalen Neuronen (DIV8) über den RhoA/ROCK Signalweg negativ reguliert. Der hier vorgeschlagene Signalweg führt auch über die Immunkinase ZAP70, deren neuronale Funktionen bisher nur unzureichend beschrieben wurden. Interessanterweise ist die Reorganisation des Actin-Zytoskeletts durch CD3 ζ von NR2B-enthaltenden NMDA-Rezeptoren abhängig. Die Daten weisen somit auf eine bisher unbekannt Funktion dieser Rezeptoren in hippocampalen Neuronen vor Beginn der Synaptogenese hin.

Neben der Vorstellung neuer Funktionen von CD3 ζ und NR2B-enthaltenden NMDA-Rezeptoren verweist diese Arbeit auch auf die Parallelen zwischen dem zentralen Nervensystem und dem Immunsystem, obwohl sie im ersten Moment sehr unterschiedlich erscheinen. So könnte es auch zukünftig empfehlenswert sein, sich mit der Signaltransduktion in Immunzellen genauer zu befassen, um die Funktionen von CD3 ζ und anderen Immunproteinen besser zu verstehen.

1 Introduction

All cells of an organism develop from a single cell and, therefore, share the identical genetic repertoire. Cell differentiation is possible due to differentially regulated gene expression giving individual sets of molecules. Nevertheless, comparative studies have revealed striking similarities between the proteomes of different cell types (Wang *et al.*, 2009). This may be related to the tightly integrated organization of cells where complex interactive patterns of molecular organization yield common structures. Thus, it is not completely surprising that two different cell types may share similar protein expression allowing for efficient intercellular communication and regulatory interaction (Broderick *et al.*, 2013).

For decades, the central nervous system (CNS) has been seen as a secluded area due to the existence of the blood-brain barrier (BBB) thought to shield the brain from certain external influences, in particular pathogens and the subsequent immune response. However, the idea of an immune-privileged CNS has been modified over the past years. Peripheral nerve ends innervate immune organs such as the spleen or lymph nodes (Nance and Sanders, 2007), and there are resident immune cells, the microglia, in the CNS (Hanisch and Kettenmann, 2007).

Indeed, immune cells are receptive for and even synthesize classical neurotransmitters like acetylcholine, glutamate, dopamine, and serotonin (Levite, 2008; Steinman, 2004). On the other hand, neurons are responsive to cytokines (e.g. tumor necrosis factor α , interleukin- 1β) (Yirmiya and Goshen, 2011; Mousa and Bakhiet, 2013). Most data about neuroimmune interactions arose from studying autoimmune disorders, brain injury, or infection. Patients suffering from neurodegenerative diseases such as Alzheimer's or Parkinson's also show signs of neuroinflammation due to cytokine secretion and the subsequent activation of microglia that are thought to be responsible for initiating neuronal cell death (Lucin and Wyss-Coray, 2009). Even systemic autoimmune diseases have an impact on the brain. Autoantibodies in patients with systemic lupus erythematosus cross the BBB and induce neuronal cell death leading to cognitive impairment in some cases (Diamond, 2010; Xu *et al.*, 2015). Therefore, modern conception of intersystem communication recognizes that the immune and central nervous system are not only

physically connected, but that they also communicate with each other using a common chemistry-based language (Marin and Kipnis, 2013).

Interestingly, recent studies do not only imply a role of immune molecules in the pathologic brain, but also in normal neuronal functioning (Fourgeaud and Boulanger, 2010). Corriveau *et al.* (1998) showed the neuronal expression of major histocompatibility complex I (MHC I) disproving the previously prevalent opinion that neurons belonged to the few cell types not expressing MHC I and simultaneously giving more evidence to negate the hypothesis of an immune-privileged brain.

1.1 Immune Proteins in Neurons

MHC I is a cell surface protein crucial for the immune system to discriminate “self” and “non-self” parts of the organism. It is expressed in neurons of the cortex, hippocampus, thalamus, and the cerebellum with postsynaptic localization (Huh *et al.*, 2000; Goddard *et al.*, 2007). In the visual cortex, it could also be detected in presynaptic structures (Needleman *et al.*, 2010). Mice lacking cell surface expressed MHC I ($\beta 2m/TAP^{-/-}$ mice) show increased hippocampal long-term potentiation (LTP) and reduced long-term depression (LTD) (Huh *et al.*, 2000) as well as higher frequencies of miniature excitatory postsynaptic currents (mEPSCs) compared to wild-type controls (Goddard *et al.*, 2007). Deletion of two MHC I genes expressed in the lateral geniculate nucleus (LGN) leads to incomplete refinement of retinogeniculate projections with impaired segregation of eye-specific inputs in mice (Datwani *et al.* 2009). All these data imply a function for MHC I in higher cognitive brain functions.

The most prominent receptor for MHC I in immune cells is the T-cell receptor (TCR). The receptor is a heterodimer consisting of an α - and a β -chain (fig. 1A), which applies for approx. 95% of the T-cell population, or a γ - and a δ -chain. The highly variable extracellular domain recognizes the antigen presented by an MHC I-carrying cell. However, the TCR is not able to transduce signals to the intracellular space due to its short cytoplasmic tail. This is done by the cluster of differentiation (CD) 3 co-receptor (fig. 1A). It comprises three dimeric transmembrane signaling modules: CD3 γ/ϵ , CD3 δ/ϵ and CD3 ζ/ζ (Call *et al.*, 2004). Each protein contains at least one

immunoreceptor tyrosine-based activation motif (ITAM) whose tyrosine residues are phosphorylated upon TCR binding to an antigen. Phosphorylated ITAMs attract a number of other signaling molecules that diverge the incoming signal.

Studies to prove the presence of the TCR in neurons have revealed the expression of the TCR β genomic locus in neurons of the murine brain suggesting the probable existence of a neuronal TCR. However, an equivalent protein could not be detected so far (Syken and Shatz, 2003; Nishiyori *et al.*, 2004). The more astonishing it is, that proteins of the CD3 co-receptor are expressed in neurons. CD3 ϵ is expressed on cerebellar Purkinje cells and seems to play a role in establishing proper neuronal architecture during development. CD3 γ and δ , but not CD3 ζ mRNAs were also detected in Purkinje cells (Nakamura *et al.*, 2007). However, CD3 ζ is expressed in most other parts of the brain including the hippocampus and has been the focus of recent studies aiming at elucidating the function of immune molecules in neurons (Corriveau *et al.*, 1998; Baudouin *et al.*, 2008).

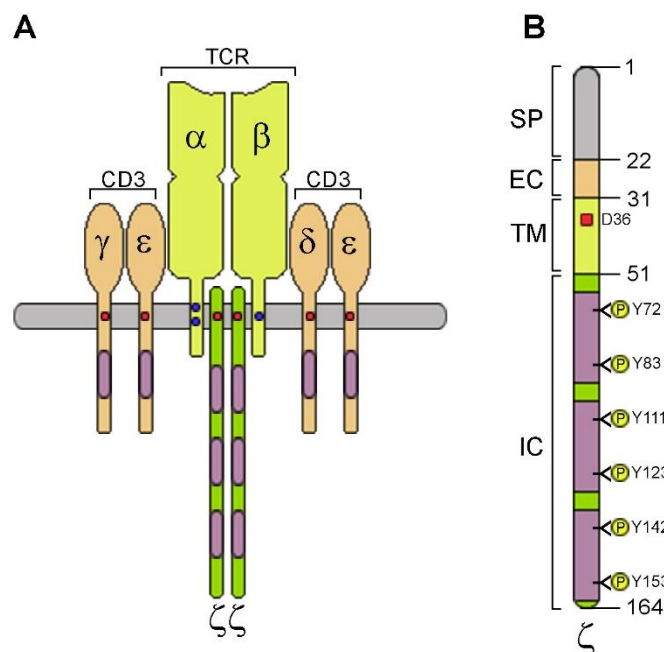


Figure 1: Structure of the TCR complex (A) and CD3 ζ (B). (A) The TCR complex consists of the α - and β -chain of the T-Cell receptor and dimers of the CD3 co-receptor – $\gamma\epsilon$, $\delta\epsilon$, and $\zeta\zeta$. They interact with each other through acidic (red dots) and basic (blue dots) amino acid residues within their transmembrane domains. Whereas the TCR is responsible for antigen recognition, the CD3 co-receptor induces the intracellular signal transduction by phosphorylation of the ITAMs (purple). (B) CD3 ζ is the crucial signaling subunit of the TCR complex with a length of 164 amino acids. It comprises a signaling peptide (SP), a short extracellular domain (EC), a transmembrane domain (TM) with an acidic aspartate residue (D36), and an intracellular domain (IC) mostly consisting of three ITAMs with two tyrosine residues each.

1.1.1 CD3 ζ - Structure and Function in T-cells

CD3 ζ is a disulfide-linked homodimer of two 143 amino acid-long transmembrane proteins (fig. 1B). The unprocessed molecule also comprises a signaling peptide of 21 amino acids. Due to a very short extracellular tail of only nine amino acids, CD3 ζ is not able to receive any incoming signals and, therefore, needs an associated receptor such as the TCR to function properly. A negatively charged aspartate residue in the transmembrane domain of CD3 ζ interacts with a basic arginine residue located within the transmembrane domain the TCR α -chain (Wucherpfennig *et al.*, 2010). This connection allows the transmission of extracellular signals from the TCR itself to the CD3 ζ subunits that contain three ITAMs with two tyrosine residues each in the intracellular domains. Each ITAM can be phosphorylated and can engage in downstream signaling independently. This makes CD3 ζ a crucial adaptor protein in TCR signal transduction (fig. 2).

The tyrosine residues of the ITAMs are phosphorylated by two Src kinase family members: Lck and Fyn. This triggers the recruitment of the kinase ZAP70 that binds the two phosphorylated tyrosines within the ITAM with its tandem SH2 domains leading to its activation (Wange and Samelson, 1996). ZAP70 is a major signaling hub in T-cells connecting the TCR and CD3 ζ to the actin cytoskeleton, gene expression, and immune response regulation (Baniyash, 2004). However, CD3 ζ function and signaling in neurons remains poorly understood.

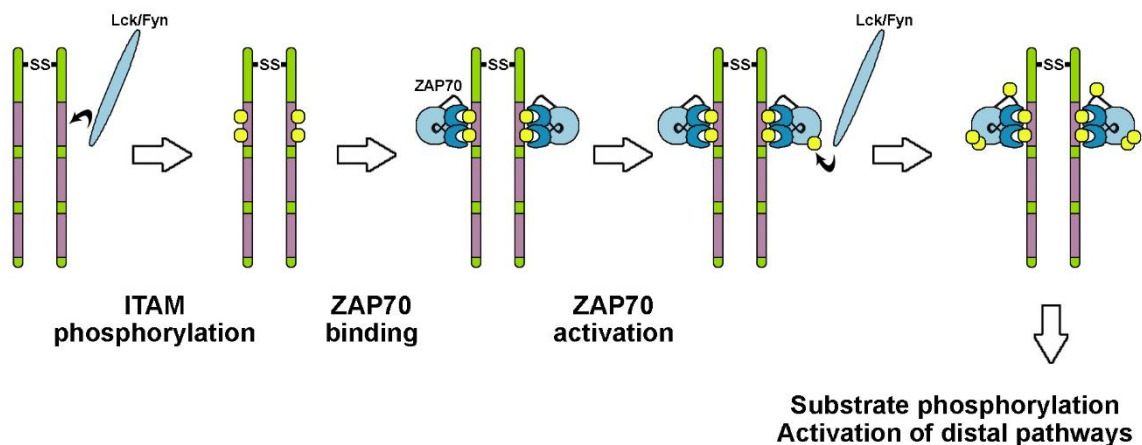


Figure 2: CD3 ζ Signaling in T-cells. Upon TCR activation by antigen binding, the tyrosine residues of CD3 ζ are phosphorylated by one of src family kinases Lck or Fyn. ZAP70 kinase is recruited by binding the phosphorylated tyrosines with its tandem SH2 domains which induces a conformational change allowing for the activation of ZAP70 by Lck or Fyn. Active ZAP70 serves as a major signaling hub by interacting with and phosphorylating several adaptor proteins and other kinases leading to the initiation of distal pathways. (Tyrosine phosphorylations are depicted as yellow circles.)

1.1.2 CD3 ζ in Neurons

First evidence for the involvement of CD3 ζ in higher brain function came from electrophysiological studies in CD3 ζ knockout mice that showed enhanced hippocampal LTP, but no LTD (Huh *et al.*, 2000). This phenomenon was abolished by applying the inhibitor D-APV suggesting N-methyl-D-aspartate receptor (NMDAR)-dependent mechanisms. Baudouin *et al.* (2008) published that CD3 ζ expression is mostly neuronal with an enriched localization of the protein at dendritic tips and the axonal growth cone during development. They also found a functional implication for CD3 ζ in dendrite outgrowth regulation. Indeed, cultured CD3 $\zeta^{-/-}$ retinal ganglion cells (RGC) show an abnormally complex dendritic arbor compared to wildtype neurons (Xu *et al.*, 2010). At the same time, dendritic motility seems to be reduced though. Furthermore, RGC axonal projections to the lateral geniculate nucleus are disrupted in CD3 $\zeta^{-/-}$ mice starting from the second postnatal week on. Around the same time, glutamate receptor-dependent RGC synaptogenesis is also impaired in knockout mice.

Studies from the H el ene Boudin Lab brought further insights into CD3 ζ functioning in hippocampal and cortical neurons. Overexpression of CD3 ζ in neural progenitor cells was shown to disrupt neurogenesis (Angibaud *et al.*, 2011a). Consequently, CD3 ζ is only expressed in postmitotic neurons where it plays a role very early in neuronal development nevertheless. Here, CD3 ζ represses early neuritogenesis in an ephrinA4 receptor-dependent manner upon stimulation with ephrinA1. Furthermore, this interaction also seems to be responsible for induced axonal growth cone collapse. Both processes were abrogated in neurons from CD3 $\zeta^{-/-}$ mice (Angibaud *et al.*, 2011b). The authors were also able to show the involvement of ZAP70 kinase in both phenomena.

In an elegant study, Louveau *et al.* (2013) demonstrated that mice lacking CD3 ζ exhibited deficits in spatial learning and memory formation. On the molecular level, these mice showed reduced synaptic localization of the NMDAR subunit NR2A and a reduced interaction with its downstream signaling partner calcium/calmodulin-protein kinase II (CamKII) in cortical neurons. They also showed that CD3 ζ is necessary for CamKII phosphorylation in a chemically induced LTP protocol.

Taken together, there are strong implications for the involvement of neuronal CD3 ζ in dendritic arborization as well as synapse development and function. These processes are partially controlled by NMDARs that, according to the above-mentioned studies, might be putative upstream regulators of CD3 ζ .

1.2 NMDA Receptors

There are two types of glutamate receptors expressed in neurons: metabotropic and ionotropic receptors. NMDARs belong to the latter category that also includes α -amino-3-hydroxy-5-methyl-4-isoxazolepropionic acid receptors (AMPA) and kainate receptors. Ionotropic glutamate receptors form a channel with their subunits allowing the influx of cations that subsequently trigger intracellular reactions. In contrast, metabotropic glutamate receptors are G-protein coupled receptors and set off signal transduction via the direct interaction with their corresponding G-protein and further related molecules.

NMDARs have certain characteristics that distinguish them from other ligand-gated ion channels. In resting state, their pore is blocked by Mg²⁺ which can only be removed by prior membrane depolarization. Once the channel is open, NMDARs show a high permeability for Ca²⁺ unlike e.g. AMPARs that are mostly permissive for sodium and potassium. Furthermore, they possess slow kinetics due to the gradual unbinding of glutamate. Apart from glutamate, NMDARs need glycine or D-serine as a co-agonist to open (Traynelis *et al.*, 2010; Cull-Candy and Leszkiewicz, 2004; Paoletti, 2011). Their long C-terminal domains allow for various interactions with multiple intracellular proteins (Sprengel *et al.*, 1998; Martel *et al.*, 2009; Sanz-Clemente *et al.*, 2013). However, all these properties largely depend on subunit composition.

The NMDAR is a heterotetramer consisting of two GluN1 (NR1) and two GluN2 (NR2) subunits or one GluN2 and one GluN3 (Paoletti *et al.*, 2013). The NR2 subunits can be divided into NR2A through D. As NR2C and D containing receptors are only a small pool, the focus here will be on NR2A and NR2B containing NMDARs, the most common subunits especially in higher function brain areas such as the hippocampus (Watanabe *et al.*, 1992; Monyer *et al.*, 1994). While NR2B is already present in developing neurons from embryonic stages on, NR2A expression starts shortly after

birth and rises progressively (Sheng *et al.*, 1994). Both receptors are found in the postsynaptic compartment of neuronal contacts. While NR2A is exclusively located within the postsynaptic density (PSD), an electron-dense signaling meshwork at the postsynapse (fig. 3), NR2B is also found in peri- and extrasynaptic areas (Hardingham and Bading, 2010; Petralia *et al.*, 2010; Gladding and Raymond, 2011). These subunits are highly mobile and may change their localization through lateral diffusion (Groc *et al.*, 2006). Apart from subunit composition, the different localization of NMDARs also accounts for their distinct functions.

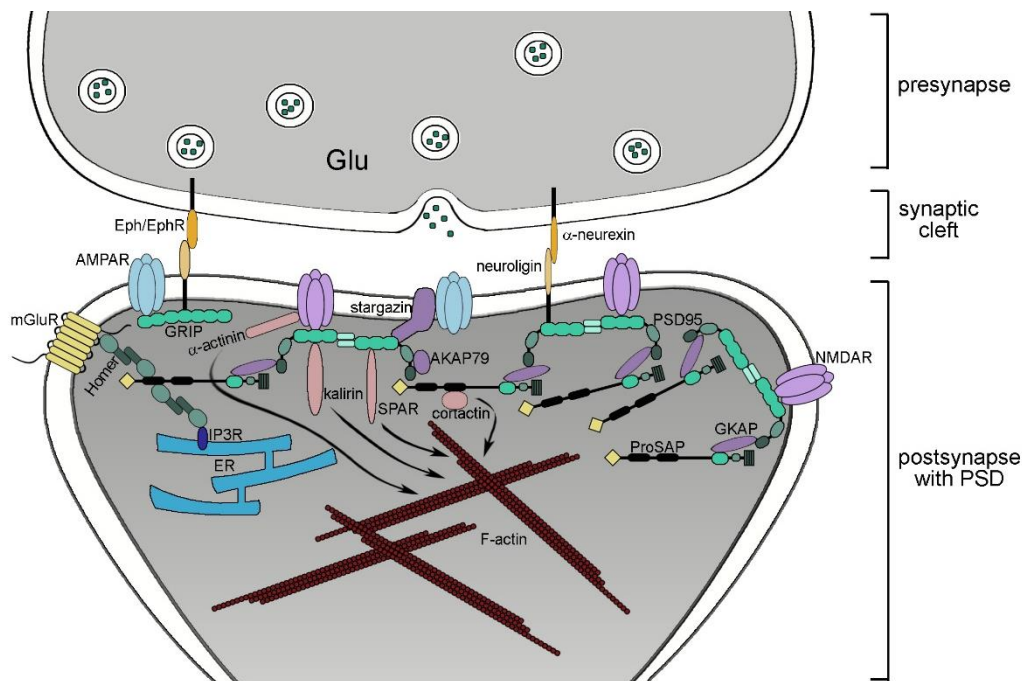


Figure 3: Structure of the postsynaptic density (PSD). When glutamate (Glu) is released from an axon terminal, the presynapse, it diffuses through the synaptic cleft and binds its receptors at the postsynaptic site. NMDARs, AMPARs and mGluRs are anchored in the PSD by a variety of scaffolding proteins such as PSD95 (postsynaptic density protein 95), ProSAP (proline-rich synapse-associated protein) or GRIP (glutamate receptor-interacting protein). This network is interconnected and stabilized by stargazin, GKAP (guanylate kinase-associated protein) and AKAP79 (A-kinase anchor protein 79). mGluRs are directly connected to the IP3 receptor (IP3R) of the endoplasmic reticulum (ER), the intracellular calcium store. Ionotropic glutamate receptors, and in particular the Ca^{2+} -permeable NMDARs, regulate the actin cytoskeleton through, e.g., actin-binding proteins cortactin and α -actinin or the GTPase activating protein SPAR and the Rho guanine nucleotide exchange factor kalirin. Further regulation of actin is established by the activation of distinct kinases (for details see fig. 4). The cell-cell contact is stabilized by cell adhesion molecules such as neuroigin/neurexin or trans-interaction complexes such as the ephrin/ephrin receptor (Eph/EphR) complex. (Interactions are indicated by direct contact of the geometric shapes representing the proteins. The influence of certain proteins on the actin cytoskeleton is shown with arrows.)

Stimulation of synaptic NMDARs induces the expression of cell survival and plasticity genes. A well-described pathway is the regulation of cAMP response element binding protein (CREB)-driven gene expression. Ca^{2+} -influx through open NMDA receptors activates the fast-acting Ca^{2+} /Calmodulin dependent protein kinase (CaMK) pathway. Furthermore, the slower acting, but longer lasting Ras-extracellular-signal-regulated kinase 1/2 (ERK1/2) pathway is set off. Both signaling cascades lead to the phosphorylation of CREB, a prerequisite for the recruitment of the co-activator CREB binding protein (CBP). Extrasynaptic NMDARs (mostly NR2B) inactivate the Ras-ERK1/2 pathway leading to CREB dephosphorylation. In addition, synaptic NMDA receptors mediate the phosphorylation of forkhead box proteins O (FOXO) via the PI3K/Akt pathway promoting the nuclear export of the transcription factor. Extrasynaptic NMDARs have the opposite effect and enable FOXO to bind and transcribe DNA sequences coding for apoptotic genes. (Hardingham and Bading, 2010)

Glutamate receptors play a crucial role in synaptic plasticity, a process describing the activity-dependent changes in synaptic structure and function. If a presynaptic and a postsynaptic cell are active at the same time, and, therefore, the latter underlies constant stimulation by the first over hours, so-called long-term potentiation (LTP) is induced. Sustained Ca^{2+} influx through NMDARs leads to the activation of the previously described CaMK pathway and the subsequent phosphorylation of AMPARs by CaMKII increasing their conductance. Furthermore, additional AMPARs taken from a non-synaptic pool are inserted into the postsynaptic membrane. Enhanced AMPAR responses increase NMDAR signaling promoting synaptic strength. The late phase of LTP requires protein synthesis and gene expression allowing the sustainable rearrangement of the synaptic cytoarchitecture. The weakening of synapses is called long-term depression (LTD). Low frequency stimulation leads to lower intracellular Ca^{2+} levels in the postsynapse promoting the activation of protein phosphatases. They mediate the endocytosis of AMPARs followed by a decrease of synaptic strength (Lüscher *et al.*, 1999; Lüscher and Malenka, 2012).

Both LTP and LTD trigger changes in the cytoskeleton of synaptic spines. The spinoskeleton (Rácz and Weinberg, 2012) consists of both linear and branched filamentous actin (F-actin) networks starting at the spine base and reaching up to the

PSD. Induction of LTP leads to actin polymerization and the enlargement of the spine. Conversely, LTD results in the loss of actin and spine shrinkage (Koleske, 2013). The reorganization of the spinoskeleton is in part controlled by NMDARs. However, they do not only exert this function in spines of mature neurons, but also in dendrites already during neuronal development (McAllister, 2000). In *Xenopus laevis* tadpoles, NMDAR activity is crucial for the dendritic development and outgrowth of optic tectal neurons (Rajan *et al.*, 1998; Sin *et al.*, 2002). Interestingly, even axon branch stabilization depends on dendritic NMDAR activation in *Xenopus* RGCs (Ruthazer *et al.*, 2003). In cultured rat hippocampal neurons, overexpression of NR2B leads to a more complex dendritic arbor at DIV7, but not in mature cells (Bustos *et al.*, 2014).

A number of possibilities of how NMDARs influence the cytoskeleton have been proposed. For example, they interact directly or indirectly with various actin-binding proteins such as α -actinin, cortactin, or profilin (Rácz and Weinberg, 2012). Furthermore, NMDAR stimulation leads to the activation of CaMKII and phosphoinositide 3-kinase (PI3K) that regulate guanine nucleotide exchange factors (GEFs) to stimulate small GTPases of the Rho subfamily, critical regulators of the actin cytoskeleton and present in all eukaryotic cells and therefore also in T-cells (Luo, 2000; Tada and Sheng, 2006) (fig. 4).

1.3 Molecular Mechanisms of Cytoskeleton Reorganization

The cytoskeleton is a highly dynamic structure supporting both cell shape and function. In all eukaryotic cells, it is formed by two major components: microfilaments and microtubules. Microfilaments, consisting of linear polymers of G-actin, directly underlie the plasma membrane and drive local changes in cell shape (Rohn and Baum, 2010). Microtubules are long hollow cylinders formed by the polymerization of α - and β -tubulin. They play crucial roles in cell migration, mitosis, and the intracellular transport of proteins and their complexes (Vale, 2003). Many animal cells also contain a third type of structure: the intermediate filaments. They are composed of a variety of proteins, and their size ranges between microfilaments and microtubules (Herrmann *et al.*, 2007). While the cytoskeleton of different organisms are composed of similar proteins, the dynamics and function may be very

different depending on the organism and the cell type (Wickstead and Gull, 2011; Gunning *et al.*, 2015).

In neurons, the actin cytoskeleton plays a role in differentiation, i.e. the outgrowth of neurites as well as the formation and plasticity of synaptic spines (Hotulainen and Hoogenraad, 2010; Matus, 2000; Pak *et al.*, 2008). In mature neurons, the actin polymers are found directly underneath the PSD where they stabilize synaptic proteins and drive morphological changes in response to stimuli (Kapitein and Hoogenraad, 2011). The actin bundles are highly dynamic. Depolymerization occurs at the so-called pointed ends, whereas ATP-dependent nucleation takes place at the barbed ends facing the plasma membrane. Their growth towards the cell boundaries creates an outward force resulting in morphological changes (Pollard and Cooper, 2009; Kapitein and Hoogenraad, 2011).

Actin dynamics are regulated by a number of actin-binding proteins and their upstream signaling molecules among which the group of Rho GTPases is essential. The best-characterized members are RhoA, Rac1, and Cdc42 (Jan and Jan, 2010). They function as molecular switches cycling between an active GTP bound state and an inactive GDP bound state (Van Aelst and D'Souza-Schorey, 1997). Whereas RhoA activation leads to dendrite retraction (Chen and Firestein, 2007; Jan and Jan, 2010), Cdc42 and Rac1 have been shown to regulate pathways responsible for outgrowth and branching (Leemhuis *et al.*, 2004; Scott *et al.*, 2003). Rho GTPases are regulated by a number of extracellular cues activating NMDARs, AMPARs, and other neuronal receptors. Their final targets are actin-binding proteins such as cofilin and profilin. The detailed signaling pathways related to NMDARs are shown in figure 4.

Cofilin is an actin disassembling factor whereas profilin polymerizes actin (Okamoto *et al.*, 2009). Both proteins are inactivated due to phosphorylation as a consequence of RhoA, CDC42 or Rac1 signaling. The finely concerted modulation of cofilin and profilin by Rho GTPases determines the polymerization and disassembly of actin fibers.

The same processes can be found in T-cells as a response to the binding of the TCR with the epitope-MHC-complex of an antigen presenting cell. This interaction initiates the formation of an immunological synapse which is – in analogy to a neuronal

synapse – a complex signaling platform at the contact site of two immune cells (Yamada and Nelson, 2007). After the activation of the TCR, signaling subdomains, each characterized by a distinct subset of proteins, are formed. These so-called supramolecular activation clusters (SMAC) surround the binding site in a concentric manner (Dustin and Colman, 2002). Both the formation of SMACs and the correct trafficking of proteins such as the TCR complex to their designated location require proper actin functioning (Kumari et al., 2013; Ritter *et al.*, 2013).

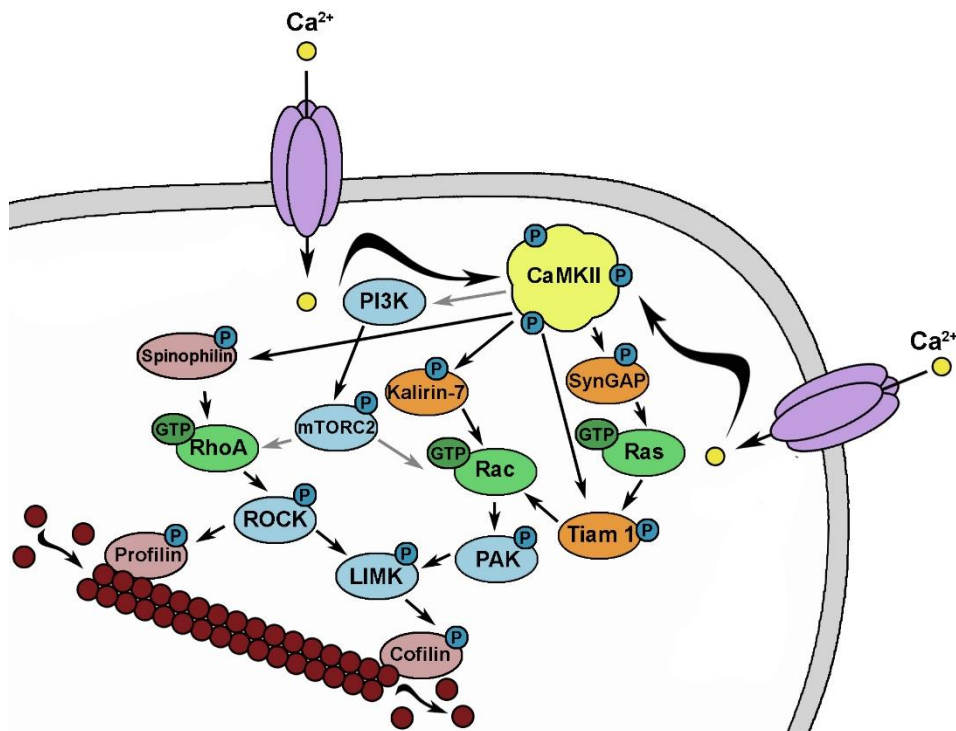


Figure 4: Regulation of the actin cytoskeleton by NMDARs. Ca²⁺ influx through open NMDARs triggers the activation of CaMKII that subsequently phosphorylates its substrates such as the GEFs kalirin-7 and tiam 1, SynGAP (Synaptic Ras GTPase-activating protein 1) as well as the actin-binding protein spinophilin (neurabin II). The next crucial step is the activation of small GTPases of the Rho subfamily (RhoA, Rac) and their downstream kinases ROCK, PAK and LIMK (Rho-associated protein kinase, p21 activated kinase, LIM domain kinase 1). ROCK and LIMK phosphorylate and thereby inactivate the actin disassembling factor cofilin and the actin monomer binder profilin. An alternative, though not fully understood pathway is the activation of PI3K, which also might depend on CaMKII (Lin et al., 2011), and the phosphorylation of its substrate mTORC2, a supposed regulator of RhoA and Rac (Jacinto et al., 2004). This complex interaction network allows a very finely regulated reorganization of the actin cytoskeleton.

Since CD3 ζ is the crucial signaling subunit of the TCR complex, we can conclude that the reorganization of the actin cytoskeleton in T-cells primarily depends on this protein. Interestingly, studies have also connected CD3 ζ with the neuronal cytoskeletal due to its regulation of dendrite outgrowth as well as its colocalization

with actin in distinct subcellular compartments (Baudouin *et al.*, 2008). Taking all these facts together, it gives rise to the hypothesis that CD3 ζ is a regulator of the actin cytoskeleton in neurons. The characterization of the underlying mechanisms will be the topic of this thesis.

1.4 Objectives

Studies have shown that neurons and T-cells have a lot in common at the molecular level despite their different morphologies and functions. Conducting an extensive database and literature research, this thesis aimed at providing a comparison between TCR signaling and neuronal signaling based on the published expression of participating proteins. The central TCR signaling subunit CD3 ζ was then chosen as a candidate protein, not only because of its immunological and neuronal expression, but mostly due to the fact that the protein needs a yet unknown neuronal receptor to transduce signals.

Apart from further characterizing CD3 ζ regarding its subcellular localization in neurons, the main objective of this thesis was to assess CD3 ζ functioning in cytoskeletal reorganization. Developing hippocampal neurons with their high dendrite dynamics were chosen as a model and subjected to Sholl analysis after the transfection with CD3 ζ loss-of-function mutants and pharmacological treatments. Biochemical analyses were then used to assess the influence of selected signaling molecules on CD3 ζ phosphorylation.

Furthermore, this study aimed at elucidating the role of NMDARs in the activation of CD3 ζ again with special focus on cytoskeletal signaling events by means of interaction and colocalization experiments as well as pharmacological studies in cell cultures.

2 Material and Methods

2.1 Material

2.1.1 Chemicals

All chemicals were obtained from BioRad, Roche, Invitrogen, Merck, Roth, Serva, Thermo Fisher Scientific, or Sigma-Aldrich and were of analytical grade. Special chemicals and solutions are detailed in the corresponding method descriptions.

2.1.2 Antibodies

2.1.2.1 Primary Antibodies

Antibody	Species	Supplier	Dilutions
anti-Bassoon	ms, monoclonal	Stressgen	IF: 1:400
anti-CD3 ζ	ms, monoclonal	Santa Cruz	IB: 1:200
anti-CD3 ζ	rb, polyclonal	Abcam	IF: 1:200 IP
anti-Cofilin	rb, monoclonal	Cell Signaling	IB: 1:500
anti-Cofilin (phospho S3)	rb, polyclonal	Abcam	IB: 1:500
anti-FLAG M2	ms, monoclonal	Sigma	IB: 1:2000
anti-GAPDH	ms, monoclonal	Abcam	IB: 1:10000
anti-GFP	rb, polyclonal	Abcam	IB: 1:10000 IF: 1:2000
anti-GluR1	ms, monoclonal	NeuroMAB	IB: 1:1000
anti-GluR2	ms, monoclonal	NeuroMAB	IB: 1:1000
anti-Homer	rb, polyclonal	Synaptic Systems	IF: 1:400
anti-Homer	rat, polyclonal	Acris	IF: 1:200
anti-MAP2	gp, polyclonal	Synaptic Systems	IF: 1:1000
anti-NR2B	ms, monoclonal	BD Transduction Laboratories	IB: 1:250 IF: 1:50
anti-NR2B	rb, polyclonal	Alomone Labs	IF: 1:20 (live)
anti-Synaptophysin	gp, polyclonal	Synaptic Systems	IF: 1:500
anti-TrkB	ms, monoclonal	BD Transduction Laboratories	IB: 1:500
anti- α -Tubulin	ms, monoclonal	Sigma	IB: 1:2000
anti- β III-Tubulin	ms, monoclonal	Sigma	IB: 1:2000 IF: 1:500
anti-phospho-Tyrosine	ms	BD Transduction Laboratories	IB: 1:2000

Abbreviations: IB - immunoblot, IF - immunofluorescence, IP - immunoprecipitations

2.1.2.2 Secondary Antibodies

Antibody	Species	Supplier	Dilutions
Anti-mouse IgG HRP	Goat, polyclonal	Dianova	IB: 1:10000
Anti-rabbit IgG HRP	Goat, polyclonal	Dianova	IB: 1:10000
Anti-rabbit IgG Alexa Fluor™ 488	Goat, polyclonal	Molecular Probes	IF: 1:1000
Anti-rabbit IgG cy3, cy5	Goat, polyclonal	Molecular Probes	IF: 1:1000
Anti-mouse IgG cy3, cy5	Goat, polyclonal	Molecular Probes	IF: 1:1000
Anti-guinea pig, cy3, cy5	Goat, polyclonal	Molecular Probes	IF: 1:1000

Abbreviations: IB – immunoblot, IF – immunofluorescence

2.1.3 Bacterial Strains and Culture Media

For transformations and preparations of plasmid DNA from bacteria, the bacterial strain XL10-GOLD with the genotype *endA1 glnV44 recA1 thi-1 gyrA96 relA1 lac Hte (mcrA)183 Δ(mcrCB-hsdSMRmrr) 173 tetR F'[proAB lacIqZΔM15 Tn10(TetR Amy CmR)]* (Stratagene) was used.

LB-medium	5g/l yeast-extract, 10g/l bacto-tryptone, 5g/l NaCl
LB-plates	1000ml LB-medium, 15g agar
SOC-medium	20g/l bacto-tryptone, 5g/l yeast-extract, 10mM NaCl, 2,5mM KCl, 10mM MgSO ₄ , 10mM MgCl ₂ , 20mM glucose

2.1.4 Animals

In this study, Wistar rats from the Leibniz Institute for Neurobiology (Magdeburg, Germany) animal facilities were used. Animal housing and experimental procedures were authorized and approved by the Institutional State and Federal Government regulations (Land Sachsen-Anhalt, Germany).

2.2 Methods

2.2.1 Molecular Biological Methods

Molecular procedures followed established protocols as described in Green and Sambrook (2012). Therefore, all protocols are described briefly unless they were significantly altered.

2.2.1.1 PolyA+-RNA Preparation and Reverse Transcription

Rats at different ages were anesthetized and transcardially perfused with a 0.9% NaCl solution. Tissue from spleen, hippocampus, and cortex were used to isolate RNA employing the RNeasy Mini Kit from Qiagen. Reverse transcription of 1 μ g RNA into cDNA was done with the Omniscript Reverse Transcription Kit from Qiagen. All procedures followed the supplier's protocols.

2.2.1.2 Polymerase Chain Reaction (PCR)

Taq DNA Polymerase: Qiagen
Primers (dissolved in ddH₂O): Biomers
Deoxyribonucleotide Set (dNTPs): Thermo Scientific

For the detection of CD3 ζ cDNA in rat spleen, hippocampus, or cortex as well as for subcloning, DNA was amplified using specific primers. The reagent concentrations in a 50 μ l reaction sample and the PCR program used are shown below. The annealing temperature (T_m) was adjusted depending on the primers in use (see section 6.3).

cDNA	1 μ g	Initial denaturation	5min	95°C	} 35 cycles
Primer 1	0.5 μ M	Denaturation	45sec	95°C	
Primer 2	0.5 μ M	Annealing	45sec	T_m	
dNTPs	0.5mM	Elongation	1min	72°C	
Taq polymerase	5U	Final Elongation	10min	72°C	
10x buffer	5 μ l				
ddH ₂ O	ad 50 μ l				

2.2.1.3 Site-directed Mutagenesis

To substitute base pairs within the CD3 ζ sequence, mutations were introduced into two overlapping DNA fragments using accordingly altered primers (see section 6.3)

in two separate PCR reactions. In a second step, the fragments were fused and elongated. A detailed protocol can be found in *PCR, Labor im Fokus, Spektrum Akademischer Verlag* (Newton and Graham, 1997).

2.2.1.4 DNA Restriction

Restriction enzymes: Thermo Scientific

Several restriction enzymes were used according to the recommendations of the manufacturer to digest DNA fragments.

2.2.1.5 Agarose Gel Electrophoresis and DNA Extraction from Agarose Gels

Agarose:	Molecular biology grade, SERVA
50x TAE:	2M Tris, 0.05M EDTA
Ethidium bromide:	1mg/ml, Roth
6x Loading Dye:	10mM Tris-HCl (pH 7.6), 0.03% bromophenol blue, 0.03% xylene cyanol FF, 60% glycerol, 60mM EDTA
GeneRuler 1kb DNA ladder:	Thermo Scientific
NucleoSpin ExtractII Kit:	Macherey-Nagel

Separation of DNA fragments for analytical or preparative purposes was accomplished using one-dimensional agarose gel electrophoresis. 1% (w/v) agarose gels were prepared by dissolving agarose in 1x TAE buffer under heat using a microwave. To visualize DNA fragments under UV light, ethidium bromide was added to a final concentration of 0.5µg/ml. Gels were run at 80mV in 1x TAE buffer.

DNA fragments for subcloning were excised from the gel, and DNA was extracted using the NucleoSpin ExtractII Kit following the manufacturer's protocol.

2.2.1.6 Cloning of DNA Fragments into Plasmid Vectors

T4 DNA ligase: New England Biolabs

Both vectors and DNA fragments underwent restriction with according restriction enzymes. Digested DNA was submitted to agarose gel electrophoresis and was then extracted from the gel as described above. For ligations, ATP-dependent T4 DNA ligase was employed at a final concentration of 1U in a 10µl reaction sample. The molar ratio between DNA fragment and vector was 3:1. The sample was incubated at

23°C for 2h.

2.2.1.7 Transformation of Chemically Competent Bacteria

For the transformation of *E.Coli* XL10-GOLD, 5µl ligation sample was added to 100µl of bacteria and incubated on ice for 10 minutes. After a 45-second heat shock at 42°C, the samples were put back on ice for 2 minutes before they were transferred to 1ml preheated SOC medium. The bacteria were incubated at 37°C for 1h with constant shaking and then plated on LB-agar plates with respective antibiotics. Plates were incubated overnight at 37°C.

2.2.1.8 Preparation of Plasmid DNA (mini and midi preparations)

Buffer P1:	50mM Tris-HCl (pH 8.0), 10mM EDTA, 100µg/ml RNase A
Buffer P2:	200mM NaOH, 1% (w/v) SDS
Buffer P3:	3M potassium acetate (pH 5.5)
Midi preparation:	NucleoBond® Xtra Midi, Macherey-Nagel

To define positive clones after transformation, colonies were cultivated in 2ml LB-medium containing the respective antibiotics at 37°C overnight. The preparation protocol was modified from Birnboim and Doly (1979). Bacteria were pelleted and resuspended with 300µl P1. Cells were lysed with 300µl P2 for 5min, neutralized with 300µl P3, and then incubated on ice for 5min. Precipitated proteins were removed by centrifugation at 20.000xg for 10min. The DNA in the supernatant was precipitated with isopropanol. Plasmid DNA was collected by centrifugation (20000xg, 10min) and washed with 70% ethanol. After drying, the pellet was resuspended in 25µl 10mM Tris-HCl (pH 7.5). Large quantities of plasmid DNA with high purity were prepared from 250ml overnight cultures using the NucleoBond® Xtra Midi Kit according to the supplier's protocol.

2.2.1.9 Generation of Expression Constructs

Constructs used in this study are listed in section 6.2 (appendix). All constructs were generated by subcloning or PCR and were sequenced.

2.2.1.10 Sequencing and Sequence Analysis

Sequencing was done by the company SeqLab. The program Standard Nucleotide Blast by NCBI was used for sequence analysis.

2.2.2 Biochemical Methods

2.2.2.1 Subcellular Fractionation of Tissues

All subcellular fractionations were performed at 4°C.

2.2.2.1.1 Preparation of a Crude Membrane Fraction (P2)

Buffer A: 320mM sucrose, 5mM HEPES (pH 7.4)
Protease inhibitors: Complete®, Roche

Rats were anesthetized and decapitated. Both spleen and forebrain were taken and either directly submitted to fractionation or frozen on dry ice and stored at -80°C until use. The tissue was homogenized with 10ml/g Buffer A containing protease inhibitors with a homogenizer (12x 900rpm) and centrifuged for 10min at 1000xg. The pellet was washed in the same amount of Buffer A as before and centrifuged. The supernatants from both centrifugations were pooled and pelleted at 12000xg for 15min. The supernatant (S2) contained the cytosolic protein fraction. The pellet was washed in Buffer A. The subsequent centrifugation step (12000xg, 20min) resulted in a crude membrane fraction (P2) that was then used for further subcellular fractionations.

2.2.2.1.2 Synaptosome Preparation from Rat Forebrain

Buffer B: 320mM sucrose, 5mM Tris-HCl (pH 8.1)
Sucrose solutions: 0.85/1.0/1.2M sucrose, 5mM Tris-HCl (pH 8.1)

To prepare a synaptosome-enriched fraction, P2 was resuspended in 1.5ml/g (wet tissue weight) Buffer B and transferred to a step gradient with 9.1ml each of 0.85/1.0/1.2M sucrose solutions. After a 2-hour centrifugation at 85.000xg the following fractions are obtained: myelin at 0.32/0.85M sucrose interface, light membranes at 0.85/1.0M sucrose interface, synaptosomes at 1.0/1.2M sucrose interface, and mitochondria as a pellet.

2.2.2.1.3 Lipid Raft Preparation from Rat Forebrain

Lysis buffer: 5mM HEPES (pH 7.4), 1% Triton X-100, protease inhibitors
Resuspension Buffer: 5mM HEPES (pH 7.4), 2M sucrose
Sucrose solutions: 0.85/1.5M sucrose, 5mM HEPES (pH 7.4)

For the preparation of a lipid raft enriched fraction, P2 was lysed in 1ml/g (wet tissue weight) lysis buffer and incubated for 30min under agitation. Detergent-resistant membranes were collected at 20.000xg for 30min. The pellet was resuspended in 1ml/g (initial tissue weight) resuspension buffer and placed at the bottom of a step gradient with 9ml each of 0.85M and 1.5M sucrose solution. The remaining volume of the centrifuge tube was filled with 5mM HEPES (pH 7.4) up to 0.5cm underneath the rim. After centrifugation (2h 100000xg), lipid rafts were harvested at the 0M/0.85M sucrose interface.

2.2.2.2 Determination of Protein Concentrations

2.2.2.2.1 Bicinchoninic Acid Assay

BC Assay Protein Quantitation Kit: Uptima
Bovine Serum Albumin (BSA): Interchim

The BC Assay is a colorimetric assay derived from the Biuret reaction (Gornall *et al.*, 1949). The protein concentrations of fractionation samples were determined in triplets. Different dilutions of BSA served as standards. The reaction was performed according to the recommendations of the supplier. The protein concentration is directly proportional to the optical absorbance measured at a wavelength of 562nm.

2.2.2.2.2 Amido Black Protein Assay

Amido black solution: 23mM amido black 10B (Merck) in methanol/acetic acid
Methanol/acetic-acid: Methanol : acetic acid 9:1
BSA: Interchim

The quantification of precipitated and in 2x SDS sample buffer resuspended proteins samples was done using the amido black protein assay (Popov *et al.*, 1975). Different dilutions of BSA served as standards. The protein concentrations of both protein and BSA samples were determined in triplets. Samples were incubated with amido black solutions in a 96-well reaction plate at room temperature for 10min and centrifuge at 3200xg for 10min. The pellets were washed three times with methanol/acetic acid

and centrifuged as before in-between. After drying, the pellet was resuspended in 300µl 0.1N NaOH. Optical Absorbance was measured at 620nm with a photometer (VERSAmax microplate reader, Molecular Devices). The program Soft Max Pro 4.8 was used for further analysis of the data.

2.2.2.3 Protein precipitation

4x SDS sample buffer: 250mM Tris (pH 6.8), 1% (w/v) SDS, 40% (v/v) glycerol, 20% (v/v) β-mercaptoethanol, 0.004% (w/v) bromophenol blue

Fractionation samples containing 500µg of protein (determined by BC assay) were incubated in ice-cold 80% ethanol at -20°C overnight. Precipitated proteins were pelleted and then washed three times with ice-cold 80% ethanol employing centrifugation at 20.000xg at 4°C for 10min. The final pellet was dried and resuspended in 2x SDS sample buffer.

2.2.2.4 Sodium Dodecyl Sulfate Polyacrylamide Gel Electrophoresis (SDS-PAGE)

4 x SDS sample buffer: 250mM Tris (pH 6.8), 1% (w/v) SDS, 40% (v/v) glycerol, 20% (v/v) β-mercaptoethanol, 0.004% (w/v) bromophenol blue

Electrophoresis buffer: 192mM glycine, 0.1% (w/v) SDS, 25mM Tris (pH 8.3)

Protein ladder: Precision Plus Protein™ Prestained Standard Dual Color, Bio-Rad

Separation of proteins by molecular weight was achieved by employing SDS-PAGE under denaturing conditions following a protocol by Laemmli (1970). Depending on the protein samples, either a homogenous running gel (12% polyacrylamide) or a continuous gradient gel (5-20% polyacrylamide) with 5% polyacrylamide stacking gel was used. Protein samples were solubilized in SDS sample buffer and incubated at 95°C for 5min. Electrophoresis was performed at a constant current of 10mA. The gels were either stained with Coomassie Brilliant Blue or used for immunoblotting.

2.2.2.5 Coomassie blue staining of SDS-PAGE gels

Coomassie Brilliant Blue staining solution: 0.125% (w/v) Coomassie Brilliant Blue R250, 50% (v/v) methanol, 10% (v/v) acetic acid

Destaining solution: 7% (v/v) acetic acid

Conservation solution: 50% (v/v) methanol, 5% (v/v) glycerol

Gels were stained in Coomassie Brilliant Blue staining solution at room temperature overnight and destained with 7% acetic acid until protein bands were clearly visible.

For conservation, gels were incubated in conservation solution for 10min and spanned in a frame between two cellophane sheets (Roth) for drying.

2.2.2.6 Western Blotting and Immunodetection of Proteins

Blotting buffer:	192mM glycine, 0.2% (w/v) SDS, 20% (v/v) Methanol, 25mM Tris (pH 8.3)
PonceauS solution:	0.5% (w/v) PonceauS in 3% (v/v) trichloroacetic acid
10x TBS:	200mM Tris/HCl (pH 7.6), 1.37M NaCl
TBS-A:	0.02% (w/v) NaN₃ in 1xTBS
TBS-T:	0.1% (v/v) Tween-20 in 1x TBS
Blocking buffer:	5% (w/v) dried milk in 1x TBS-T
Nitrocellulose membrane:	PROTRAN® pore size 0.45µm, Whatman®
ECL:	Pierce® ECL Western Blotting Substrate, PierceImmobilon™ Western, Millipore
Light-sensitive films:	Amersham Hyperfilm™ ECL, GE Healthcare

The electrophoretic transfer of proteins to a nitrocellulose membrane followed a protocol by Towbin *et al.* (1979) in a 4°C-cooled blotting chamber by Hoefer at constant current of 200mA. Blotting time for endogenous CD3ζ was 1h, for all other samples 90min. After the transfer, the membrane was incubated in PonceauS solution for 15min at room temperature before blocking with blocking buffer for 1h. Incubation with the primary antibody was either done 1h at room temperature or overnight at 4°C under constant shaking. The antibody diluted in TBS-A, 5% BSA in TBS-TA, or blocking buffer depending on the supplier's recommendations. Before and after the 1h incubation with secondary antibody in blocking solution, the membrane was washed four times 10min in TBS-T. Induction of chemiluminescence was achieved with an ECL reagent following the manufacturer's protocol. Protein bands were detected using either light-sensitive films and the developer machine Agfa Crux 60 or the INTAS ECL Chemocam Imager (INTAS Science Imaging).

2.2.2.7 Expression and Purification of Tandem-Affinity-Purification-Tagged CD3ζ (CD3ζ-TAP)

10x PBS:	1.4M NaCl, 83mM Na₂HPO₄, 17mM NaH₂PO₄, pH 7.4
Lysis Buffer:	50mM Tris/HCl (pH 8.0), 150mM NaCl, 1% Triton X-100
Wash Buffer:	50mM Tris/HCl (pH 8.0), 150mM NaCl
Protease Inhibitors:	Complete (Roche)
Anti-FLAG® M2 Affinity Gel:	Sigma
FLAG® peptide:	Sigma

HEK 293-T cells in 175cm² flasks were transfected as described in 2.2.3.1. 24h after

transfection, cells were harvested in cold PBS, pelleted at 1000xg for 3min, and then lysed for 1h at 4°C under constant rotation with 250µl lysis buffer containing protease inhibitors. Insoluble cell debris was removed by centrifugation (20min, 20000xg, 4°C). Prior to adding the supernatant to the Anti-FLAG® M2 Affinity Gel (75µl/175cm² flask of cells) in 10ml flow-through columns (Pierce), the matrix was washed three times with 0.1M glycine (pH 3.5) and equilibrated five times with wash buffer. After a 1h incubation on an overhead rotator at 4°C, the gel was washed four times with protease inhibitor containing washing buffer and then twice with the same buffer with 5µg/µl FLAG peptide. Bound protein was eluted with 2x SDS sample buffer and analyzed by SDS-PAGE and subsequent Coomassie staining for purity.

2.2.2.8 Antibody Generation and Affinity Purification of Polyclonal Antisera

10x PBS: 1.4M NaCl, 83mM Na₂HPO₄, 17mM NaH₂PO₄, pH 7.4
Blocking Buffer: 5% (w/v) BSA in 1xPBS, 0.1% (v/v) Tween-20, 0.025% (w/v) NaN₃
Wash buffer: 0.1% (w/v) BSA in 1x PBS, 0.1% (v/v) Tween-20
Elution buffer: 100mM glycine (pH 2.5)
Neutralization buffer: 1M Tris-HCl (pH 8.0)

The immunization of rabbits and guinea pigs with four different peptides of the CD3ζ sequence (2 animals per peptide) was carried out by BioGenes, Berlin, Germany. The immune reactivity of crude sera at different time points after the immunization was tested. If CD3ζ-TAP expressed in HEK-293 T could be detected via immunoblot analysis, the animal was sacrificed to collect the complete serum.

For the affinity purification of antisera, purified CD3ζ-TAP was subjected to SDS-PAGE and Western blotting. Staining of the nitrocellulose membrane with PonceauS solution showed a clear band of approximately 25kDa, which was excised and cut into pieces. The blot pieces were blocked for 1h at room temperature in blocking buffer and incubated with 1.5ml crude serum at 4°C overnight. After washing three times with wash buffer, polyclonal antibodies were eluted with 900µl elution buffer and immediately neutralized with 90µl 1M Tris-HCl (pH 8.0). Aliquots were stored at -80°C.

2.2.2.9 Co-Immunoprecipitation using Magnetic anti-GFP Microbeads

μMACS™ Epitope Tag Protein Isolation Kit: Miltenyi Biotec
Protease inhibitors: Complete (Roche)

HEK 293-T cells co-expressing CD3ζTAP and GFP, CD3ζGFP or either one of the mutants were harvested in PBS and pelleted for three minutes at 1000xg. The pellet was lysed for 1h at 4°C using the lysis buffer of the μMACS™ Epitope Tag Protein Isolation Kit supplemented with protease inhibitors. Insoluble cell debris was removed by centrifugation (20min, 20000xg, 4°C). The supernatant was subjected to immunoprecipitation as described in the manufacturer's protocol. Elution was done using 2x SDS sample buffer. Samples were analyzed by immunoblot.

2.2.2.10 Co-Immunoprecipitation using Protein G magnetic beads

Wash buffer: 50mM Tris/HCl (pH 8.0), 150mM NaCl
Lysis buffer: 50mM Tris/HCl (pH 8.0), 150mM NaCl, 1% Triton X-100, protease inhibitors
Protease inhibitors: Complete (Roche)
Dynabeads Protein G: Life Technologies (Thermo Fisher Scientific)

Rat synaptosome fraction containing 1mg of protein were washed twice with 5ml wash buffer and centrifuged at 100000xg at 4°C to remove residual sucrose. The pellet was lysed with 500μl lysis buffer on an overhead rotator at 4°C for 1h, and insoluble cell debris was removed by centrifugation (20000xg, 20min, 4°C). The supernatant was incubated with 2μg anti-CD3ζ antibody or rb IgG coupled to protein G magnetic beads overnight on an overhead rotator at 4°C. After washing three times with 500μl lysis buffer, precipitated proteins were eluted with 2x SDS sample buffer.

2.2.2.11 Biotin-labeling and Isolation of Cell Surface Proteins

Pierce Cell Surface Protein Isolation Kit: Thermo Fisher Scientific
Protease Inhibitor: Complete (Roche)

Hippocampal neurons (300000/ well in 6-well plate) were transfected with GFP, CD3ζGFP or either one of the mutants using lentivirus on DIV10. Six days later, neurons were used for cell surface protein biotinylation using Pierce cell surface protein isolation kit. In short, cells were washed twice with ice-cold PBS and incubated with a 0.25mg/ml biotin solution on ice while shaking for 30 minutes. After adding 50μl of quenching solution, cells were washed with TBS and lysed in 50μl lysis

buffer supplemented with protease inhibitors on ice for 20 minutes. Cell suspension of two wells was collected in a tube, and insoluble cell debris was removed by centrifugation (20000xg, 5min, 4°C). 100µl equilibrated NeutrAvidin agarose suspension was added to the supernatant and incubated for 1h at room temperature while rotating. After four times washing with washing buffer, bound proteins were eluted with 2x SDS sample buffer.

2.2.3 Cell Culture

2.2.3.1 Cultivation and Transfection of Mammalian Cell Lines

HEK 293-T cells:	American Type Culture Collection (ATCC)
COS7 cells:	American Type Culture Collection (ATCC)
Culture dishes:	(Nunc)
Solution A:	500mM CaCl₂
Solution B:	140mM NaCl, 50mM HEPES, 1.5mM Na₂PO₄, pH 7.05
Culture Medium:	DMEM, 10% (v/v) fetal bovine serum (FBS), 2mM L-glutamine, 100U/ml penicillin, 100µg/ml streptomycin (all Gibco)
TrypLE™ Express:	1x (Gibco)
HBSS:	(Gibco)

Human embryonic kidney (HEK) 293-T cells and COS7 cells derived from African green monkey kidney were used for overexpression studies. Cultures were maintained at 37°C, 5% CO₂ and 95% humidity in an incubator. Confluent cultures were passaged twice a week. After washing with warm HBSS, cells were trypsinized with 1x TrypLE™ for three minutes at 37°C. For cell line maintenance, cells were split in a 1:10 ratio into fresh culture medium. For transfection, cells were split to achieve 80% confluency within 24 hours.

Transfection of cell lines was performed with calcium phosphate precipitates. For a 75cm² culture flask, 1ml solution A was mixed with 25µg plasmid DNA. After adding 1ml solution B, the mix was incubated for one minute at room temperature before adding it dropwise to the flask. Culture medium was exchange for new one six hours after transfection. For smaller culture flasks or plates, the amount of transfection reagents and DNA was scaled down. Cells were processed 24 hours after transfection.

2.2.3.2 Cultivation and Transfection of Hippocampal Primary Cells

Plating medium:	DMEM, 10% (v/v) FBS, 100U/ml Penicillin, 100µg/ml, Streptomycin, 2mM L-glutamine (all Gibco)
Culture Medium:	Neurobasal™, 1x B27 , 0.8mM L-glutamine (all Gibco)
Culture dishes:	(Nunc)
Coverslips:	(Roth)
HBSS:	(Gibco)
Trypsin:	10x Trypsin (-EDTA), (Gibco)
Poly-D-lysine:	100 mg/l in 0.15 M boric acid, pH 8.4
OptiMEM™:	(Gibco)
Lipofectamin 2000:	Life Technologies (Thermo Fisher Scientific)

Preparation of hippocampal neuronal culture followed the method introduced by Kaech and Banker (2006) with slight modifications. E18 rat embryos were decapitated, and hippocampi were dissected from the brain in HBSS. The tissue was trypsinized for 15 minutes at 37°C and washed three times with plating medium to remove residual trypsin. Dissociation of hippocampi was achieved by repeatedly pipetting up and down with a Pasteur pipette with a narrowed tip (achieved by flaming). After determining the cell density, neurons are seeded in plating medium onto poly-D-lysine treated coverslips or culture dishes. One hour after seeding, plating medium is exchanged for culture medium. Partial exchange of culture medium to verify optimal feeding of cells followed once per week. Medium of low-density cultures (20000 cells/12mm coverslip) used for immunofluorescence was supplemented with conditioned medium. Biochemical procedures were performed with hippocampal neurons in 6-well plates (300000/well). High-density cultures (60000 cells/12mm coverslip) were used for transfection.

Transfection of neurons was performed using lipofection. Culture medium of 24-well plates was exchanged for 450µl OptiMEM™ and stored for later use in the culture incubator at 37°C. Per well 25µl OptiMEM™ were incubated with 1µl Lipofectamin 2000 for 5min at room temperature after vigorous mixing. Then another 25µl OptiMEM™ containing 1µg of plasmid DNA were added. After 20 minutes of incubation, suspension was added dropwise to the well. Four hours later, cells were washed three times with OptiMEM™. Neurons were maintained in their old culture medium in the culture incubator until further use.

2.2.3.3 Generation of Lentiviruses

Medium I:	DMEM, 10% (v/v) FBS, 2mM L-Glutamine, 100U/ml Penicillin, 100µg/ml Streptomycin (all Gibco)
Medium II:	DMEM, 4%FBS, 2mM L-glutamine, 100U/ml Penicillin, 100µg/ml Streptomycin (alles Gibco)
Sterile filter:	(Corning)
Centrifugation tubes:	(Beckmann Ultra clear)

Lentiviral expression vectors were generated by integrating DNA fragments amplified by PCR into the FUGW vector (Lois *et al.*, 2002). Used constructs are listed in the appendix (section 6.2).

Production of lentiviruses in HEK 293-T cells followed protocols described in Dittgen *et al.* (2004) und S2 security conditions. Transfer vector and the helper vectors VSVg and pSPAX2 were transfected into HEK 293-T cells using the calcium phosphate method (see 2.2.3.1) with a ratio of 10µg/5µg/7.5µg. The culture medium (medium I) was replaced with medium II 24h after transfection. On the next day, this medium was collected for virus harvest. Cell debris was removed by centrifugation for 5min at 2000xg and subsequent filtration through a previously blocked sterile filter (pore size 0.45µm). Viral particles were pelleted at 19700xg for 2h and resuspended Neurobasal™. Aliquots were stored at -80°C until use.

Optimal virus concentrations for infection of hippocampal neurons were tested for all constructs in both low-density and high-density cultures. Depending on the experiment, neurons were infected on DIV3 and harvested on DIV8 or infected on DIV10 and used six days later.

2.2.3.4 Stimulation of Cultured Hippocampal Neurons

2.2.3.4.1 Pervanadate Treatment of Cultured Hippocampal Neurons

Na ₃ VO ₄ :	200mM in H ₂ O (pH 10.0) (Sigma)
H ₂ O ₂ :	30% (v/v) (Sigma)
HBSS +/-:	(Gibco)

Pervanadate is an irreversible inhibitor of tyrosine phosphatases (Huyer *et al.*, 1997). It is used to maintain the phosphorylated state of tyrosine residues of target proteins. 20min before treatment, the culture medium of the neurons was exchanged for HBSS +/- (HBSS containing Ca²⁺ and Mg²⁺) – 500µl/well in 24-well plates or 1ml/ well in 6-well plates. The next protocol steps are described for 24-well plates. Amounts can be

up-scaled for use in larger culture dishes. For stimulation, 15µl 200mM Na₃VO₄ and 1µl H₂O₂ were added per well. Neurons were incubated for 5min at 37°C before washing twice with ice-cold HBSS +/- . Cells were harvested with 25µl 2x SDS buffer per well. Samples were boiled at 95°C for 5min before immunoblot analysis. The experiment was performed both on DIV8 and DIV16 hippocampal neurons.

2.2.3.4.2 NMDA Stimulation of Hippocampal Neurons

Tyrodes buffer: 12.5mM HEPES (pH 7.4), 1.25mM KCl, 15mM glucose, 120mM NaCl, 2mM MgCl₂, 2mM CaCl₂
1000x NMDA: 100mM in H₂O
1000x glycine: 2mM in H₂O (prepared directly before use)

This experiment was performed on DIV16 hippocampal neurons. Culture medium was exchanged for Tyrodes buffer at least 20min prior to stimulation. Three minutes of incubation with 1xNMDA/1xglycine at 37°C was followed by three times washing with tyrodes buffer. Water was used instead of NMDA/glycine as vehicle control. After 20min neurons were harvested in 25µl 2x SDS buffer. Samples were boiled at 95°C for 5min before immunoblot analysis.

2.2.3.4.3 Inhibition of Neuronal Receptors and Kinases

200x D-APV: 10mM in DMSO (Sigma)
1000x CNQX: 10mM in DMSO (Sigma)
1000x Ifenprodil: 10mM in DMSO (Sigma)
1000x Damnacanthal: 100µM in DMSO (Tocris)
1000x Piceatannol: 10mM in DMSO (Sigma)
1000x PP2: 1mM in DMSO (Sigma)
1000x Wortmannin: 50µM in DMSO (Sigma)
1000x Y-27632: 10mM in H₂O (Sigma)

The inhibitors were used for Sholl analysis experiments (DIV8) and pervanadate treatment experiments (DIV8 and DIV16) with hippocampal neurons. For Sholl analysis, neurons were transfected with Lipofectamin 2000 (see 2.2.3.2) in OptiMEM™. When replacing OptiMEM™ with culture medium, inhibitors or vehicle (DMSO or H₂O in case of Y-27632) were added. Cells were kept in the incubator at 37°C for 5h before fixing with 4% PFA as described in 2.2.3.5. For pervanadate treatment (see 2.2.3.4.1), inhibitors were added to the neurons 1h before the experiment.

2.2.3.5 Immunocytochemistry

PFA: 4% (w/v) paraformaldehyde in 1xPBS
Blocking solution: 5% (w/v) bovine serum albumin (BSA), 10% (w/v) horse serum (HS),
0.1% (v/v) Triton X-100 in 1x PBS
Mowiol: 10% (w/v) Mowiol, 25% (v/v) Glycerol, 100mM Tris/HCl (pH 8.5)

Cells were grown on Ø 12 mm coverslips and fixed with 4% PFA in 1xPBS for 7 at room temperature. Coverslips were washed four times 10min with PBS to remove the PFA. Cells were blocked for 30min with blocking solution. The incubation with primary antibodies diluted in blocking solution followed for 1h at room temperature or overnight at 4°C. After thorough washing, cells were incubated with secondary antibodies diluted in blocking solution for 1h at room temperature. Then, cells were washed four times 10min with PBS, rinsed briefly in bidistilled water and mounted in 7µl mowiol.

Live Staining of Surface NR2B

To visualize surface NR2B molecules, hippocampal neurons were treated with an anti-NR2B antibody recognizing an extracellular epitope (Alomone Labs). The antibody was diluted 1:20 in culture medium, and insoluble parts were removed by centrifugation for 5min at 10000xg. Coverslips were incubate with the antibody solution for 15min at 37°C. After short washing with warm culture medium, cells were fixed with 4% PFA and the protocol proceeded as described in the section above.

2.2.3.6 Image Acquisition and Analysis

Fluorescence was visualized with the Axio Imager.A2 microscope (Zeiss, Oberkochen, Germany), and images were acquired with the CoolSNAP MYO camera by Photometrics (Tucson, USA). The imaging software VisiView (Visitron Systems GmbH, Puchheim, Germany) was used for image documentation.

2.2.3.6.1 Sholl Analysis of Cultured Hippocampal Neurons

To assess dendrite complexity, DIV8 hippocampal neurons were fixed and mounted on microscope slides 9h after transfection. Images were acquired with a 20x objective

and 2x camera binning to improve visualization of dendrites.

Soma and dendrites of neurons were traced using Adobe Photoshop (Adobe Systems, San José, USA). The trace copy of the neuron was subjected to Sholl analysis (Sholl Analysis Plugin for ImageJ, public domain, imagej.nih.gov/ij/) with the following parameters:

Starting radius:	0 μ m
Ending radius:	200 μ m
Radius Step Size:	5 μ m
Radius Span:	0
Span Type:	Median

2.2.3.6.2 Optic Density Analysis of Overexpressed Proteins in Dendrites

To examine the distribution of CD3 ζ and its mutants in hippocampal neurons, cells were fixed 6h after transfection and subjected to immunocytochemical staining of the somatodendritic compartment with an anti-MAP2 antibody. Images were acquired with a 63x (1.4 NA) objective and 1x camera binning. Optic density distribution within a dendrite was measured using ImageJ software by tracing the branch with the “Segmented Line” tool and taking the “Plot Profile”.

2.2.3.6.3 Analysis of Synaptic Structures and NR2B-positive puncta

Images were acquired with a 63x (1.4 NA) objective and 1x camera binning (pixel size = 0.072 μ m x 0.072 μ m, pixel depth = 8 bytes). Dendritic segments of 50 μ m² approx. were cropped and used as templates for quantifications. The size, number, and fluorescence intensity of puncta were quantified for each individual channel using “Analyze Particle” tool of the Fiji software by setting the following parameters: brightness and contrast range = 30 to 255; color threshold filter pass range = 70 to 255; range of particle size = 0.04–0.6 μ m² as in detail described previously (Herrera-Molina *et al.*, 2014). Lists of raw data were automatically generated as an Excel-compatible file for further statistical analysis. Data were normalized on the base of 10 μ m² of dendrite.

After quantification of number and size of pre- and post-synaptic proteins, 1-bit masks were created for each individual channel using the “Analyze Particle” tool of the Fiji software. To quantify the number of synapses, I used complementary masks (from pre- and post-synaptic markers) and the “Image calculator” function of the Fiji software. By this procedure, a synapse results from the contact of at least one pre- and one postsynaptic punctum and, thus, it is robust in detecting tightly matched complementary synaptic markers (Herrera-Molina *et al.*, 2014).

3 Results

3.1 A Comparative Study of Immune and Neuronal Signaling Pathways

Computational systems biology provides a holistic approach to understand complex signal transduction networks. In an effort to describe the components and dynamics of T cell receptor (TCR) signaling, Saez-Rodriguez *et al.* (2007) published a model relying on Boolean algebra. It comprises 94 nodes and 123 interactions. The model allows following the global behavior of the network at any given condition, e.g. inhibition of certain proteins. To gain deeper insights into postsynaptic signaling, we used an extended version of the model as a blueprint (104 nodes including 95 proteins). In a first step, we compared the expression of listed proteins between T-cells and neurons. Peer-reviewed publications were searched for information regarding the expression of proteins in rat, mouse or human neurons and glia cells with special focus on the brain regions hippocampus and cortex. Apart from published data we also used a variety of databases, namely the Allen Brain Atlas, the Human Protein Atlas, and SynProt.

The Allen Brain Atlas is a project initiated by the Allen Institute for Brain Science in Seattle, USA. It comprises several atlases of human and mouse brain of which the latter one was used for this study. The mouse atlas provides information on gene expression in the adult mouse brain (Lein *et al.*, 2007, Jones *et al.*, 2009). Nissl staining of the brain sections allows for localization of mRNA to neuronal cells. Information on glial mRNA expression is not available.

The second database used was the Human Protein Atlas hosted by the Royal Institute of Technology in Stockholm, Sweden (Uhlén *et al.*, 2015). They follow an antibody-based approach to characterize the protein expression in a large variety of human tissues, cancer types as well as cell lines. Brain tissue expression is specified for neurons, glia cells, epithelia, and neuropil in cortical, hippocampal, cerebellar, and lateral ventricle area.

Information on the synaptic presence of the proteins could be found in the database SynProt (Pielot *et al.*, 2012). This database is a meta-study of proteomics screens

detecting proteins in the detergent-resistant synaptic junctions fraction. The classification system of the database gives information on glial or neuronal protein expression as well as on pre- or postsynaptic localization.

Detailed results can be seen in the appendix section 6.4. Figure 5 gives an overview over the entire network depicting all the nodes and providing color-coded information on protein expression. Abbreviations are explained in table 1. In short, 69 out of 95 proteins were found to be expressed in hippocampal pyramidal cells according to published data (green nodes). Also shown in green are the second messengers calcium (Ca^{2+}), diacylglycerol (DAG) and phosphatidylinositol (3,4,5)-trisphosphate (PIP3). Another eight proteins could be detected in cortical or other neurons (grey) with no information available regarding their hippocampal expression. Neuronal localization of 18 proteins has not been published so far. However, seven of these can be found in either one of the databases with expression in neurons (grey stripes).

The TCR complex is shown with green stripes. It comprises several proteins of which some are expressed in neurons. Therefore, a detailed overview is given in figure 6 with an explanation of the abbreviations in table 2. Neither the α - nor the β -chain of the TCR can be found in neurons. Syken and Shatz (2003) report findings of TCR β mRNA, but no evidence of respective proteins. Subunits of the T-cell surface glycoprotein CD3 can be detected in neurons. The γ -, δ -, and ϵ -chain are found in cerebellar granule neurons (nodes shown in grey). However, little is known about their functions there (Nakamura *et al.*, 2007). On the contrary, the CD3 ζ chain has been described in hippocampal pyramidal cells and its functional characterization in neurons has yielded interesting links toward NMDA receptor signaling. This study will complement and extend already published data on neuronal CD3 ζ .

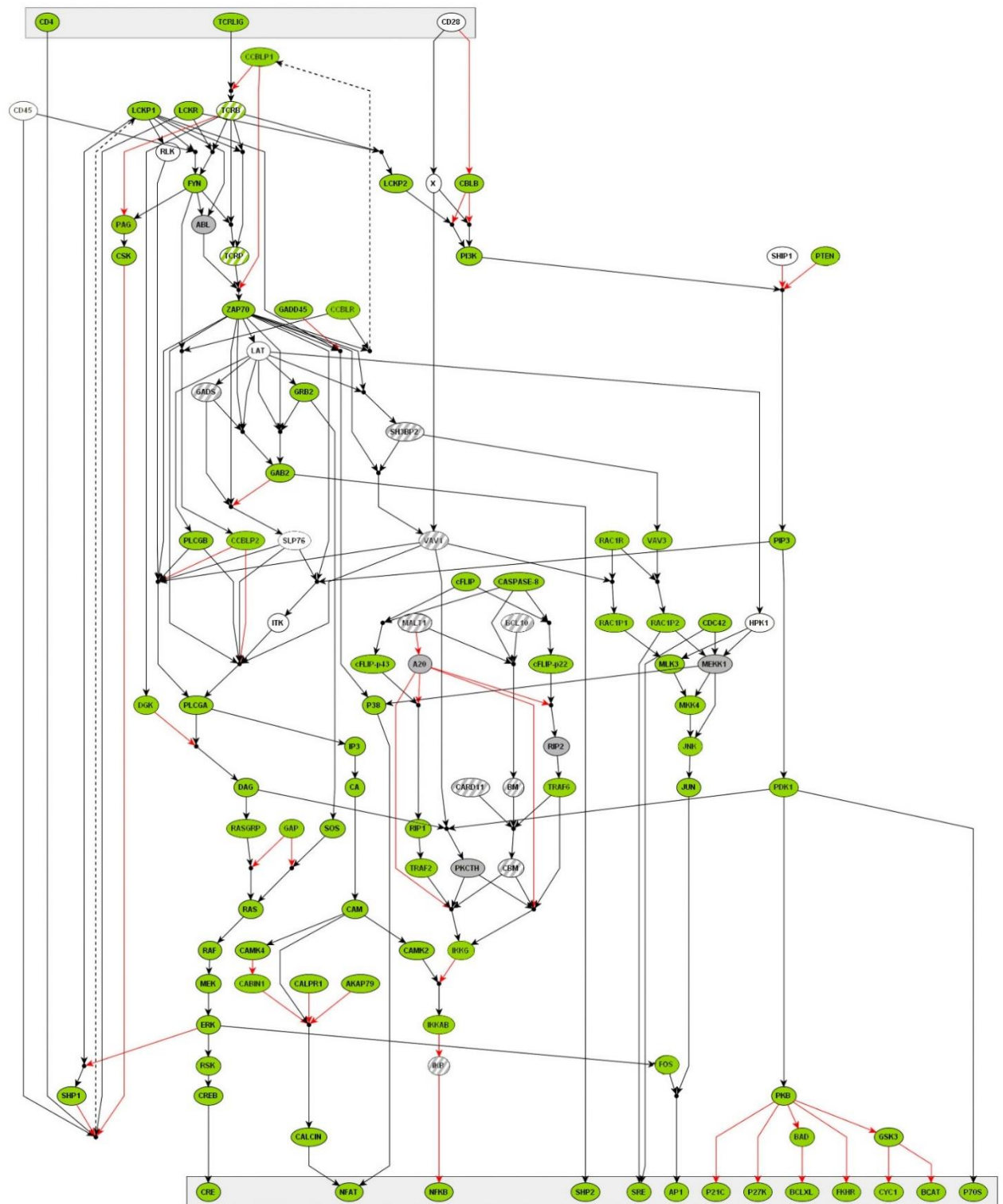


Figure 5: Scheme of TCR signaling components and their expression in neurons. Nodes represent proteins or second messengers connected by black (activation) or red (inhibition) arrows. The Boolean operation “and” is depicted as a dot implying the concerted action of connected proteins to activate or inhibit further signaling. Arrowheads pointing directly at a node stand for “or” connections that allow for alternative upstream pathways to regulate the respective species. Green-colored proteins are expressed in hippocampal neurons and grey ones in cortical neurons according to published data. Information on grey-striped nodes regarding their neuronal expression could only be found in databases. For white proteins, there are no data about neuronal expression available. The TCR complex is depicted in green stripes and shown in detail in figure 2. Full protein names can be found in table 1.

Table 1: Full protein names for nodes in TCR signaling network shown in figure 1.

Abbreviation	Full Name	Abbreviation	Full Name
A20	TNF α -induced protein 3	CRE	cAMP responsive element
ABL	Tyr-protein kinase ABL1	CREB	CRE-binding protein
AKAP79	A-Kinase Anchor protein 5	CSK	Tyr-protein kinase CSK
AP1	Transcription factor AP-1	CYC1	Cytochrome c1
BAD	Bcl2-associated agonist of cell death	DAG	Diacylglycerol
BCAT	Catenin β -1	DGK	Diacylglycerol kinase alpha
BCL10	B-cell lymphoma/leukemia 10	ERK1	MAPK 3
BCLXL	Bcl-2-like protein 1 (XL)	ERK2	MAPK 1
BM	BCL10-MALT1-Complex	FKHR	Forkhead box protein O1
Ca	Calcium	FOS	Proto-oncogene c-fos
CABIN1	Calcineurin-binding protein Cabin-1	FYN	Proto-oncogene tyrosine-protein kinase Fyn
CALCIN	Calcineurin	GAB2	GRB2-associated-binding protein 2
CALPR1	Calciressin-1	GADD45	Growth arrest and DNA-damage-inducible protein
CAM	Calmodulin	GADS	GRB2-related adapter protein 2
CAMK2	Ca ²⁺ /calmodulin-dependent protein kinase type II	GAP	GTPase activating proteins
CAMK4	Ca ²⁺ /calmodulin-dependent protein kinase type IV	GRB2	Growth factor receptor-bound protein 2
CARD11	Caspase recruitment domain-containing protein 11	GSK3	Glycogen synthase kinase-
CASPASE-8	Caspase-8	HPK1	MAPK kinase kinase 1
CBLB	E3 ubiquitin-protein ligase CBL-B	IKB	NF κ B inhibitor
CBM	CARD11-BM-Complex	IKKAB	Inhibitor of NF κ B kinase
CCBLP1	Phosphorylated CBL-C	IKKG	NF κ B essential modulator
CCBLP2	Phosphorylated CBL-C	IP3	Inositol-trisphosphate 3-kinase
CCBLR	E3 ubiquitin-protein ligase CBL-C	ITK	Tyr-protein kinase ITK
CD28	T-cell-specific surface glycoprotein CD28	JNK	MAPK 8
CD4	T-cell surface glycopr. CD4	JUN	Transcription factor jun
CD45	Receptor-type tyrosine-protein phosphatase C	LAT	Linker for activation of T-cells family member 1
CDC42	Cell division control protein 42 homolog	LCKP1	Phosphorylated LCK
cFLIP	CASP8 and FADD-like apoptosis regulator	LCKP2	Phosphorylated LCK
cFLIP-p22	Cleavage product of cFLIP	LCKR	Proto-oncogene tyrosine-protein kinase LCK

Abbreviation	Full Name	Abbreviation	Full Name
cFLIP-p43	Cleavage product of cFLIP	MALT1	Mucosa-associated lymphoid tissue lymphoma translocation protein 1
MEK	Dual specificity MAPK kinase 1	RAF	RAF proto-oncogene ser/thr-protein kinase
MEKK1	MAPK kinase kinase 1	RAS	GTPase HRas
MEK4	Dual specificity MAPK kinase 4	RASGRP	RAS guanyl-releasing protein 1
MLK3	MAPK kinase kinase 11	RIP1	Receptor-interacting ser/thr-protein kinase 1
NFAT	Nuclear factor of activated T-cells, cytoplasmic	RIP2	Receptor-interacting ser/thr-protein kinase 2
NFKB	Nuclear factor NF-kappa-B	RLK	TXK tyrosine kinase
P21C	Cyclin-dependent kinase inhibitor 1	RSK	Ribosomal protein S6 kinase alpha-1
P27K	Cyclin-dependent kinase inhibitor 1B	SH3BP2	SH3 Domain Binding Protein
P38	Mitogen-activated protein kinase 14	SHIP1	Phosphatidylinositol-3,4,5-trisphosphate 5-phosphatase 1
P70S	Ribosomal protein S6 kinase beta-1	SHP1	Tyr-protein phosphatase non-receptor type 6
PAG	Phosphoprotein associated with glycosphingolipid-enriched microdomains 1	SHP2	Tyr-protein phosphatase non-receptor type 11
PDK1	3-phosphoinositide-dependent protein kinase 1	SLP76	Lymphocyte cytosolic protein 2
PI3K	Phosphatidylinositol-4,5-bisphosphate 3-kinase	SOS	Son of sevenless homolog 1
PIP3	Phosphatidylinositol (3,4,5)-trisphosphate	SRE	Serum response Element
PKB	RAC- α ser/thr-protein kinase	TCRB	T-cell receptor complex
PKCTH	Protein kinase C theta type	TCRLIG	T-cell receptor ligand
PLCGA	Phospholipase C gamma 1	TCRP	Phosphorylated TCRB
PLCGB	Phospholipase C gamma 1 (Non-active form)	TRAF2	TNF receptor-associated factor 2
PTEN	PIP3-phosphatase and dual-specificity protein phosphatase PTEN	TRAF6	TNF receptor-associated factor 6
RAC1P1	Phosphorylated RAC	VAV1	Proto-oncogene vav
RAC1P2	Phosphorylated RAC	VAV3	Guanine nucleotide exchange factor VAV3
RAC1	Ras-related C3 botulinum toxin substrate 1	ZAP70	Tyrosine-protein kinase ZAP-70

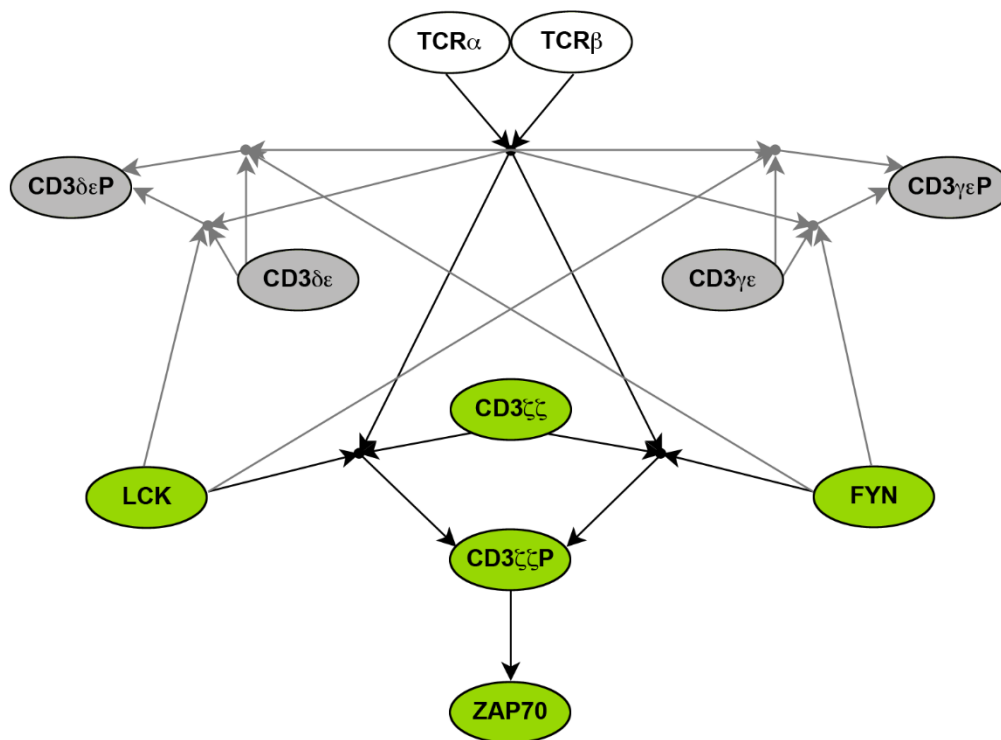


Figure 6: Detailed view of TCR complex signaling. Nodes represent proteins involved in initial TCR signaling color-coded for hippocampal (green) or cerebellar (grey) expression. The α - and β -chain of the TCR (white) cannot be found in neurons. For better visibility, signaling connected to the crucial TCR signaling subunit CD3 ζ is shown in black as opposed to grey for all other connections. Boolean operations apply as described above in figure 5.

Table 2: Full protein names for nodes in TCR complex signaling shown in figure 6.

Abbreviation	Full Name
CD3 $\gamma\epsilon$	T-cell surface glycoprotein CD3 gamma/epsilon chain dimer
CD3 $\gamma\epsilon$ P	Phosphorylated T-cell surface glycoprotein CD3 gamma/epsilon chain dimer
CD3 $\delta\epsilon$	T-cell surface glycoprotein CD3 delta/epsilon chain dimer
CD3 $\delta\epsilon$ P	Phosphorylated T-cell surface glycoprotein CD3 delta/epsilon chain dimer
CD3 $\zeta\zeta$	T-cell surface glycoprotein CD3 zeta chain dimer
CD3 $\zeta\zeta$ P	Phosphorylated T-cell surface glycoprotein CD3 zeta chain dimer
FYN	Proto-oncogene tyrosine-protein kinase Fyn
LCK	Proto-oncogene tyrosine-protein kinase LCK
TCR α	T-cell receptor alpha chain
TCR β	T-cell receptor beta chain
ZAP70	Tyrosine-protein kinase ZAP-70

3.2 Characterization of CD3 ζ in the Brain

3.2.1 CD3 ζ mRNA is found in Hippocampus and Cortex of Young and Adult Rats

To initiate our studies, I aimed at showing the existence of CD3 ζ mRNA in the brain of both adult (P56) and young (P5) rats. To that end, the animals were perfused with a saline solution to avoid contamination of tissue samples with hematopoietic cells. Total RNA was isolated from hippocampus, cortex, and spleen and then subjected to reverse transcription PCR (RT-PCR). The resulting cDNA was used as a template for quantitative PCRs either amplifying CD3 ζ or GAPDH as a control. cDNA from spleen served as a positive control for CD3 ζ expression (Baudouin *et al.*, 2008).

CD3 ζ mRNA can be detected in both hippocampus and cortex of young and adult rats as shown in figure 7. The expression levels in young animals were lower than in older animals. Further data are needed to confirm this impression.

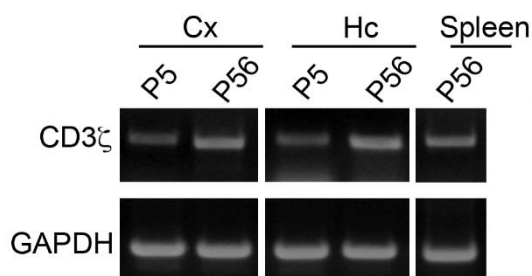


Figure 7: CD3 ζ transcripts in rat brain. CD3 ζ cDNA can be amplified from both young (P5) and adult (P56) rat hippocampus and cortex. cDNA from spleen was taken as a positive control for CD3 ζ . Amplification of GAPDH served as a loading control. Image is representative for three independent experiments.

3.2.2 CD3 ζ Localization at Different Developmental Stages of Hippocampal Neurons

Next, I examined the localization pattern of CD3 ζ protein in cultured hippocampal neurons at different developmental stages – days *in vitro* (DIV) 2, 7, 11, and 21. After fixation, neurons were stained with an anti-CD3 ζ antibody as well as with antibodies directed against cytoskeletal marker proteins such as actin, MAP2 or β III-tubulin. In mature neurons, synaptic formations were labeled with the postsynaptic marker homer or the presynaptic marker bassoon.

CD3 ζ can be detected in hippocampal neurons at all investigated stages with differences in localization though. At DIV2, CD3 ζ and actin immunofluorescences are overlapping at the axonal growth cone and at dendritic tips (figure 8). The latter localization of CD3 ζ can still be observed at DIV7 when visualizing the somatodendritic compartment with MAP2. Around the time point of synaptogenesis (DIV11) (Ziv *et al.*, 1996), CD3 ζ colocalizes with homer positive puncta and can no longer be detected at dendritic ends. This is also true for CD3 ζ localization in mature neurons at DIV21 (figure 9). To exclude presynaptic localization of CD3 ζ , a staining with bassoon was performed. CD3 ζ fluorescence hardly showed any overlapping with bassoon fluorescence. Thus, I concluded that CD3 ζ localization is mainly postsynaptic.

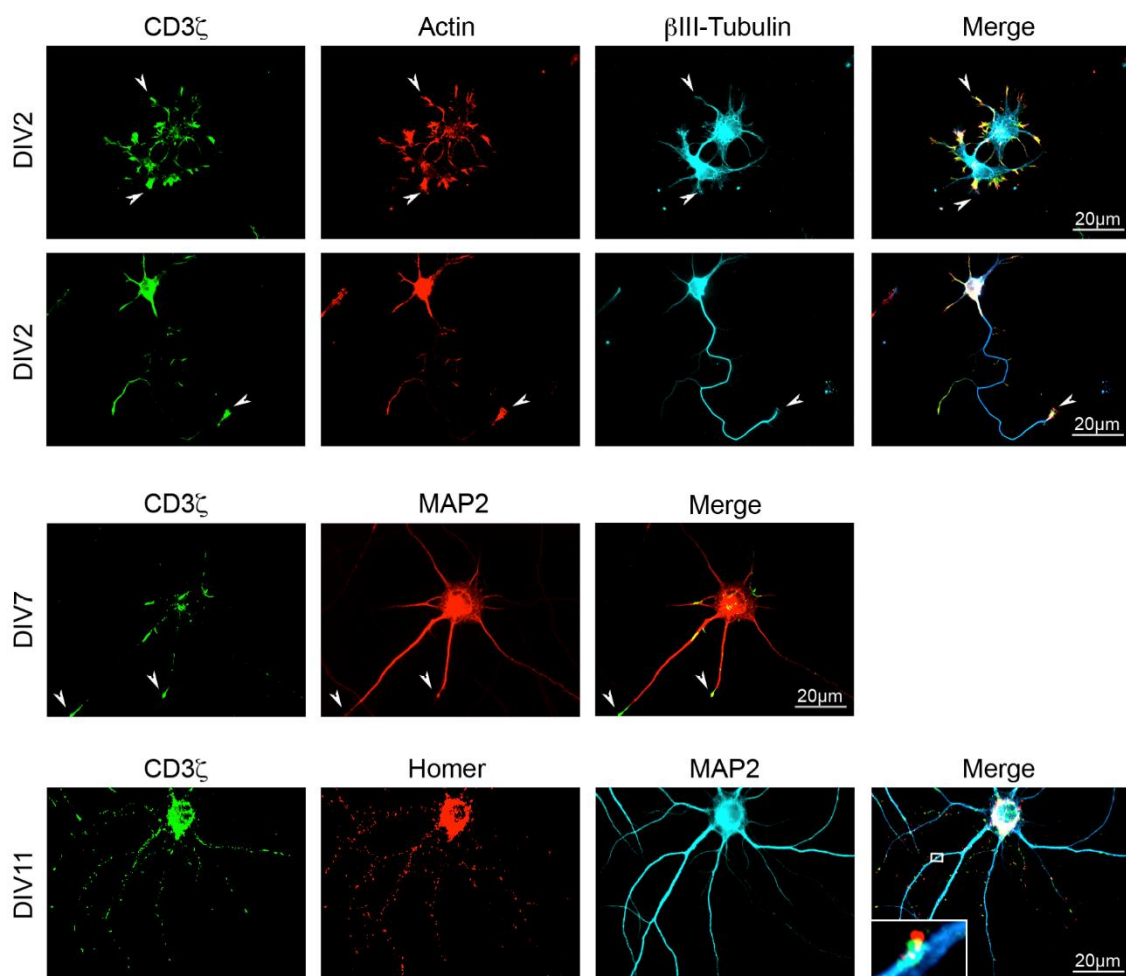


Figure 8: Localization of CD3 ζ in hippocampal neurons at different developmental stages. Cultures were fixed prior to immunofluorescent labeling of indicated proteins. At DIV2 CD3 ζ is detected at dendritic and axonal growth cones. The latter localization vanishes over time with labeling of dendritic tips left at DIV7. CD3 ζ moves to homer positive synaptic puncta around the time point of synaptogenesis (DIV11).

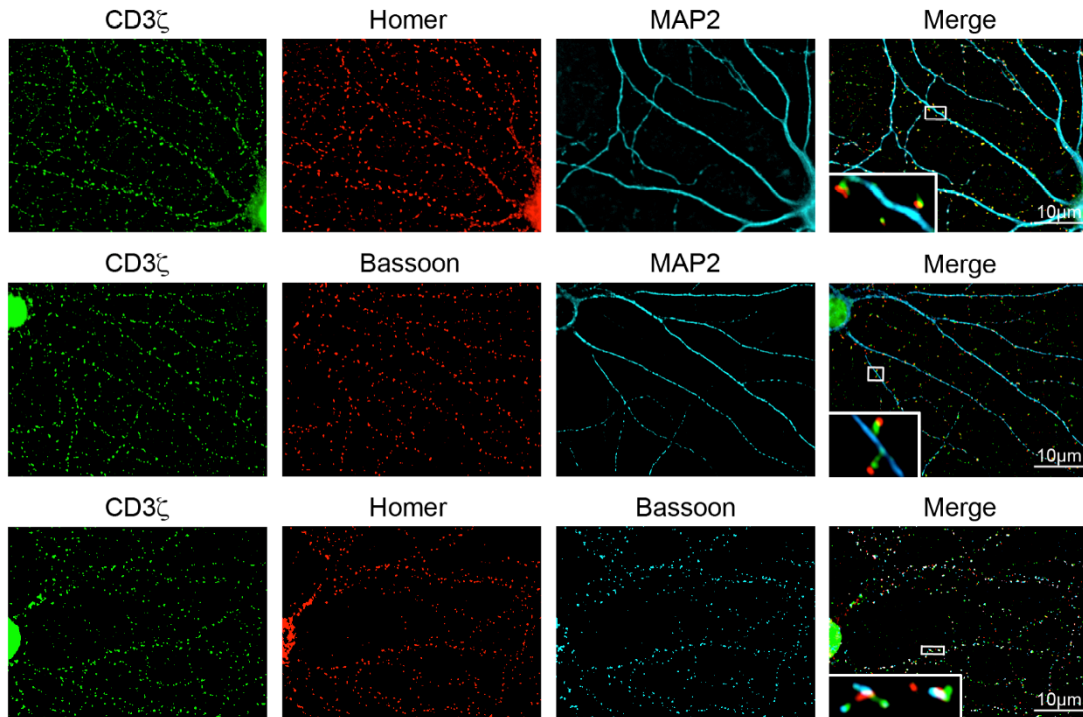


Figure 9: Postsynaptic localization of CD3 ζ in mature hippocampal neurons. Cultures were fixed prior to immunofluorescent labeling of indicated proteins. At DIV21, CD3 ζ immunofluorescence shows a partial overlap with homer-positive postsynaptic puncta, but hardly any colocalization with bassoon-positive presynapses leading to the assumption of a postsynaptic localization of the protein.

3.2.3 CD3 ζ is Abundant in Rat Brain Fractions

To further elucidate the localization of CD3 ζ , subcellular fractions of adult rat forebrain were prepared using a sucrose gradient centrifugation approach. The samples were then probed on Western Blot with an anti-CD3 ζ antibody and compared to a spleen membrane fraction control. Equal amounts (60 μ g) of each fraction were loaded (figure 10).

In spleen control the antibody detects a single band at approximately 25kDa as expected for CD3 ζ (Sakaguchi *et al.*, 2003). This band can also be found in brain homogenate (Hom), the membrane fraction (P2), the cytosolic fraction (S2) as well as in synaptosomes (Syn) and detergent resistant membranes (DRM) derived from P2. However, all brain samples also reveal yet uncharacterized bands at 30kDa, 50kDa, and with the exception of DRM at 75kDa. The existence of stable dimer formations of CD3 ζ , explaining the signal at 50kDa, is conceivable pending further investigation.

Another possible explanation is a certain unspecificity of the antibody in neurons. Therefore, we aimed at raising new antisera against different CD3 ζ epitopes to confirm our previous observations.

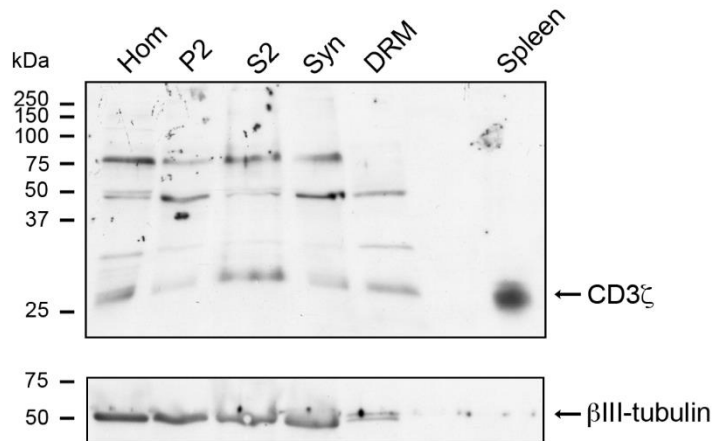


Figure 10: Subcellular fractionation of adult rat forebrain. CD3 ζ can be detected at 25kDa in homogenate (Hom), membrane (P2) and cytosolic (S2) fraction as well as in synaptosomes (Syn) and detergent resistant membranes (DRM) derived from P2. Spleen membrane fraction serves as a positive control. Bands at 30kDa, 50kDa and 75kDa are of unknown origin. Equal amounts (60 μ g) of each fraction were loaded.

3.3 Generation of Tools to Characterize CD3 ζ in Neurons

3.3.1 Generation of Antisera against CD3 ζ

Specific antisera are an important tool to characterize a protein regarding its biochemical and cellular properties. Polyclonal antisera were raised in either rabbits or guinea pigs by immunizing the animals with peptides with sequences corresponding to previously selected CD3 ζ epitopes (see figure 11). Both the extracellular and the transmembrane epitope are frequently used in commercial CD3 ζ antibodies (Santa Cruz Biotechnology sc-1239, Alexis Biochemicals ALX-210-828). The two intracellular epitopes (IC1 and IC2) were chosen according to their proteomic properties such as accessibility and the lack of putative posttranslational modifications.

All antisera were tested on Western Blot to recognize a CD3 ζ TAP fusion protein and in immunofluorescent stainings to detect overexpressed CD3 ζ GFP in COS7 cells. CD3 ζ TAP was overexpressed in HEK293T cells. Total cell lysate was then used for immunoblot analysis. For immunofluorescent stainings, COS7 cell were transfected

with CD3 ζ GFP and fixed 24 hours later. All antisera, except anti-CD3 ζ -TM, recognized both the adequate band at 25 kDa on Western Blot and the overexpressed fusion protein, but not GFP alone in COS7 cells (figure 12, data for anti-CD3 ζ -TM not shown). The functional antisera were subjected to affinity purification using CD3 ζ TAP purified via an anti-FLAG M2 column (Gloeckner *et al.*, 2007).

Purified antisera produced much weaker bands of CD3 ζ TAP on Western Blot compared to native antisera (figure 12 A). They also lost the ability to detect overexpressed CD3 ζ GFP in COS7 cells (figure 12 E). Neither the native nor the purified antisera were able to recognize endogenous CD3 ζ from a spleen membrane fraction where a band of 25kDa would be expected as detected by a commercial anti-CD3 ζ antibody. Anti-CD3 ζ -IC1 and IC2 show a band at approximately 20kDa of unknown origin (figure 12 B). The antisera were also not able to detect endogenous CD3 ζ in cultured hippocampal neurons (data not shown). While commercial antibodies showed stainings comparable to the ones presented in figure 12, signals obtained by antisera application did not exceed background levels.

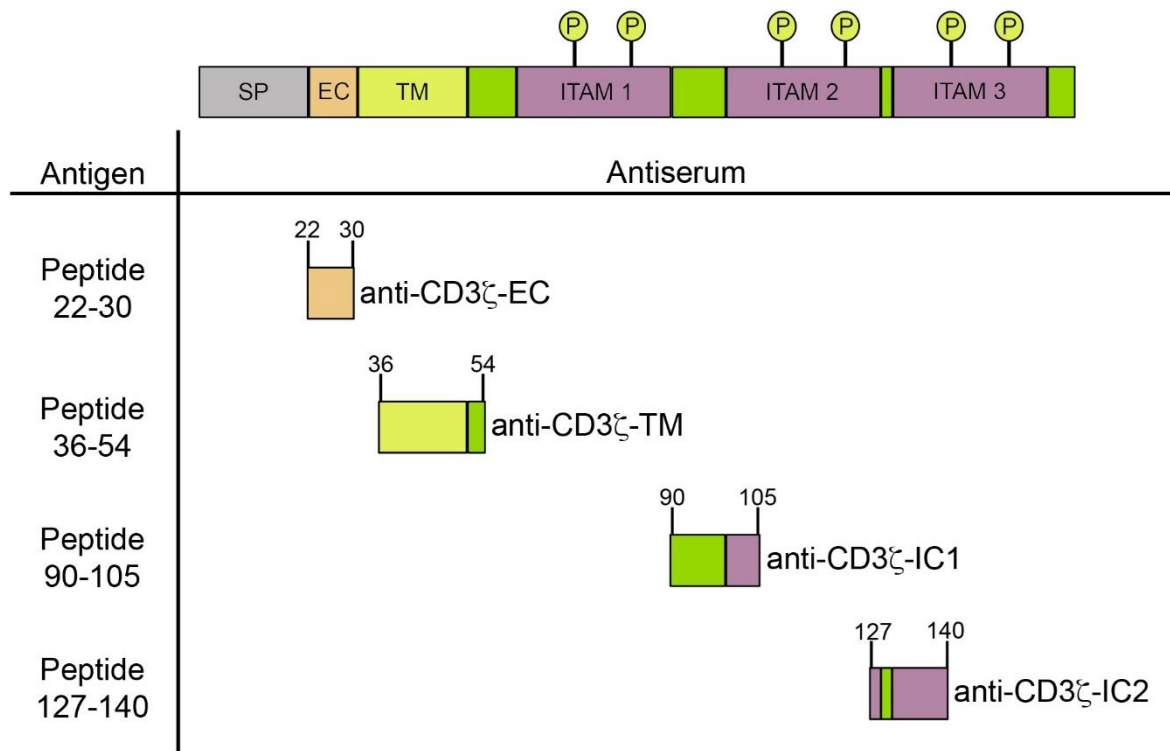


Figure 11: Overview over the antigen epitopes and the names of the corresponding CD3 ζ antisera. Anti-CD3 ζ -EC and IC2 were raised in guinea pigs, anti-CD3 ζ -TM and IC1 in rabbits.

These results suggest an insufficient elution of the antibodies from the nitrocellulose membrane. Indeed, probing the blot pieces used for purification on Western Blot revealed pronounced bands corresponding to light and heavy chains of antibodies (data not shown) indicating incomplete elution from the nitrocellulose membrane. The lack of a suitable antibody to further characterize CD3 ζ in neurons led to an alternative strategy: the generation of CD3 ζ mutants to extend our toolbox and assess functional properties of CD3 ζ in neurons.

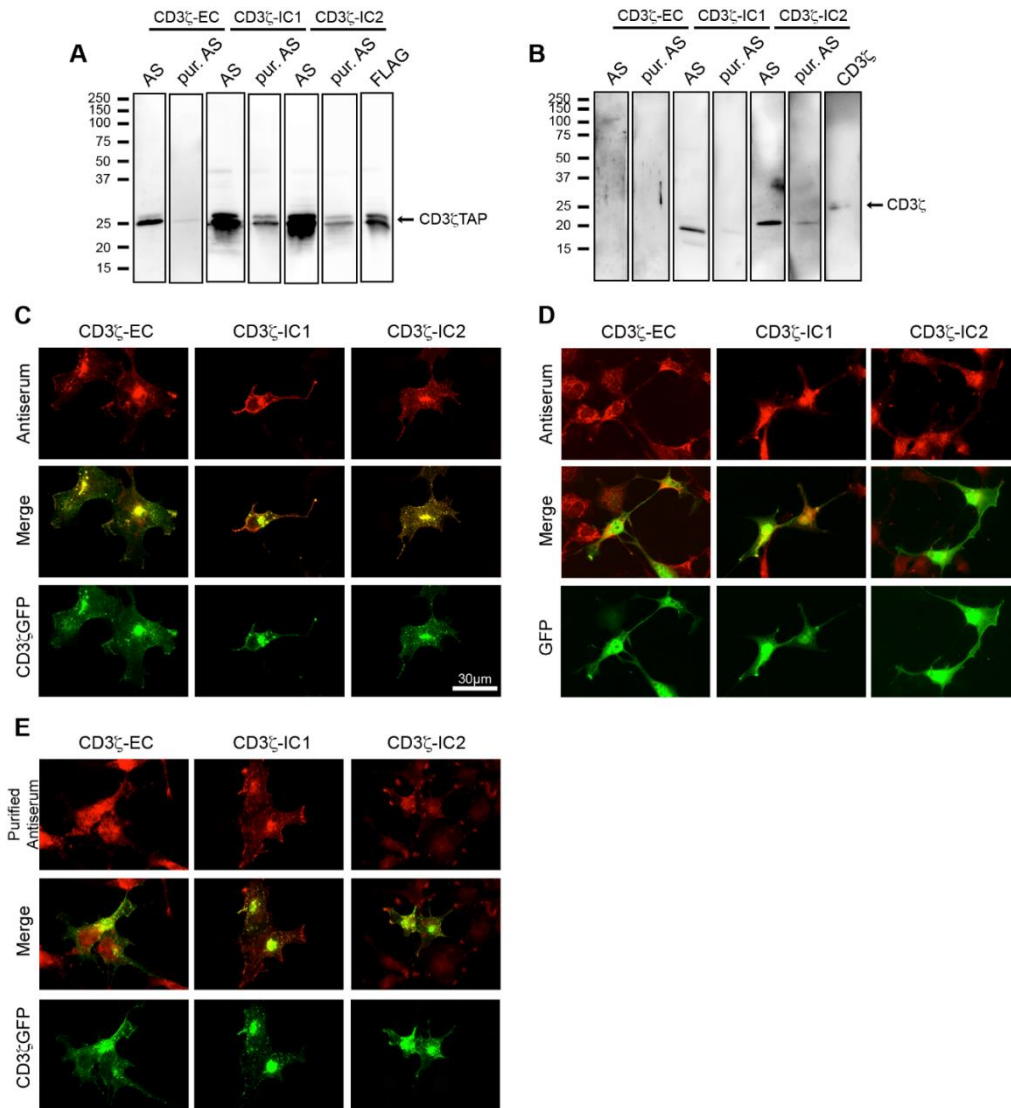


Figure 12: Characterization and specificity of antisera. (A) Antisera (AS) and CD3 ζ TAP affinity purified antisera (pur. AS) were tested on immunoblots with a CD3 ζ TAP fusion protein overexpressed in HEK cells. Equal amounts of total cell lysate were loaded. Detection with an anti-FLAG M2 antibody served as positive control. (B) Antisera and CD3 ζ TAP affinity purified antisera were tested on immunoblots with a spleen membrane fraction (30 μ g loaded). Detection of CD3 ζ with a commercial anti-CD3 ζ antibody (Santa Cruz) served as positive control. (C) and (D) COS7 cells overexpressing CD3 ζ GFP (C) or GFP as a control (D) were stained with antisera. Antisera recognize the CD3 ζ GFP fusion protein, but not GFP alone. (E) Purified antisera were applied to detect CD3 ζ GFP overexpressed in COS7 cells. Lack of overlapping (yellow) immunofluorescence indicates that the purified antisera do not recognize the fusion protein.

3.3.2 Generation and Characterization of Two CD3 ζ Mutants

To elucidate functional properties of CD3 ζ in neurons, we generated two different mutants as GFP fusion proteins. In the sequence of CD3 ζ -6YF, tyrosine residues within the three ITAM's Y72, Y83, Y111, Y123, Y142, and Y153 were exchanged for phenylalanine to prevent phosphorylation and subsequent signaling. This mutant has previously been described as a loss-of-function mutant in the literature (Baudouin *et*

al., 2008). For the second mutant, I replaced the aspartate residue at position 36 by alanine (D36A). This mutation alters the properties of the transmembrane region subsequently preventing the formation of the TCR complex in T cells (Rutledge *et al.*, 1992; Call *et al.*, 2002). An overview of both mutants is given in figure 13.

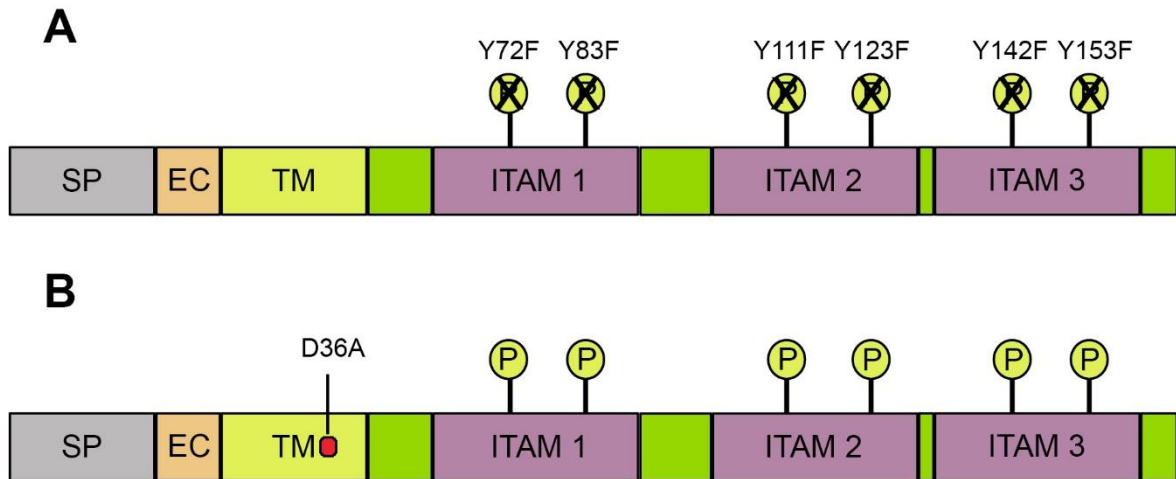


Figure 13: Overview over both CD3 ζ mutants. (A) For the CD3 ζ -6YF mutant, all tyrosine residues within the ITAM's were replaced by phenylalanine to prevent phosphorylation at these amino acid residues. **(B)** In the CD3 ζ -D36A, the aspartate residues within the transmembrane domain was exchanged for alanine.

3.3.3 CD3 ζ Fusion Protein and its Mutants Form Dimers

Dimer formation is an essential part for CD3 ζ functionality (Wange and Samelson, 1996). Therefore, we assessed the ability of both mutants to interact with TAP-tagged wild type (wt) CD3 ζ by means of immunoprecipitation (IP). CD3 ζ TAP, CD3 ζ GFP, CD3 ζ -6YF-GFP, CD3 ζ -D36A-GFP, and GFP as a control were overexpressed in HEK cells. Total cell lysates were then incubated with anti-GFP tagged magnetic beads. Bound proteins were eluted with SDS sample buffer. Cell lysates and eluates were subjected to immunoblotting (figure 14).

Probing the blot with an anti-GFP antibody reveals bands at 25kDa for GFP in both lysate and IP fraction. Bands at 50kDa present the GFP-tagged mutants demonstrating equal motility properties in SDS polyacrylamide gels. The 37kDa

bands in the eluate might be due to protein degradation. As the TAP tag contains the FLAG sequence, an anti-FLAG M2 antibody was used to examine the presence of CD3 ζ TAP. Equally strong bands at around 25kDa in the lysate of all samples indicate a similar expression level of the protein. The double band is most likely due to the existence of phosphorylated and non-phosphorylated CD3 ζ TAP. Bands in the eluate fraction of wt CD3 ζ and both mutants prove the presence of coprecipitated CD3 ζ TAP implying dimer formation. The lack of a band in the GFP control confirms the specificity of the interaction. The IP fraction of the D36A sample also shows a striking double band at around 60-70kDa probably presenting the dimer of CD3 ζ TAP and CD3 ζ -D36A-GFP. Quantitative analysis of the experiments shows no significant difference in the ability to form dimers between wt CD3 ζ and either one of the mutants indicating the possibility of the mutants to participate in interactions with other proteins and to fulfill basic functional requirements.

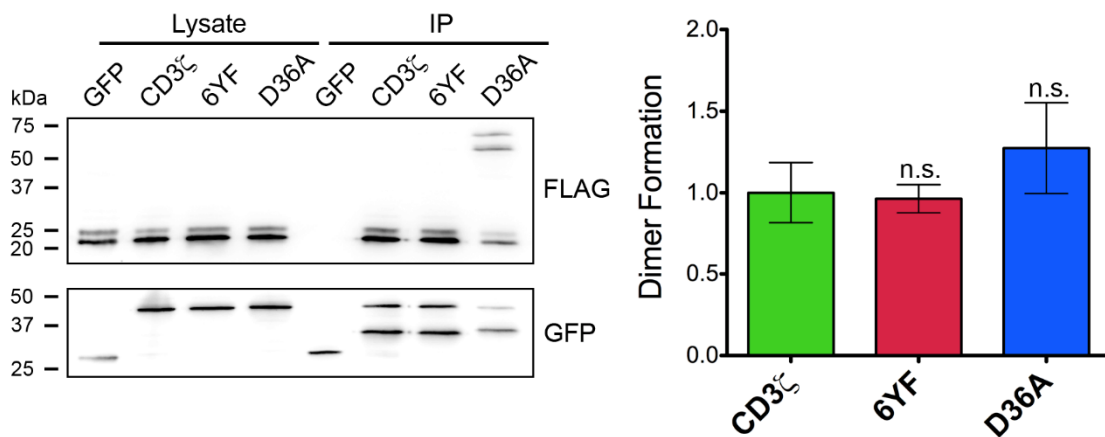


Figure 14: Dimerization of CD3 ζ mutants compared to wt CD3 ζ . GFP fusion proteins including CD3 ζ wt and mutants were overexpressed in HEK cells together with wt CD3 ζ TAP. Total cell lysates were subjected to immunoprecipitation with GFP-coupled magnetic beads. Western Blots were probed with an anti-GFP and an anti-FLAG M2 antibody. Optic density of the bands was measured using Quantity One. Statistical analysis of three independent experiments (One-way ANOVA) resulted in no significant difference between the means ($p>0.05$). Error bars present the SEM.

3.3.4 Phosphorylation of CD3 ζ -D36A-GFP is Reduced Compared to CD3 ζ GFP

In T cells, CD3 ζ signaling is initiated by its phosphorylation by the kinase Fyn (Wange and Samelson, 1996). As neurons also express a variety of src kinases including Fyn, the next experiment aims at evaluating the phosphorylation properties of CD3 ζ GFP

and the D36A mutant when overexpressed in cultured hippocampal neurons applying lentivirus at DIV3. Five days after transfection, cells were submitted to a 5-minute pervanadate treatment. Pervanadate blocks tyrosine phosphatases and prevents the dephosphorylation of proteins at these sites. The neurons were then harvested with SDS sample buffer and subjected to immunoblotting (figure 15).

Probing the blot membrane with an anti-GFP antibody reveals bands at around 50kDa in CD3 ζ wt as well as in both mutant samples. Whereas CD3 ζ -6YF-GFP is shown as a clear band, CD3 ζ GFP and CD3 ζ -D36A-GFP show a slight smear suggesting posttranslational modifications. The use of a pan phospho-tyrosine (pTyr) antibody confirms this observation. The pTyr antibody produces a very broad band in the CD3 ζ GFP sample; the band of the transmembrane mutant is rather weaker. The 6YF sample shows no band and therefore no tyrosine phosphorylation as expected. Statistical analysis reveals a significant difference in the phosphorylation properties. CD3 ζ -D36A-GFP phosphorylation is reduced by approximately 75% compared to CD3 ζ GFP meaning that the transmembrane mutant may not be able to transmit signals to a full extend.

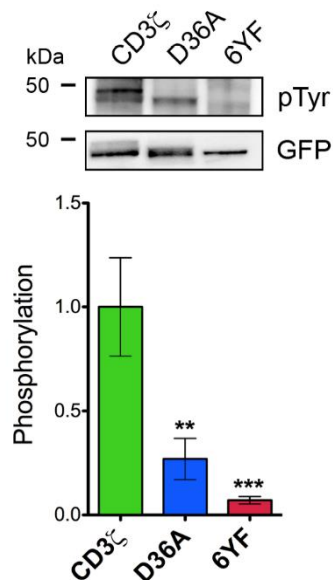


Figure 15: Phosphorylation of overexpressed CD3 ζ wt and mutants. GFP fusion proteins were overexpressed in cultured hippocampal neurons. Prior to harvesting at DIV8, cells were treated with pervanadate to inhibit tyrosine phosphatases. Immunoblots were probed with an anti-phosphotyrosine (pTyr) and an anti-GFP antibody. Optic density of the bands was measured using ImageJ. Statistical comparison of measurements using one-way ANOVA showed a clearly reduced phosphorylation of the D36A mutant ($p^{**}<0.01$, $p^{***}<0.0001$) in five different experiments. Signal in the 6YF lane can be considered background.

3.3.5 CD3 ζ Wildtype and its Mutants Localize Differently in COS7 Cells and in Neurons

A possible reason for the reduced phosphorylation of the D36A mutant might be improper localization resulting in limited accessibility for kinases. To investigate this, I transfected COS7 cells with CD3 ζ GFP, GFP, or either one of the mutants. Indeed, overexpressed CD3 ζ GFP and its mutants reveal different localization patterns when observed under the fluorescence microscope as can be seen in figure 16. GFP alone shows cytoplasmic expression, whereas CD3 ζ GFP and CD3 ζ -6YF-GFP localize to the membrane as well as to cell organelles – probably the Golgi apparatus, the endoplasmic reticulum, or transport vesicles as indicated by various small GFP-positive puncta. CD3 ζ -D36A-GFP, however, seems to accumulate within the Golgi apparatus resulting in an enlarged organelle visible as a large GFP-positive spot. There is very little membranous localization and fewer small puncta compared to CD3 ζ wt and the 6YF mutant confirming the aforementioned mislocalization phenotype of this mutant.

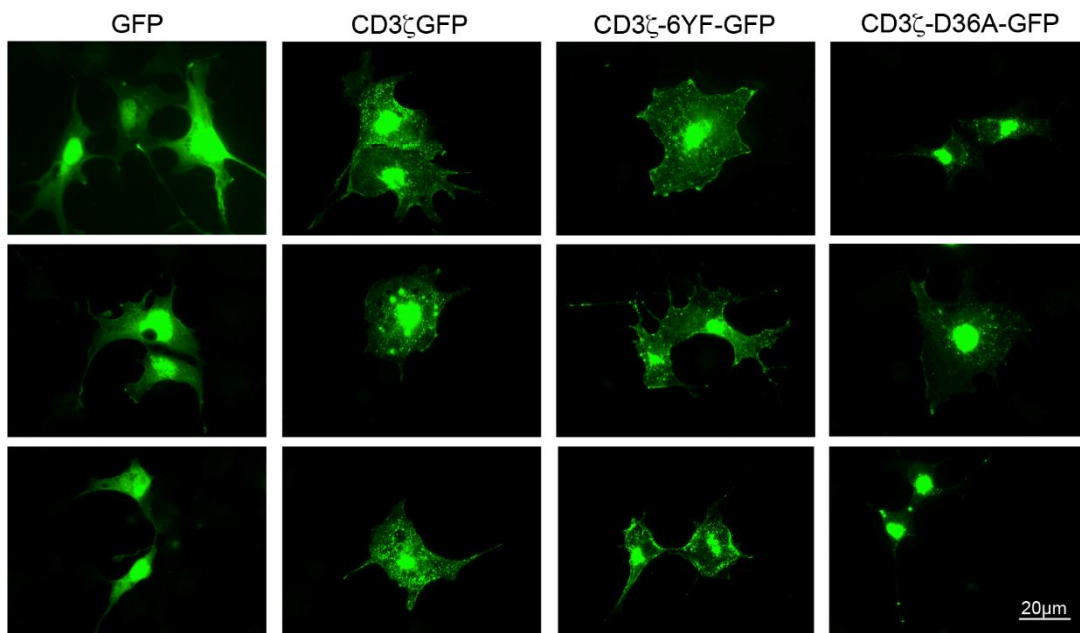


Figure 16: Localization of CD3 ζ and its mutants in COS7 cells. Cells were transfected and fixed 24 hours later. Whereas GFP shows a diffused pattern, both CD3 ζ GFP and CD3 ζ -6YF-GFP display localization at the membrane and in cell organelles. CD3 ζ -D36A-GFP fluorescence seems to be restricted to the Golgi apparatus with little to no surface expression. Images are representative for three independent experiments.

Next, I aimed at evaluating CD3 ζ distribution in neurons. Hippocampal cells were transfected at DIV7 and fixed six hours later. After a counterstaining with an anti-MAP2 antibody to visualize the cell soma and dendrites, images were taken with a fluorescence microscope. Figure 17 shows that GFP is again diffusely spread throughout the entire cell. The localization of wt CD3 ζ GFP is similar to endogenous CD3 ζ at DIV7 with large amounts of the protein visible at the dendritic tip as indicated by arrows (compare fig. 8). The 6YF mutant can be found more spread along the dendrite with a slight concentration at dendritic ends. The transmembrane mutant seems to spread throughout the dendrite showing a punctate distribution pattern. To quantify these observations, we compared the mean optical density of the dendritic tip (defined as the final 10 μ m of the branch) with the mean optical density/ μ m of the entire dendrite using ImageJ. The equal diffusion based distribution of GFP results in a ratio of around 1. The quotients of the 6YF and D36A mutant are marginally higher which is not statistically different compared to the GFP control though. The pronounced localization of wt CD3 ζ at dendritic ends can be confirmed by the quantitative analysis resulting in a more than threefold higher ratio than GFP control.

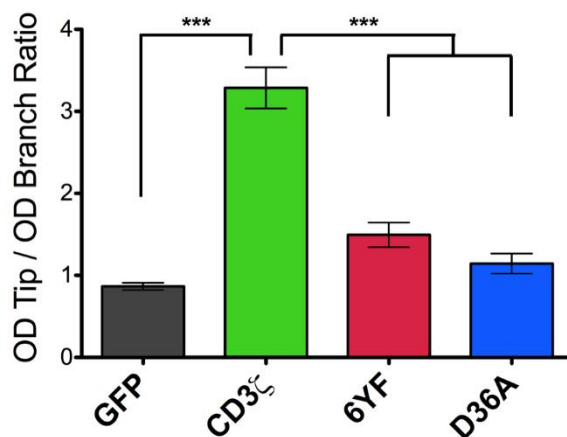
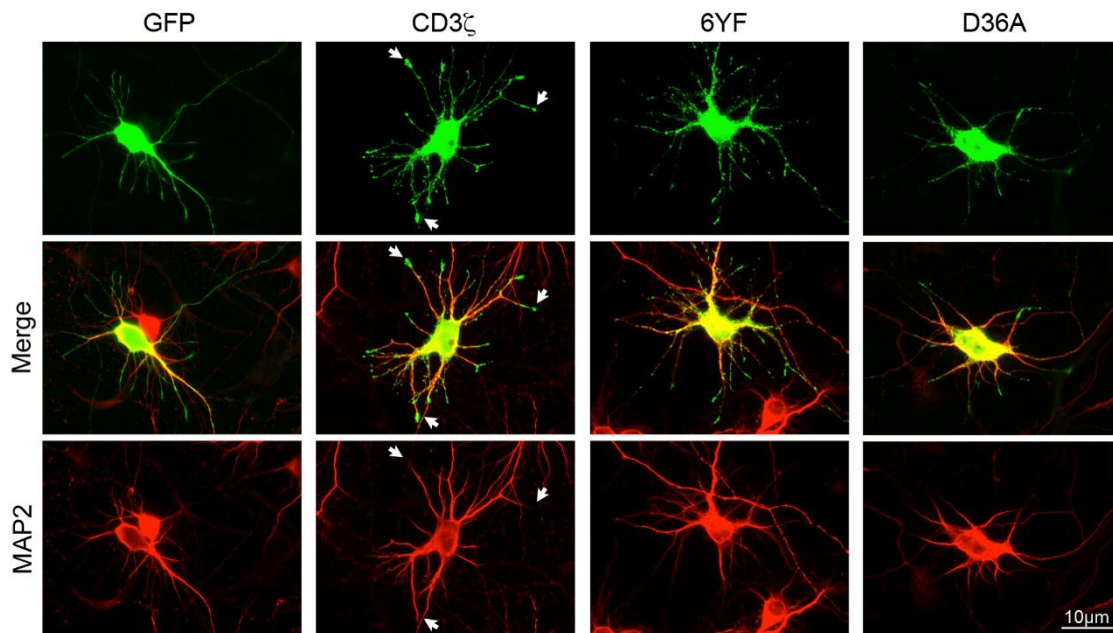


Figure 17: Distinct localization pattern of CD3 ζ GFP and its mutants in hippocampal neurons. Cells were transfected at DIV7 and fixed six hours later. After immunofluorescent labeling of the somatodendritic compartment with an anti-MAP2 antibody, images were acquired with a fluorescent microscope. Image analysis was done using ImageJ. CD3 ζ GFP immunofluorescence is pronounced at dendritic tips, whereas both mutants are more spread throughout the branch. Analysis of optic densities (OD) results in an increased OD tip to OD branch ratio for the wildtype protein compared to GFP and the mutants (One-way ANOVA, $p < 0.001$). Error bars present the SEM.

3.3.6 Cell Surface Expression of CD3 ζ GFP and its Mutants

Apart from the different distribution of the constructs, we also observed a seemingly reduced cell surface expression of CD3 ζ -D36A-GFP mutant in COS7 cells. To evaluate if this holds true in neurons, we overexpressed all CD3 ζ construct as GFP fusion proteins in hippocampal cells using lentiviral transfection at DIV 10. At DIV16, cells were subjected to cell surface biotinylation (Solé *et al.*, 2009; Kim and Kovacs, 2011).

After lysis, biotinylated proteins were isolated with a streptavidin matrix and eluted with SDS sample buffer. Cell lysate and eluate were analyzed by western blot employing an anti-GFP antibody to detect overexpressed proteins (figure 18). Comparably strong bands of CD3 ζ GFP in the lysate and eluate fraction indicate a high level of cell surface expression. The CD3 ζ -6YF-GFP signal in the eluate is weaker than in the lysate sample. The eluate of the CD3 ζ -D36A-GFP sample shows a hardly perceivable band despite high expression levels of the protein as conveyed by a strong signal in the total cell lysate. Quantitative analysis of reveals a significantly reduced cell surface expression of CD3 ζ -D36A-GFP compared to wt CD3 ζ confirming the observed differences in localization patterns of this mutant in both COS7 cells and neurons.

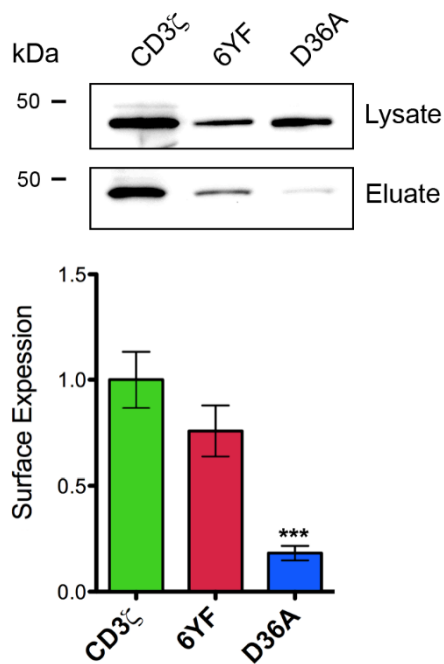


Figure 18: Cell surface expression of CD3 ζ GFP and its mutants in hippocampal neurons. Fusion proteins were overexpressed using lentiviral transfection. At DIV16, cell surface proteins were biotinylated and isolated using a streptavidin column after lysis. Total lysates and column eluates were subjected to immunoblot analysis employing an anti-GFP antibody. ODs were measured using ImageJ. OD ratio between eluates and lysates were analyzed using a one-way ANOVA revealing reduced surface expression CD3 ζ -D36A-GFP compared to CD3 ζ wt (six independent experiments, *** p <0.001). Error bars present the SEM.

3.3.7 CD3 ζ GFP Overexpression Reduces Dendrite Complexity

Previous publications have suggested a role for CD3 ζ in the regulation of dendritic branching (Baudouin *et al.*, 2008; Xu *et al.*, 2010). To further elucidate the functional influence of the phosphorylation and the localization phenotype, I performed Shall

Analysis on neurons overexpressing CD3 ζ GFP, GFP or either one of the mutants. DIV8 neurons were transfected and fixed nine hours later. Images were taken with a fluorescence microscope and analyzed using PhotoShop and ImageJ Sholl analysis. The number of intersections with the concentric circles was plotted against the distance from the soma resulting in a curve. The area under this curve was taken as a parameter to describe the complexity of the cells. As shown in figure 19, overexpression of CD3 ζ GFP clearly reduces dendritic branching compared to GFP control confirming published observations. Both mutants do not affect the dendritic arbor.

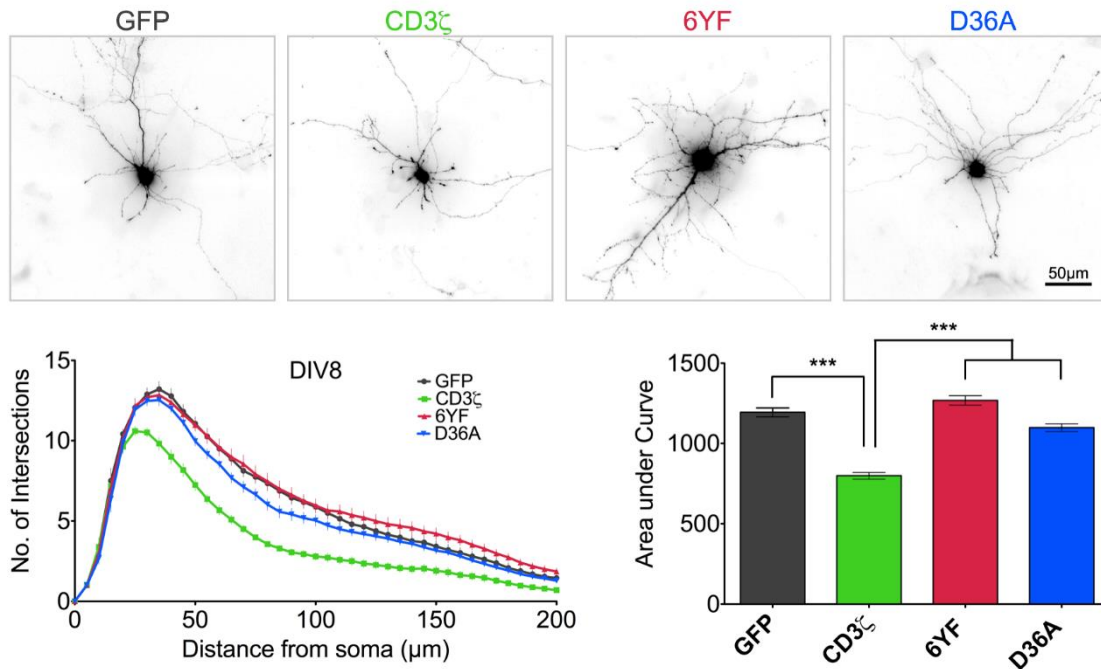


Figure 19: Overexpression of CD3 ζ GFP reduces dendritic complexity in DIV8 hippocampal neurons. Cells were transfected and fixed nine hours later. The number of intersections of a dendrite with concentric circles was plotted against the distance from the soma resulting in a curve. The area under the curve was taken as a parameter to describe dendrite complexity. Overexpression of CD3 ζ GFP leads to reduced branching, whereas neither of the mutants shows any effect on dendrite complexity (one-way ANOVA, *** p <0.001). Error bars present the SEM.

To verify this effect of CD3 ζ GFP, I aimed at knocking down the protein expecting increased neurite complexity. Four commercially available shRNA constructs were evaluated regarding their efficacy to decrease the levels of expressed CD3 ζ GFP in HEK 293T cells. Total cell lysates were subjected to immunoblot analysis. Levels of

CD3 ζ GFP were compared to an internal GAPDH control. As depicted in figure 20, shRNA 2 and 3 proved to be most efficient compared to scramble and vector controls and were chosen for use in neurons.

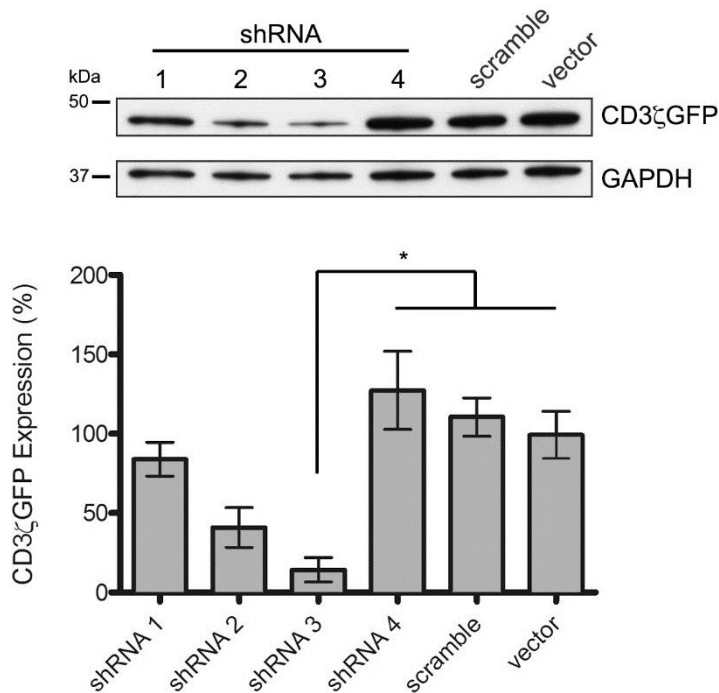


Figure 20: Efficacy of shRNAs. HEK293T cells were transfected with CD3 ζ GFP and either one of the shRNAs. Total cell lysates were subjected to immunoblot analysis and probed with an anti-GFP and an anti-GAPDH antibody. ShRNA 2 and shRNA 3 proved to be most effective in reducing CD3 ζ GFP expression. Signal intensity of each band was measured using ImageJ. The data are expressed as mean \pm SEM from three independent experiments (* p <0.05).

Hippocampal cells were transfected with shRNA 2, shRNA 3, scramble or vector control at DIV8 and fixed 24 hours later. Images were acquired with a fluorescence microscope and analyzed using PhotoShop and ImageJ Sholl analysis. Only shRNA 3 transfected cells showed a significantly increased area under curve indicating more complex branching compared to vector control (fig. 21). This verifies the role of CD3 ζ in the regulation of neuronal cytoarchitecture which will be examined in detail in the next sections. Complexity of both shRNA 2 and scramble control transfected neurons is not statistically different from vector control.

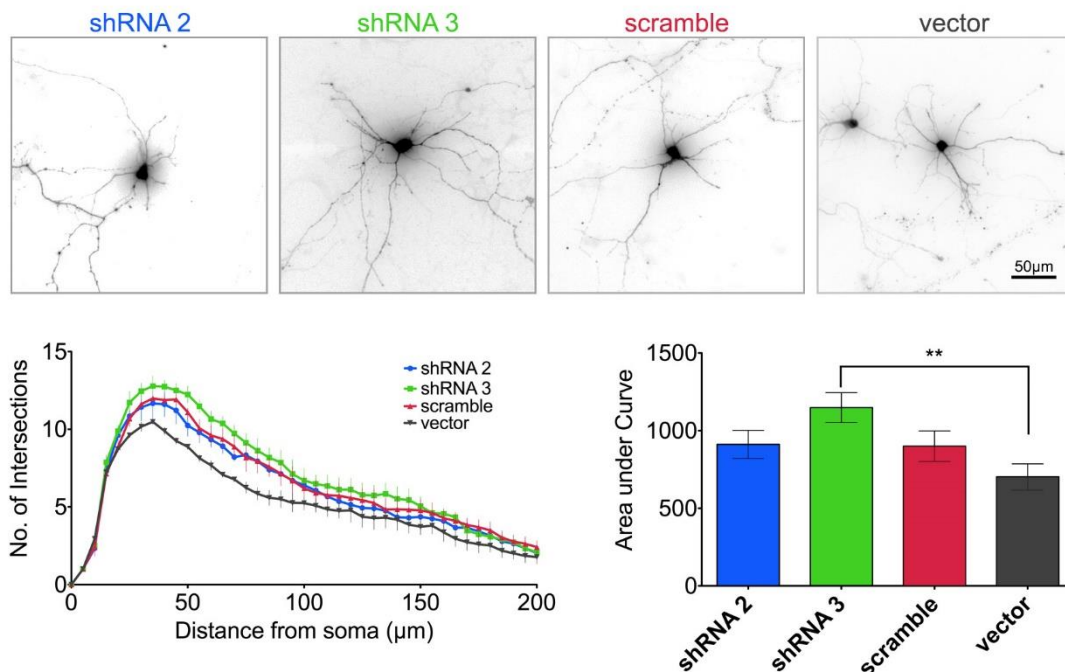


Figure 21: Knockdown of endogenous CD3 ζ increases dendrite complexity. Hippocampal neurons were transfected at DIV8 and fixed 24 hours later. Image analysis was done employing ImageJ Sholl analysis. Quantification of Sholl analysis data reveals shRNA 3 to be most effective (three experiments, one-way ANOVA, ** $p < 0.01$).

3.3.8 Involvement of CD3 ζ in Actin and Microtubule Regulation

The neuronal cytoskeleton consists of three major components: actin-based microfilaments, neurofilament-based intermediate filaments, and tubulin-based microtubules (Lee and Cleveland, 1996; Kapitein and Hoogenraad, 2011). The first and the latter have a major impact on dendrite outgrowth and stabilization. Thus, in a next step, I analyzed how CD3 ζ and its mutants influence proteins involved in actin or microtubule regulation. Microtubules consist of α -/ β -tubulin dimers (Singh *et al.*, 2008). A change in the ratio of those two proteins would indicate a modification of microtubules regarding their cytoskeleton or transportation function. Influences on actin can be monitored by analyzing the amount of phosphorylated cofilin. As an actin-binding factor, cofilin depolymerizes actin filaments and thereby regulates cytoskeletal reorganization. Phosphorylation of cofilin inactivates the protein (Okamoto *et al.*, 2009).

Developing hippocampal neurons (DIV8) overexpressing CD3 ζ GFP or either one of the mutants after lentiviral transfection were subjected to immunoblot analysis. Samples were probed for α - and β -tubulin or cofilin and phosphorylated cofilin. As shown in figure 22, measurement of signal intensities with ImageJ does not show any change in α -/ β -tubulin levels. However, a strong decrease in cofilin phosphorylation can be observed in CD3 ζ GFP and both mutant samples compared to GFP control indicating an influence on actin cytoskeleton regulation.

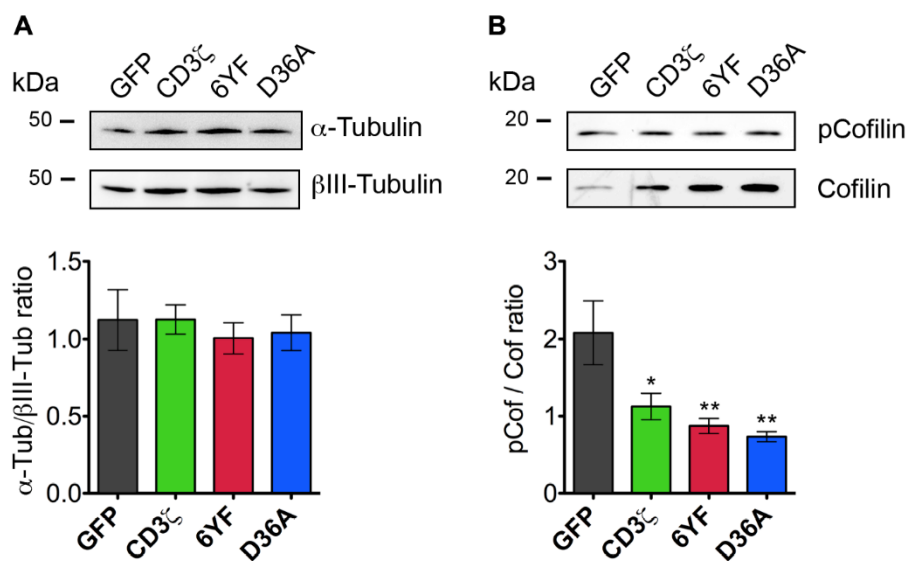


Figure 22: Influence of CD3 ζ on neuronal cytoskeleton. Hippocampal neurons (DIV8) overexpressing CD3 ζ GFP, its mutants or GFP were analyzed on immunoblots probed for α -/ β -tubulin or phosphorylated (p)cofilin and cofilin. Optic density of bands was measured using ImageJ. Samples were compared to GFP control. The data are expressed as mean \pm SEM from six different experiments (one-way ANOVA, * p <0.05, ** p <0.01, *** p <0.001)

3.3.9 Effect of CD3 ζ and its Mutants on Mature Hippocampal Neurons

Cytoskeletal changes do not only occur in developing but also in mature neurons (Kaech *et al.*, 2001). Synaptic structures highly depend on actin dynamics (Chen *et al.*, 2007; Cingolani and Goda, 2008). As shown before (fig. 9), CD3 ζ is located at the postsynapse. Therefore, it is conceivable that CD3 ζ does not only regulate dendritic complexity, but also synaptic architecture in mature neurons. Thus, I examined dendrite complexity and synapse properties in DIV16 hippocampal neurons again using lentiviral transfection at DIV10 to overexpress CD3 ζ GFP, its mutants, and GFP as a control.

To assess dendritic branching, cells were stained with anti-MAP2 antibody after fixation. Images were acquired with a fluorescence microscope using a 10x objective and 1.6x digital zoom. Sholl analysis was performed as described previously. As shown in figure 23, CD3 ζ GFP does not have any effect on the dendritic arbor in mature neurons, nor does the D36A mutant. However, CD3 ζ -6YF-GFP overexpression leads to an increase in dendrite complexity compared to the other samples indicating that correct CD3 ζ functioning still plays a role in mature neurons.

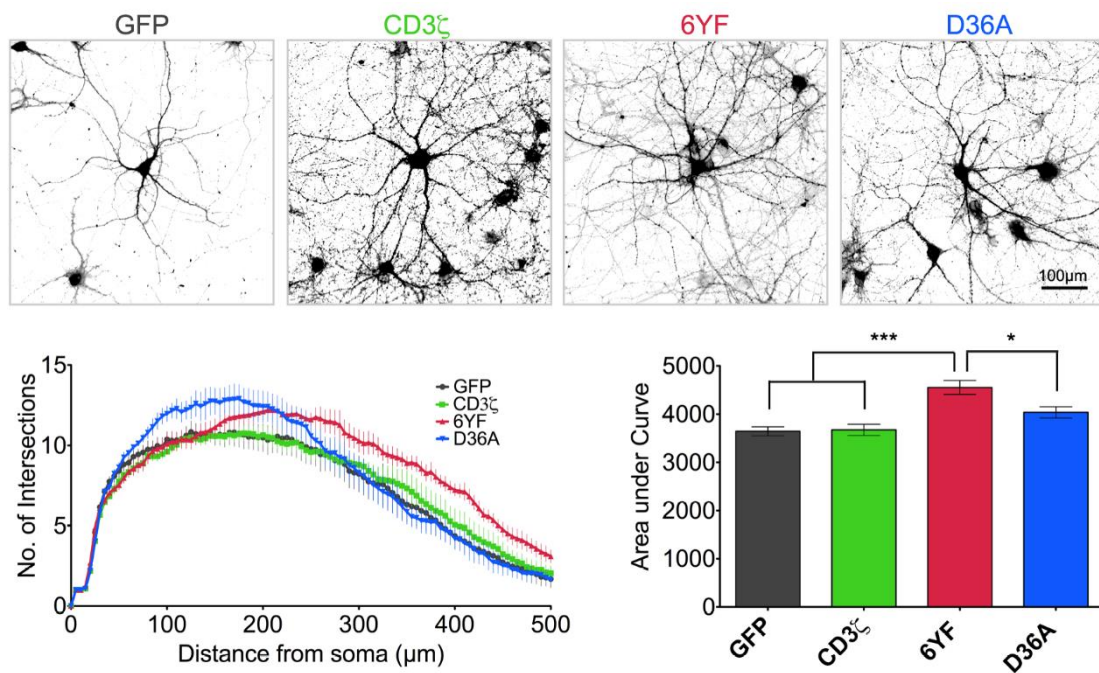


Figure 23: CD3 ζ -6YF-GFP increases dendrite complexity in mature hippocampal neurons. Cells overexpressing CD3 ζ GFP, its mutants or GFP were fixed on DIV16. Sholl analysis was done applying ImageJ software. Data from four independent experiments were subjected to one-way ANOVA (* p <0.05, *** p <0.001). Data are shown as mean \pm SEM.

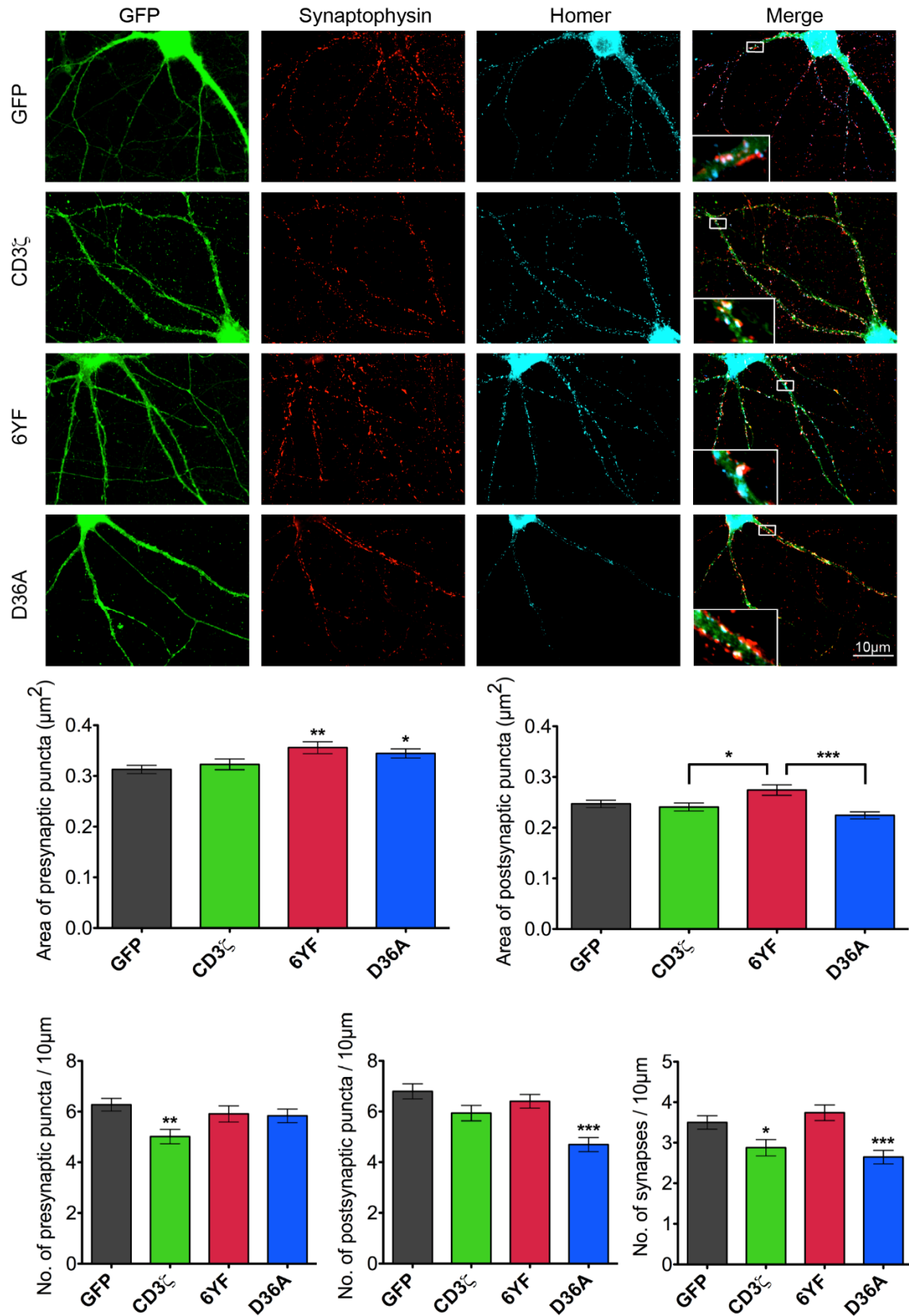


Figure 24: Influence of CD3ζ on synaptic structures in hippocampal neurons. Cells were fixed at DIV16 after a 6-day overexpression of CD3ζGFP, its mutants or GFP. Immunofluorescent labeling of pre- and postsynaptic sites was achieved by staining with anti-synaptophysin or anti-homer antibodies. Analysis of puncta size and number was done with ImageJ. Data of three different experiments are expressed as mean ± SEM (one-way ANOVA, *p<0.05, **p<0.01, ***p<0.001).

For synapse evaluation, hippocampal neurons were stained with the presynaptic marker synaptophysin (Glantz *et al.*, 2007) and the postsynaptic marker homer (Ippolito and Eroglu, 2010) after fixation. Images were taken with a fluorescence microscope and 63x magnification. ImageJ analysis allowed to count homer or synaptophysin positive dots along a dendrite and to calculate their area. Partially colocalizing pre- and postsynaptic puncta were regarded as synapses. Representative images and the statistical analyses of the experiment are shown in figure 24.

The area of presynaptic puncta of cells overexpressing the 6YF or D36A mutant is increased compared to GFP control. CD3 ζ -6YF-GFP overexpression also leads to enlarged postsynapses in comparison to CD3 ζ wt neurons. The non-phospho mutant does not affect the number of pre- or postsynaptic puncta, whereas CD3 ζ -D36A-GFP decreases the number of postsynaptic puncta, and CD3 ζ GFP the number of presynaptic puncta. In both cases, this results in a lower synapse count. These outcomes suggest an influence of CD3 ζ on synaptic structure that might be analogous to its effect on dendrite complexity.

3.4 The CD3 ζ -NMDA Receptor Complex

NMDA receptors are known to regulate actin cytoskeleton reorganization (Penzes and Cahill 2012; Penzes and Rafalovich 2012; Bustos *et al.*, 2014). Furthermore, they have been shown to be involved in CD3 ζ signaling. Huh *et al.* (2000) were able to show that CD3 ζ ^{-/-} mice have an enhanced LTP. This effect could be abolished using the NMDA receptor inhibitor APV. A later study then confirmed that the interaction between CD3 ζ and the NR2A subunit (Louveau *et al.*, 2013) influences CaMKII dependent induction of LTP. Thus, I examined whether CD3 ζ also forms a complex with the NR2B subunit and how it influences NR2B expression levels.

3.4.1 CD3 ζ and NR2B Form a Complex

Conducting an immunoprecipitation experiment, we examined if CD3 ζ also interacts with the NR2B subunit or with other receptors that are related to NMDA receptor signaling. A Triton X-100 lysate of adult rat forebrain synaptosomes was incubated with either an anti-CD3 ζ antibody or control IgG coupled to protein G magnetic beads. After washing, elution was done with SDS sample buffer. Total lysate, unbound fraction, the two last washing steps, and the eluate of CD3 ζ IP and IgG control were subjected to immunoblot analysis (fig. 25A).

The NR2B subunit could be coprecipitated with the CD3 ζ antibody, but not with control IgG. Respectively, the amount of NR2B found in the unbound fraction of the IgG control is higher than the one in the actual IP. Clean washing steps indicate that protein bands seen in the eluate stem from binding to the IP antibody and not from contamination. Neither TrkB nor the GluR1 and GluR2 subunit of AMPA receptors were detected in the CD3 ζ interactome.

The CD3 ζ -NR2B-complex should show as colocalization of both proteins in a fluorescent staining. To that end, DIV21 hippocampal neurons were fixed and subsequently incubated with an anti-CD3 ζ and an anti-NR2B antibody. Homer labeling was used to define postsynaptic sites. Figure 25B shows that CD3 ζ and NR2B partially colocalize around homer positive postsynapses proving their local proximity as a prerequisite for interaction.

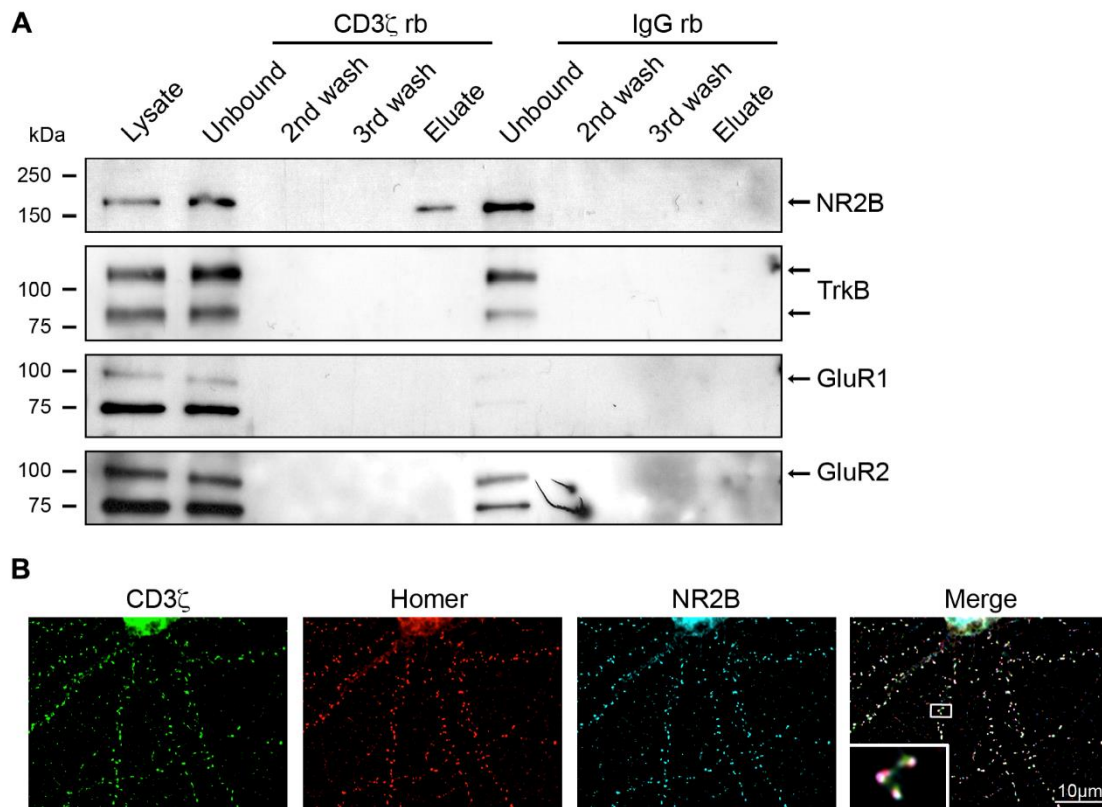


Figure 25: CD3ζ and NR2B form a complex. (A) Immunoprecipitation (IP) with an anti-CD3ζ antibody and IgG control using a Triton X-100 extract of rat forebrain synaptosomes. Total lysate, unbound, washing and eluate fractions of both IP and IgG control were subjected to immunoblot analysis and probed with an anti-NR2B, anti-TrkB, anti-GluR1 and anti-GluR2 antibody. NR2B but none of the other receptors coprecipitated with CD3ζ. A representative image of four independent experiments is shown. **(B)** Colocalization of NR2B and CD3ζ in DIV21 hippocampal neurons. Cells were fixed and stained with an anti-CD3ζ, anti-NR2B and anti-homer antibody. The enlarged cutout shows triple colocalization (white) in detail. Results could be confirmed in three independent experiments.

3.4.2 CD3ζ Affects Expression Levels of NR2B in Hippocampal Neurons

Next, I examined the functional relationship between NR2B and CD3ζ. In a first experiment, NR2B expression levels in DIV16 neurons overexpressing CD3ζGFP, GFP, or either one of the mutants were evaluated after NMDA/glycine stimulation compared to a vehicle control. Hippocampal cells were transfected using lentivirus at DIV10. Stimulation with 100μM NMDA/2μM glycine or vehicle for three minutes followed on DIV16. Cells were harvested with SDS sample buffer 20 minutes after treatment and subjected to immunoblot analysis probing for NR2B and GAPDH.

Previous studies have shown a decrease in NR2B activity and protein levels 20 minutes after stimulation due to internalization and subsequent degradation (Nong *et al.*, 2003; Snyder *et al.*, 2005; Li *et al.*, 2009). I can also observe this effect in my

experiment. In both CD3 ζ and GFP overexpressing neurons, NR2B protein levels drop down to less than 30% of the original value after treatment (fig. 26). This decrease is missing in neurons overexpressing either one of the mutants indicating a role for CD3 ζ in NMDA receptor internalization and degradation. Therefore, both mutants can be considered loss-of-function-mutants concerning NMDA receptor signaling.

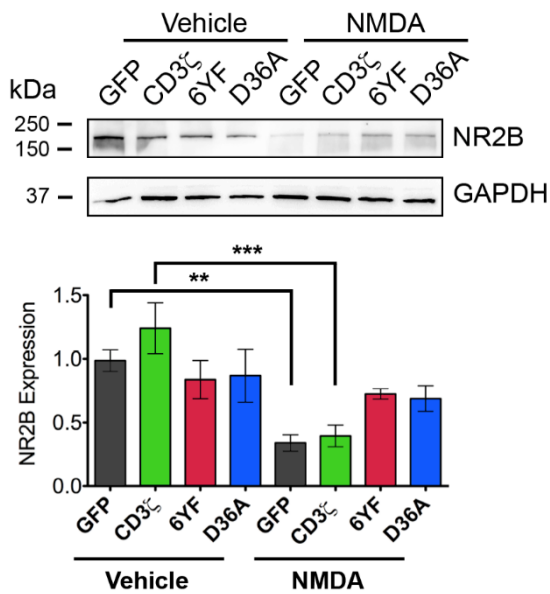


Figure 26: Expression levels of NR2B before and after NMDA receptor stimulation. Hippocampal neurons overexpressing CD3 ζ GFP, its mutants or GFP were treated with 100 μ M NMDA / 2 μ M glycine at DIV16. 20 minutes after stimulation, cells were harvested and analyzed via immunoblot probing for NR2B and GAPDH. Quantitative analysis of signal intensities was done with ImageJ. Data from seven independent experiments are expressed as mean \pm SEM (one-way ANOVA, **p<0.01, ***p<0.001).

If CD3 ζ is indeed involved in the internalization or degradation of NR2B-containing NMDA receptors, CD3 ζ GFP transfected neurons should show altered NR2B surface expression. To that end, I performed live staining of NR2B in DIV16 hippocampal neurons overexpressing GFP, CD3 ζ GFP or either one of the mutants prior to fixation. Images were acquired with a fluorescence microscope and a 63x objective. Number, area, and intensity of NR2B positive puncta were calculated using ImageJ (fig. 27).

There was no difference observed in the size of the puncta when comparing CD3 ζ GFP- to GFP- or mutant-overexpressing neurons. However, the loss-of-function mutant 6YF leads to a decrease of the amount of puncta per 10 μ m compared to wt CD3 ζ , which shows a slight, albeit not statistically significant increase in the count. The intensity of surface NR2B fluorescence is reduced in both CD3 ζ GFP and CD3 ζ -D36A-GFP overexpressing cells when compared to GFP control or 6YF mutant. Taken

together, these results indicate an influence of CD3 ζ on the distribution of surface NR2B rather than on its amount. An effect on complex clustering is conceivable pending further experiments. Merely the D36A mutant seems to reduce surface expression levels of NR2B slightly.

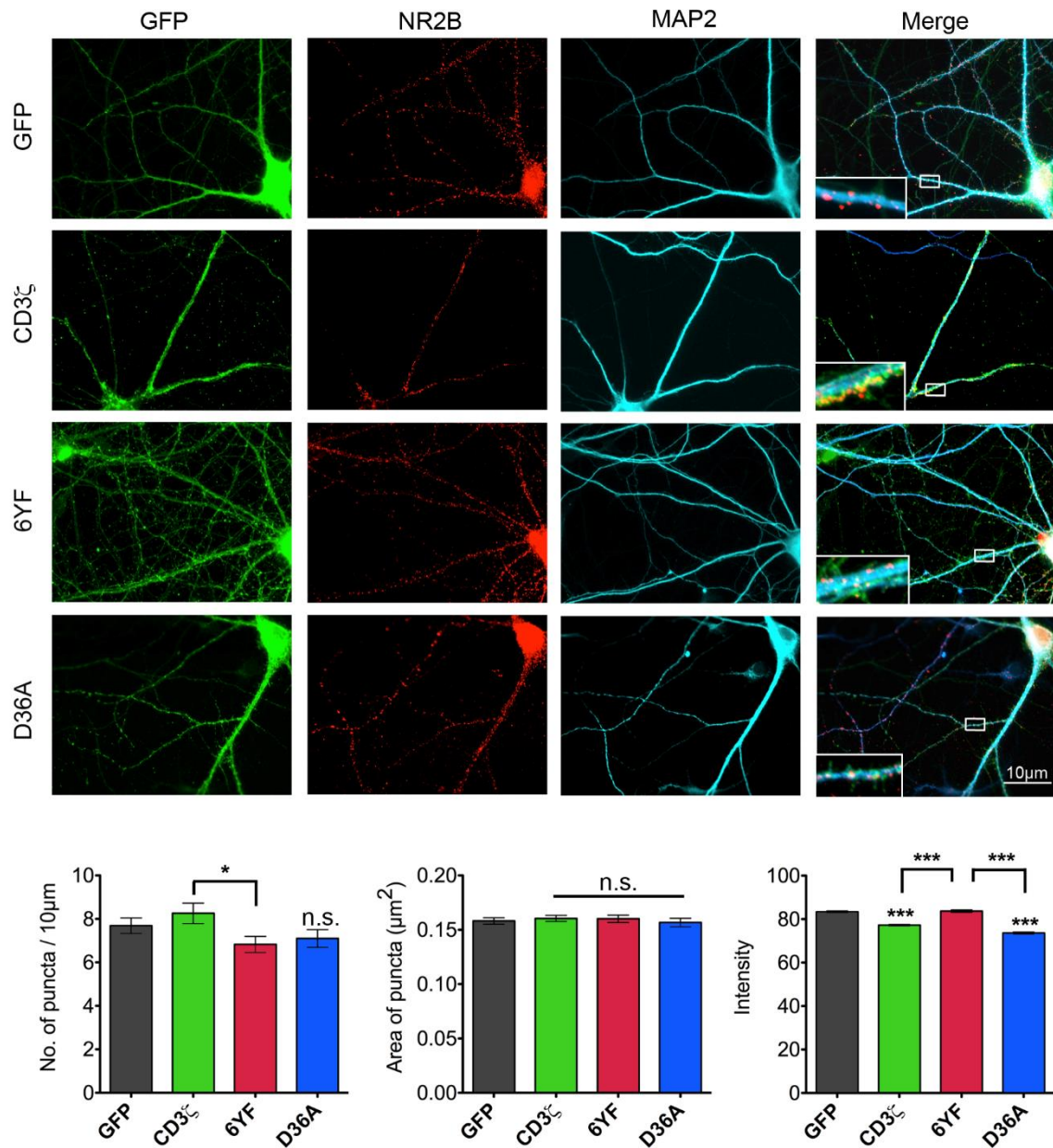


Figure 27: Immunofluorescent staining of surface NR2B. DIV16 hippocampal neurons expressing CD3 ζ GFP, its mutants or GFP were stained for surface NR2B prior to fixation. Analysis of puncta properties was done using ImageJ. Data from three different experiments are shown as mean \pm SEM (one-way ANOVA, * p <0.05, *** p <0.001).

3.4.3 NMDA Receptor Activity is needed for CD3 ζ Phosphorylation

Not only may CD3 ζ influence the function, localization, and cell surface expression features of NMDA receptors, also the reciprocal effect is possible. Therefore, I assessed the influence of a variety of receptor inhibitors on CD3 ζ phosphorylation, i.e. activation, employing a variety of inhibitors (see table 3 for detailed information). DIV10 hippocampal cells were transfected with CD3 ζ GFP lentivirus and then treated with pervanadate as described previously at DIV16. After harvesting, samples were subjected to immunoblot analysis comparing phosphorylated versus total CD3 ζ GFP. Results are shown in figure 28.

Table 3: Overview over applied inhibits and their target proteins.

Inhibitor	Target Protein	References
APV	NMDA receptor	Morris (1989)
CNQX	AMPA receptor	Honoré <i>et al.</i> (1988) Long <i>et al.</i> (1990)
Damnacanthal	Lck	Faltynek <i>et al.</i> (1995)
Ifenprodil	NR2B-containing NMDA receptor	Williams (2001)
Piceatannol	ZAP70	Geahlen <i>et al.</i> (1989) Oliver <i>et al.</i> (1994)
PP2	Src-kinases (Lck, Fyn)	Hanke <i>et al.</i> (1996)
Wortmannin	PI3K	Wymann <i>et al.</i> (1996)
Y-27632	ROCK	Uehata <i>et al.</i> (1997)

As CD3 ζ is phosphorylated by a src kinase in immune cells (Wange and Samelson, 1996), we used the general src kinase inhibitor PP2 as a control for the feasibility of the experiment. Indeed, application of PP2 leads to a decrease of phospho-CD3 ζ compared to a vehicle control. The same can be observed for the use of the NMDA

receptor blocker APV, albeit a smaller reduction than with PP2. Both the NR2B specific inhibitor ifenprodil and the AMPA receptor inhibitor CNQX do not affect CD3 ζ phosphorylation. This suggests that in mature neurons NR2A containing NMDA receptors, which are incidentally the predominant type at this stage, have the major influence on CD3 ζ signaling. In developing neurons, however, NR2B is much more prevalent than NR2A (Thomas *et al.*, 2005, Petralia 2012). Therefore, I focused the next experiments on DIV8 hippocampal neurons.

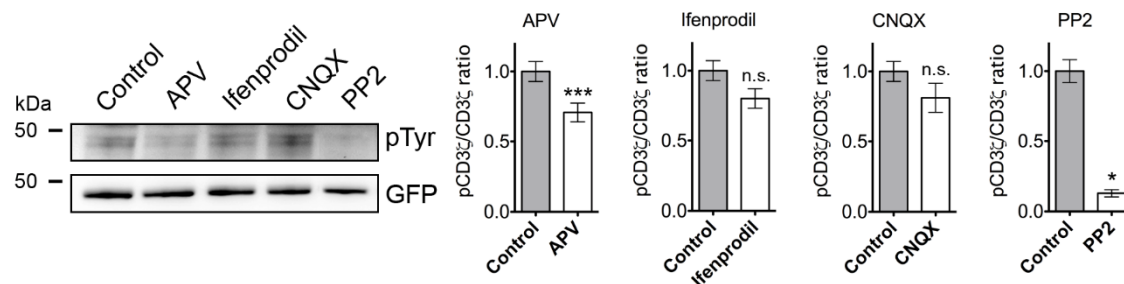


Figure 28: NMDA receptor activity is crucial for CD3 ζ phosphorylation. Receptors of hippocampal neurons (DIV16) overexpressing CD3 ζ GFP were blocked for 2 hours, and cells were subsequently treated with pervanadate. Samples were blotted against phospho-tyrosine (pTyr) detecting phosphorylated CD3 ζ GFP and total CD3 ζ GFP (GFP). Quantitative analysis of six (PP2 three) independent experiments was done with ImageJ. Data are shown as mean \pm SEM (t-test, * p <0.05, *** p <0.001).

3.4.4 Influence of CD3 ζ on NR2B Expression Levels in Developing Hippocampal Neurons

To evaluate the influence of CD3 ζ on NR2B protein levels in developing neurons (DIV8), I overexpressed CD3 ζ GFP, GFP, or either one of the mutants and immunostained the samples against an anti-NR2B and an anti-GAPDH antibody as a loading control (fig. 29). Interestingly, NR2B expression levels are reduced in all conditions compared to GFP control giving no hint to a specific influence of CD3 ζ .

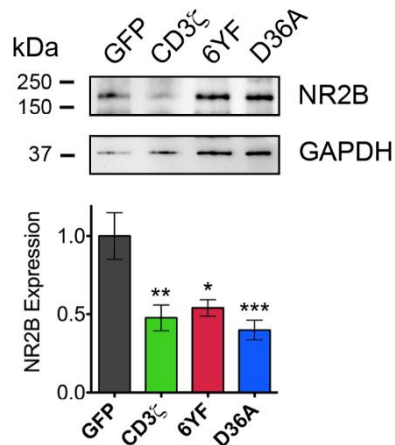


Figure 29: Effect of CD3 ζ on NR2B expression levels in DIV8 hippocampal neurons. Neurons overexpressing CD3 ζ GFP, GFP, or either one of the mutants were subjected to immunoblot analysis and probed with an anti-NR2B and an anti-GAPDH antibody as loading control. Optic density of the bands was analyzed using ImageJ. Data of six experiments are shown as mean \pm SEM (one-way ANOVA, * p <0.05, ** p <0.01, *** p <0.001)

3.5 CD3 ζ Activation Leads to Reorganization of the Actin Cytoskeleton

Now that the influence of CD3 ζ on actin cytoskeleton regulation and on NR2B expression levels was established in mature neurons, I aimed at elaborating the role of CD3 ζ in developing neurons – especially regarding the pronounced effect of CD3 ζ overexpression on dendrite complexity. Thus, I decided to use Sholl analysis and the CD3 ζ phosphorylation paradigm to characterize the influence of NMDA receptors and other proteins on CD3 ζ functioning in young neurons by applying a number of inhibitors.

For the following studies in DIV8 hippocampal neurons, cells were transfected with CD3 ζ GFP, GFP, CD3 ζ -6YF-GFP, or CD3 ζ -D36A-GFP. After four hours, the transfection medium was replaced by growth medium containing the appropriate inhibitors or vehicle. Neurons were incubated for another 5 hours and then fixed with PFA. For image acquisition, a fluorescence microscope with 20x objective was used. Image analysis was done using Adobe Photoshop and ImageJ Sholl analysis.

In all experiments, wt CD3 ζ overexpression leads to a clear reduction of dendrite complexity as described previously, whereas both mutants do not show any effect (fig. 30-32, 34-36, 38-39). By applying specific inhibitors of receptors or putative downstream actors of CD3 ζ , I aimed at deciphering the mechanism of this phenomenon (see table 3 for detailed information on inhibitors).

3.5.1 NMDA Receptor Activation is Crucial for CD3 ζ Signaling to the Cytoskeleton

To assess the contribution of NMDA receptors on CD3 ζ signaling, I applied APV, which blocks all NMDA receptors, and ifenprodil, which is specific for NR2B-containing NMDA receptors. Although CD3 ζ does not interact with AMPA receptor subunits GluR1 and GluR2 (fig. 25A), these types of glutamate receptors may still have an influence on NMDA receptor dependent CD3 ζ signaling. To remove the Mg²⁺ block of NMDA receptor to allow opening, membrane depolarization is needed. This can be achieved by previous stimulation of AMPA receptors (Horak *et al.*, 2014). Therefore, I also used the AMPA receptor inhibitor CNQX.

Blocking NMDA receptors with APV abolishes the negative influence of CD3 ζ on branching and even increases the complexity above GFP vehicle control level (fig. 30). To verify the hypothesis, that CD3 ζ signaling predominantly depends on NR2B in young neurons, I repeated the experiment with ifenprodil. Also here, I observed control levels of dendrite complexity in CD3 ζ GFP overexpressing cells when specifically inhibiting NR2B (fig. 31). None of the inhibitors had any effect on GFP or mutant overexpressing neurons.

Using the inhibitor CNQX, I assessed the impact of AMPA receptors on this paradigm. Interestingly, this inhibitor was not able to rescue the effect of CD3 ζ on neurite branching (fig. 32), nor did it have any influence on cells expressing GFP or one of the mutants. Thus, AMPA receptors do not seem to affect the influence of CD3 ζ on cytoskeleton reorganization in young neurons.

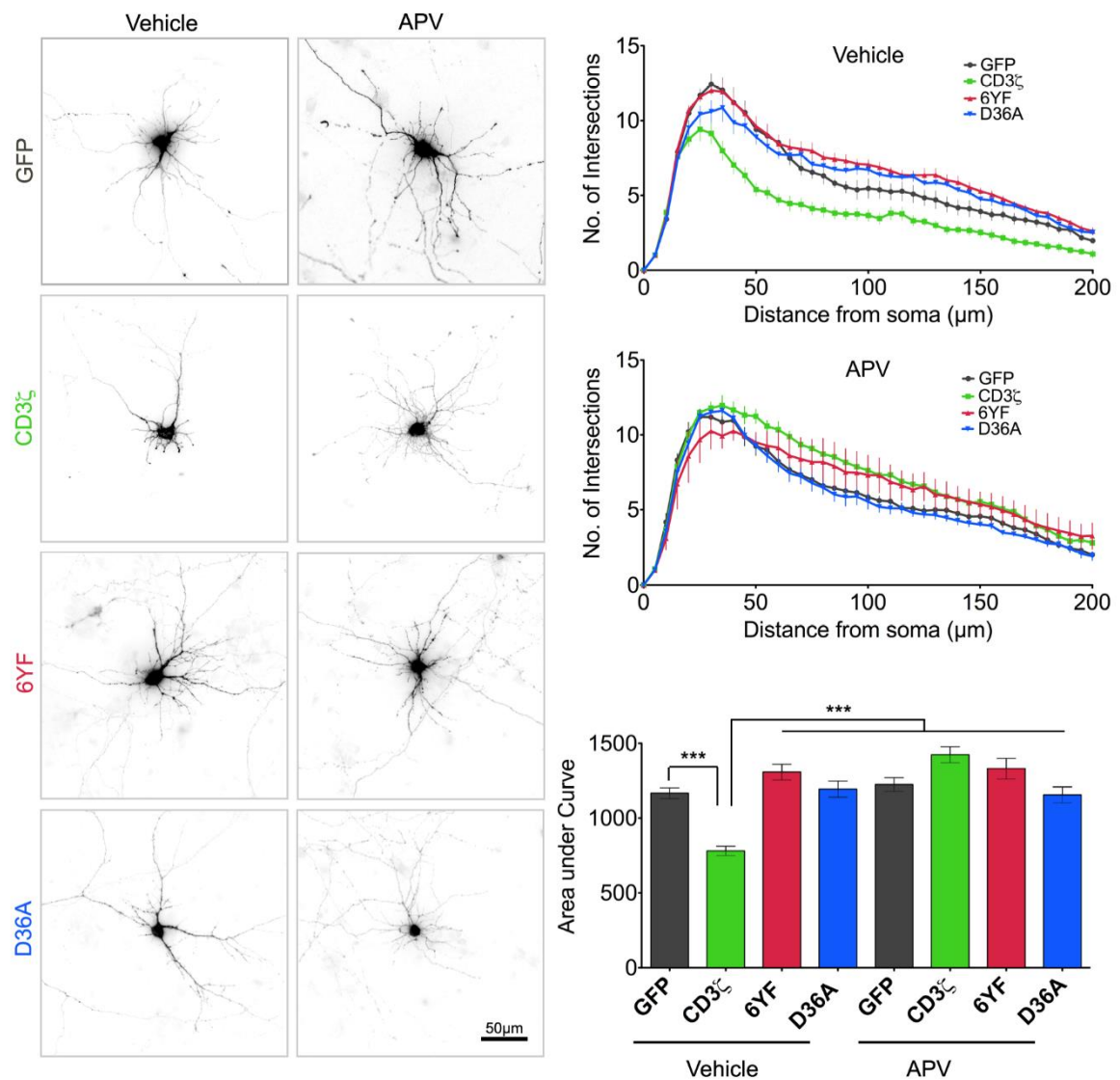


Figure 30: NMDA receptor blocker APV reverses CD3 ζ effect on dendrite complexity. DIV8 cultured hippocampal neurons were transfected with CD3 ζ GFP, GFP or either one of the mutants. 5 hours prior to fixing, 50 μ M APV was applied. Image analysis was done using Adobe PhotoShop and ImageJ Sholl analysis. The two upper graphs plot the number (No.) of intersections of dendrites with concentric circles of the Sholl analysis against the distance from the soma. The area under the curves is depicted in the column graph below. Data of four experiments are shown as mean \pm SEM (one-way ANOVA, ***p<0.001)

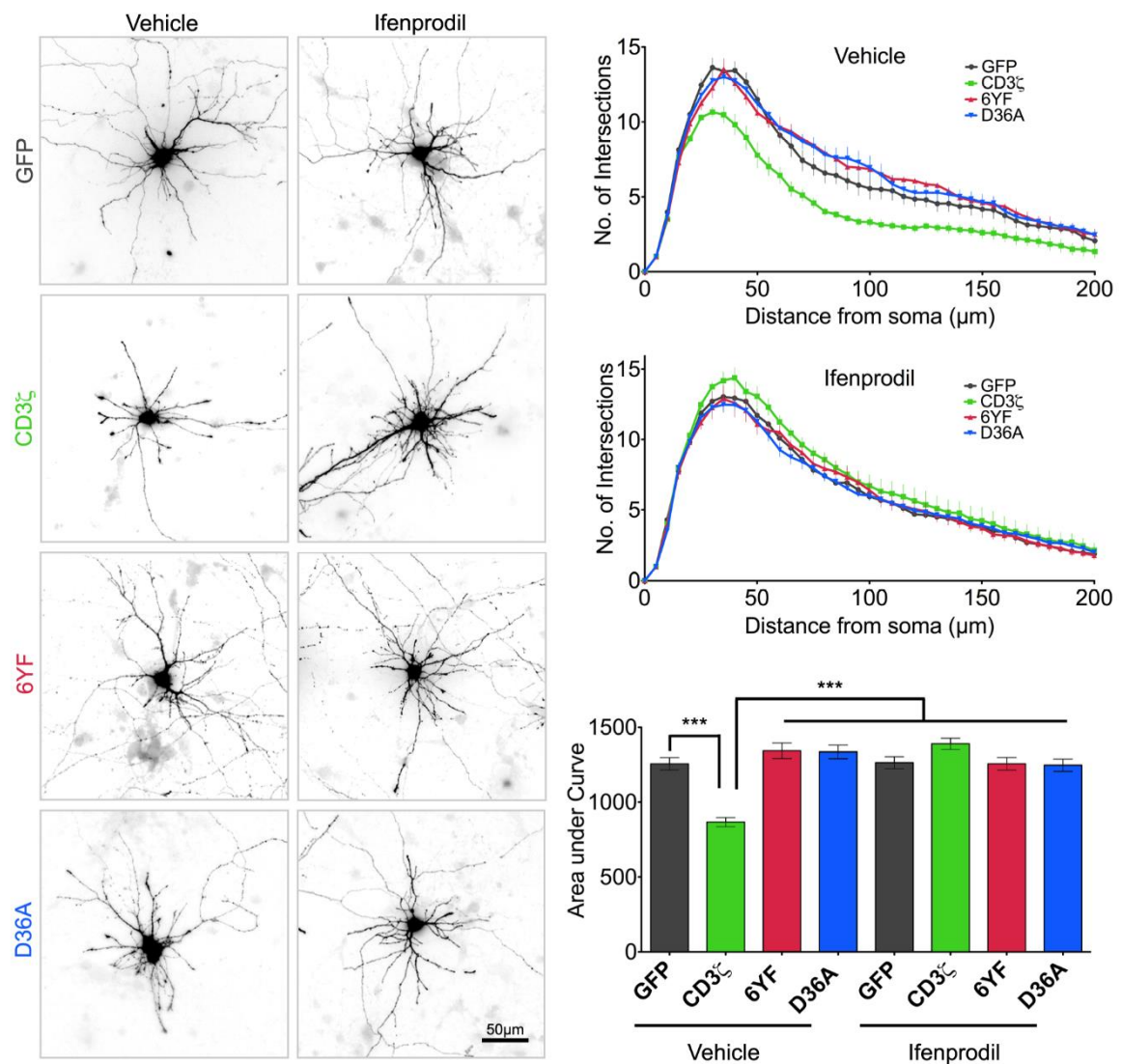


Figure 31: NR2B subunit inhibitor ifenprodil reverses CD3ζ effect on dendrite complexity. DIV8 cultured hippocampal neurons were transfected with CD3ζGFP, GFP or either one of the mutants. 5 hours prior to fixing, 10 μM ifenprodil was applied. Image analysis was done using Adobe PhotoShop and ImageJ Sholl analysis. The two upper graphs plot the number (No.) of intersections of dendrites with concentric circles of the Sholl analysis against the distance from the soma. The area under the curves is shown in the column graph below. Data of four independent experiments are expressed as mean ± SEM (one-way ANOVA, ***p < 0.001)

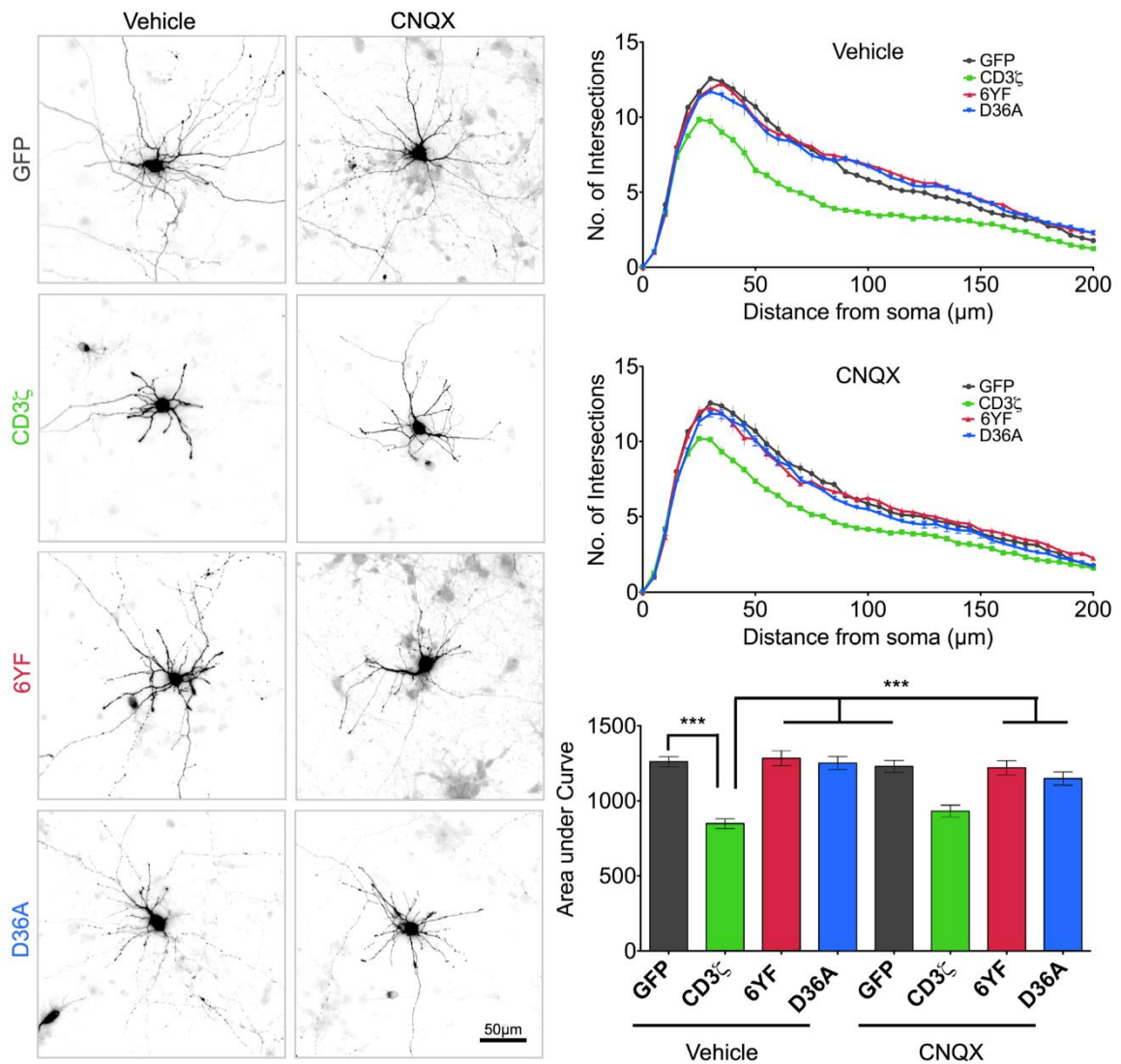


Figure 32: AMPA receptor inhibitor CNQX does not rescue the CD3ζ overexpression phenotype. DIV8 cultured hippocampal neurons were transfected with CD3ζGFP, GFP or either one of the mutants. 5 hours prior to fixing, 10μM CNQX was applied. Image analysis was performed using Adobe PhotoShop and ImageJ Sholl analysis. The two upper graphs plot the number (No.) of dendritic intersections with concentric circles of the Sholl analysis against the distance from the soma. The area under the curves is shown in the column graph below. Data of four independent experiments are expressed as mean ± SEM (one-way ANOVA, ***p<0.001)

If NMDA receptor activation regulates CD3ζ signaling in young neurons, it may also affect CD3ζ phosphorylation. To that end, I overexpressed CD3ζGFP in hippocampal neurons using lentivirus and harvested the cells after pervanadate treatment at DIV8. Immunoblot analysis for phosphorylated and total CD3ζGFP, detected with an anti-phospho-tyrosine and an anti-GFP antibody respectively, shows a reduction of CD3ζ phosphorylation when applying APV and ifenprodil, but also when using CNQX (fig.

33). The outcome suggests an impact of NMDA receptors, and more specifically of NR2B containing NMDA receptors, on CD3 ζ signaling. AMPA receptors, even though not involved in CD3 ζ dependent structuring of the cytoskeleton, may still have an influence on CD3 ζ functioning in other areas, e.g. gene expression or receptor localization.

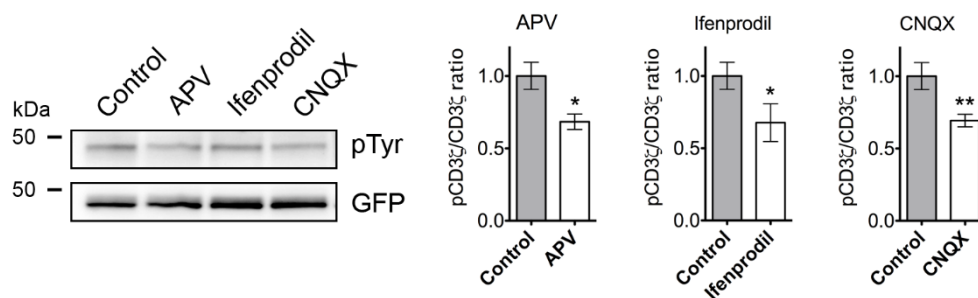


Figure 33: NMDA and AMPA receptor activity has an impact on CD3 ζ phosphorylation in developing neurons. AMPA (10 μ M CNQX) and NMDA receptors (50 μ M APV, 10 μ M ifenprodil specific for NR2B subunit) of hippocampal neurons (DIV8) overexpressing CD3 ζ GFP were blocked for 2 hours, and cells were subsequently treated with pervanadate. Samples were blotted against phospho-tyrosine (pTyr) detecting phosphorylated CD3 ζ GFP and total CD3 ζ GFP (GFP). Quantitative analysis of seven independent experiments was done with ImageJ. Data are shown as mean \pm SEM (t-test, * p <0.05, ** p <0.01).

3.5.2 Src Kinases are Required for CD3 ζ -dependent Cytoskeletal Remodeling in Developing Neurons

In T cells, CD3 ζ phosphorylation is mediated by the src kinases Fyn or Lck (Wange and Samelson, 1996). The recruitment of Lck to the TCR activation site leads to the activation of ZAP70 and PI3K (von Willebrand *et al.*, 1998; Wang *et al.*, 2010; Wange and Samelson, 1996). Both proteins are starting points for several pathways of which some regulate actin cytoskeleton remodeling (Bach *et al.*, 2007; Dustin and Cooper 2000). To decipher neuronal CD3 ζ signaling, I employed a number of inhibitors and observed their effect on dendrite complexity and CD3 ζ phosphorylation in cultured hippocampal neurons.

Blocking src kinases with PP2 led again to a phenotypical rescue of CD3 ζ overexpression in neurons. Remarkably, branching in GFP expressing control neurons was decreased with the inhibitor. PP2 had no effect on neurons expressing the mutants (fig. 34). The same could be observed when using the Lck inhibitor

damnacanthal. CD3 ζ GFP neurons showed increased and GFP neurons reduced branching when blocking Lck (fig. 35). The PI3K inhibitor wortmannin also increased dendrite complexity of CD3 ζ GFP expressing cells, but had no influence on GFP or mutants expressing neurons (fig. 36).

These results suggest an involvement of all three kinases Fyn, Lck, and PI3K in CD3 ζ dependent cytoskeletal reorganization.

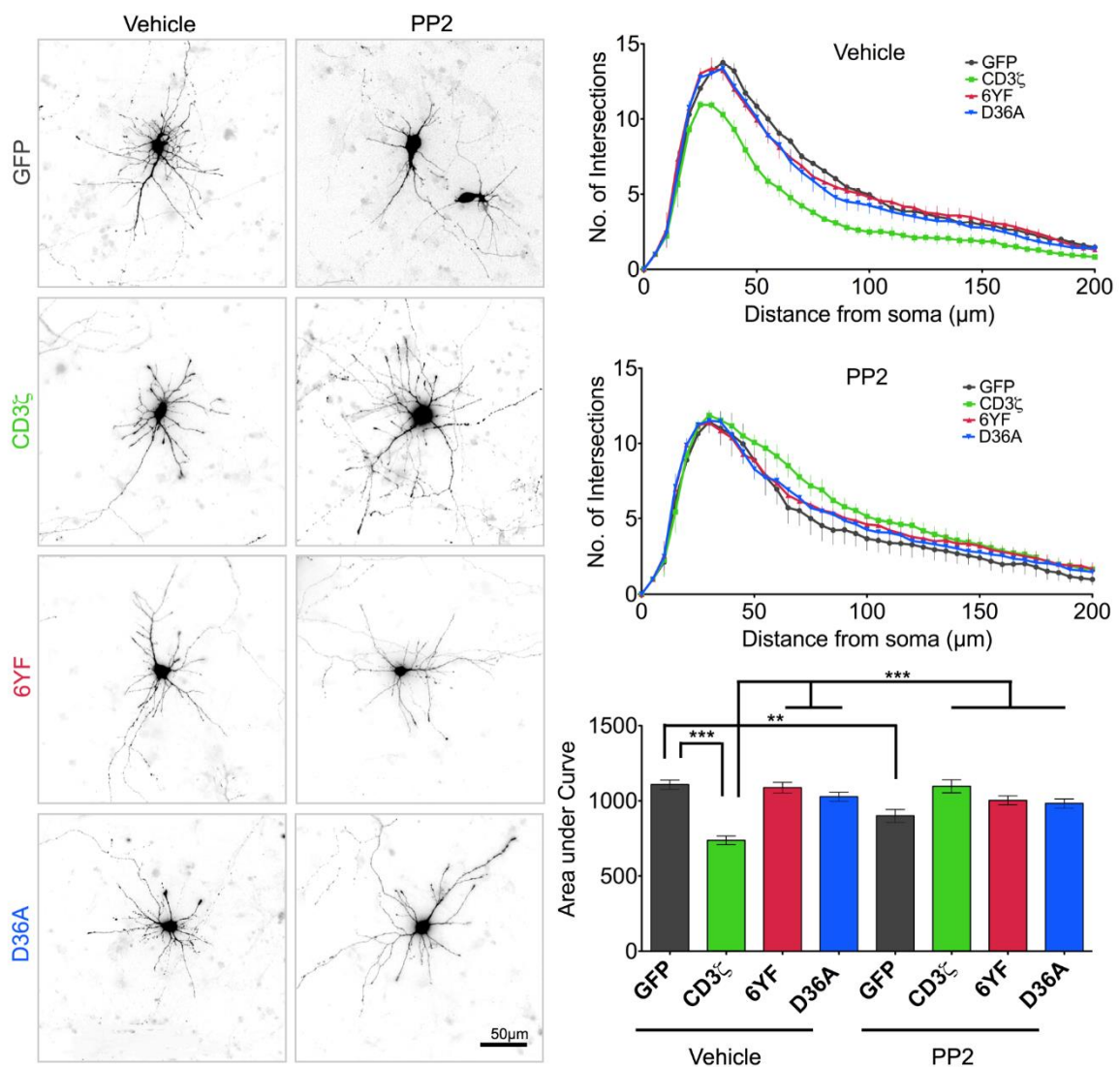


Figure 34: The general src kinase inhibitor PP2 reverses the effect of CD3 ζ on dendrite complexity. DIV8 cultured hippocampal neurons were transfected with CD3 ζ GFP, GFP or either one of the mutants. 5 hours prior to fixing, 1 μ M PP2 was applied. Image analysis was performed using Adobe PhotoShop and ImageJ Sholl analysis. The two upper graphs plot the number (No.) of dendritic intersections with concentric circles of the Sholl analysis against the distance from the soma. The area under the curves is shown in the column graph below. Data of three different experiments are expressed as mean \pm SEM (one-way ANOVA, ** p <0.01, *** p <0.001)

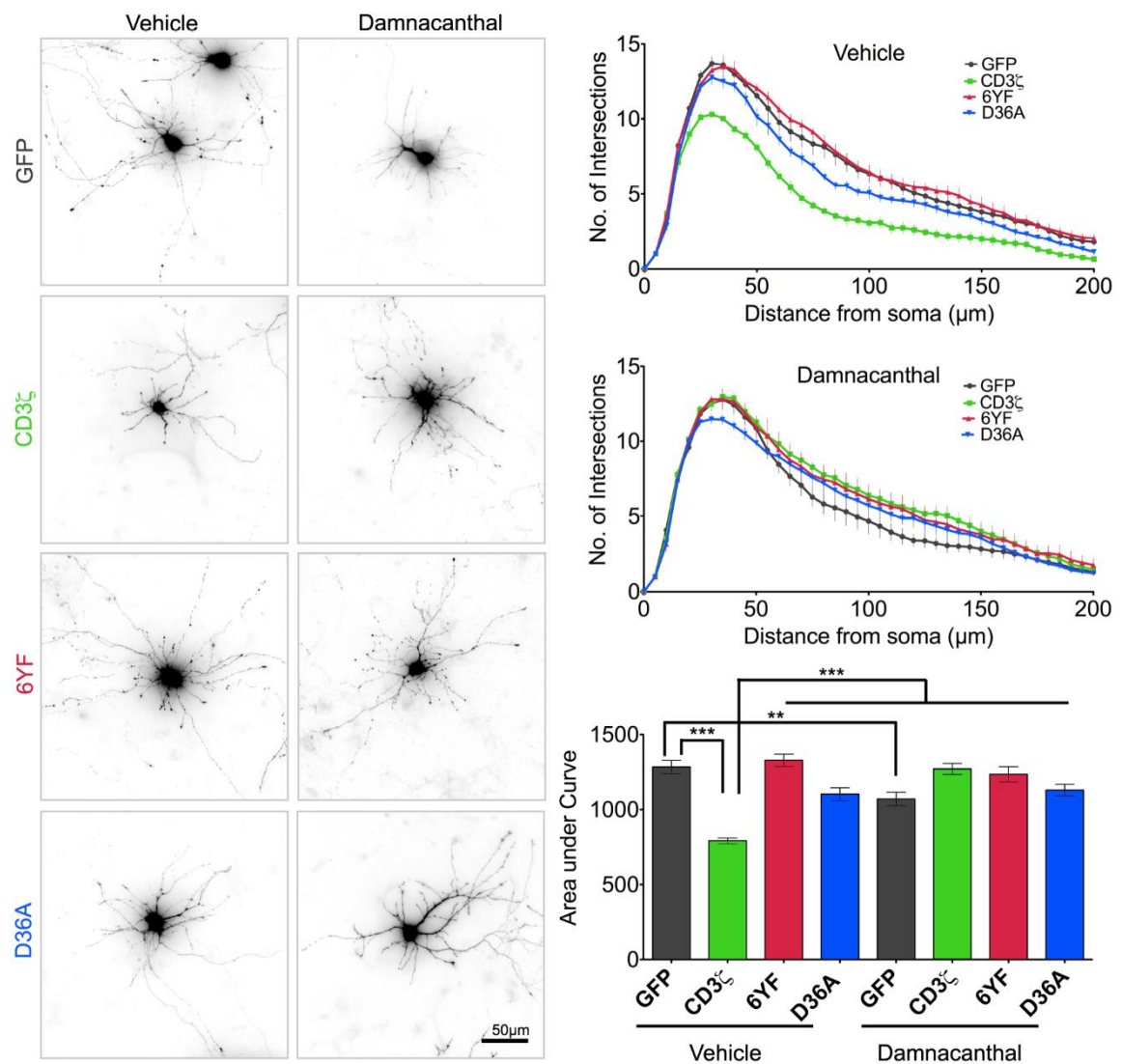


Figure 35: Lck inhibitor damnacanthal rescues the CD3ζ overexpression phenotype. DIV8 cultured hippocampal neurons were transfected with CD3ζGFP, GFP or either one of the mutants. 5 hours prior to fixing, 100nM damnacanthal was applied. Image analysis was performed using Adobe PhotoShop and ImageJ Sholl analysis. The two upper graphs plot the number (No.) of dendritic intersections with concentric circles of the Sholl analysis against the distance from the soma. The area under the curves is shown in the column graph below. Data of four different experiments are expressed as mean ± SEM (one-way ANOVA, **p<0.01, ***p<0.001)

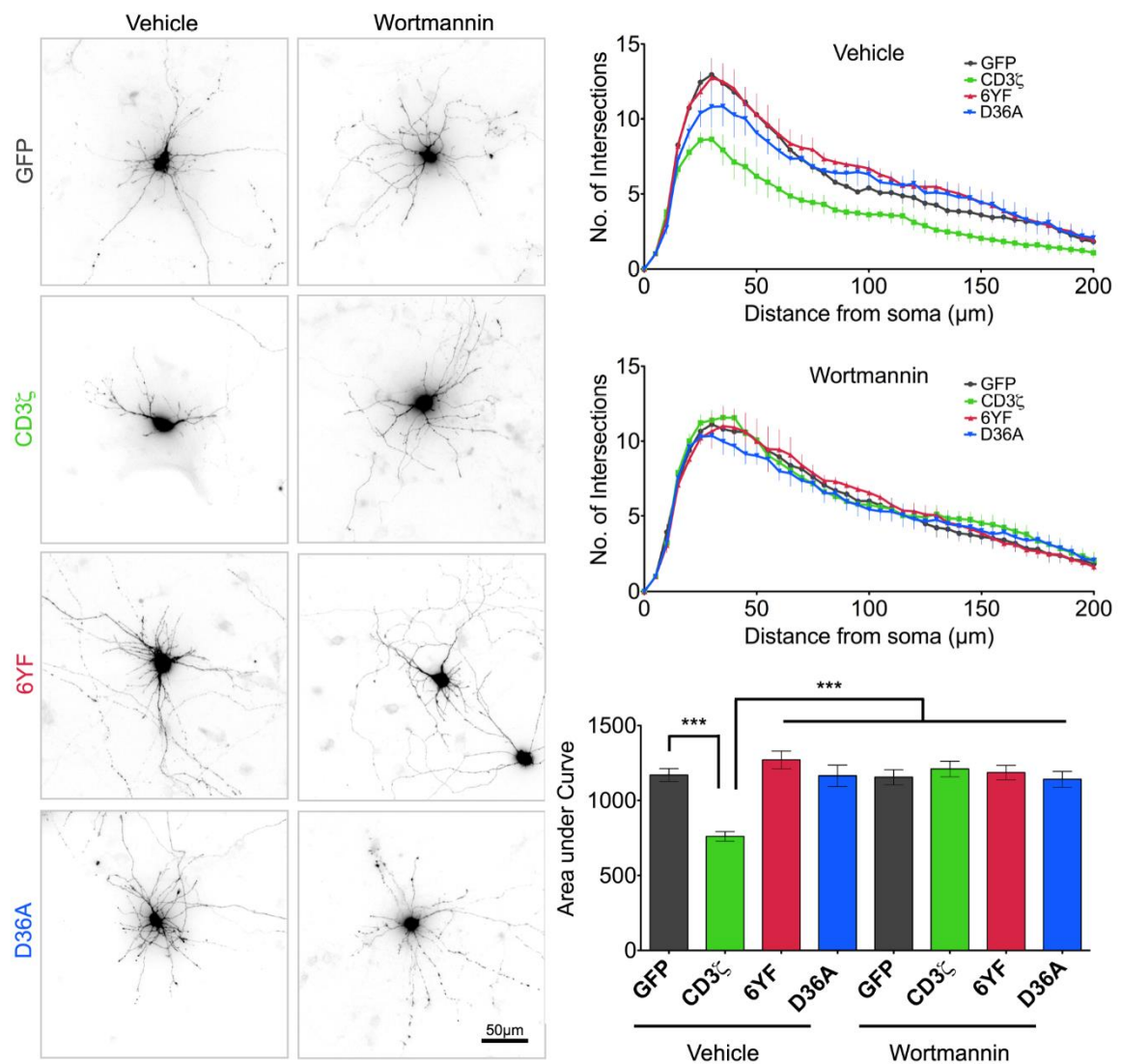


Figure 36: The PI3K blocker wortmannin rescues the CD3ζ overexpression phenotype. DIV8 cultured hippocampal neurons were transfected with CD3ζGFP, GFP or either one of the mutants. 5 hours prior to fixing, 50nM wortmannin was applied. Image analysis was performed using Adobe PhotoShop and ImageJ Sholl analysis. The two upper graphs plot the number (No.) of dendritic intersections with concentric circles of the Sholl analysis against the distance from the soma. The area under the curves is shown in the column graph below. Data of three independent experiments are expressed as mean ± SEM (one-way ANOVA, ***p<0.001)

In a next step, I aimed at determining whether the kinases function up- or downstream of CD3ζ, i.e. if they influence CD3ζ phosphorylation. Therefore, I performed the previously described CD3ζ phosphorylation experiment using pervanadate treatment in DIV8 hippocampal neurons overexpressing GFP, CD3ζGFP, or either one of the mutants after lentiviral transfection. Immunoblot analysis of the samples shows a reduction of CD3ζ phosphorylation by more than 75% when

applying PP2 (fig. 37). This effect could not be observed with any of the other two inhibitors. Thus, I conclude that Lck and PI3K are located downstream of CD3 ζ whereas a src kinase other than Lck mediates CD3 ζ phosphorylation.

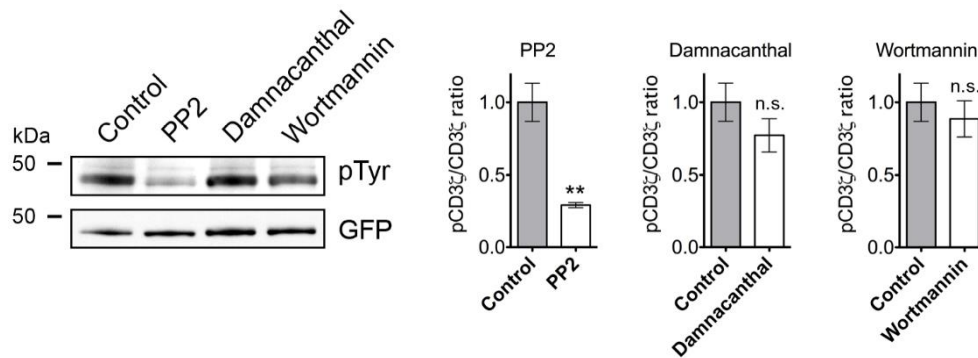


Figure 37: CD3 ζ phosphorylation is mediated by a src kinase in developing neurons. The general src kinase inhibitor PP2 (1 μ M), the Lck blocker damnacanthal (100nM), or PI3K inhibitor wortmannin (50nM) were applied on cultured hippocampal neurons (DIV8) overexpressing CD3 ζ GFP for two hours. Neurons were subsequently treated with pervanadate. Samples were blotted against phospho-tyrosine (pTyr) detecting phosphorylated CD3 ζ GFP and total CD3 ζ GFP (GFP). Quantitative analysis of four independent experiments was done with ImageJ. Data are presented as mean \pm SEM (t-test, **p<0.01).

3.5.3 Downstream Signaling of CD3 ζ is Mediated by ZAP70 Kinase Leading to the Activation of the RhoA/ROCK Pathway

The tyrosine kinase ZAP70 is a major signaling network hub in immune cells (Wang *et al.*, 2010). Studies have shown the expression of ZAP70 and the closely related kinase Syk in neurons (Hatterer *et al.*, 2011), but did not elaborate on their putative functions there. Considering the close interaction between CD3 ζ and ZAP70 in immune cells, it was conceivable to further explore the role of the kinase in the CD3 ζ dependent cytoskeletal regulation. Indeed, inhibiting ZAP70 with piceatannol leads to an increased branching of CD3 ζ overexpressing neurons bringing dendrite complexity back to GFP control levels (fig. 38).

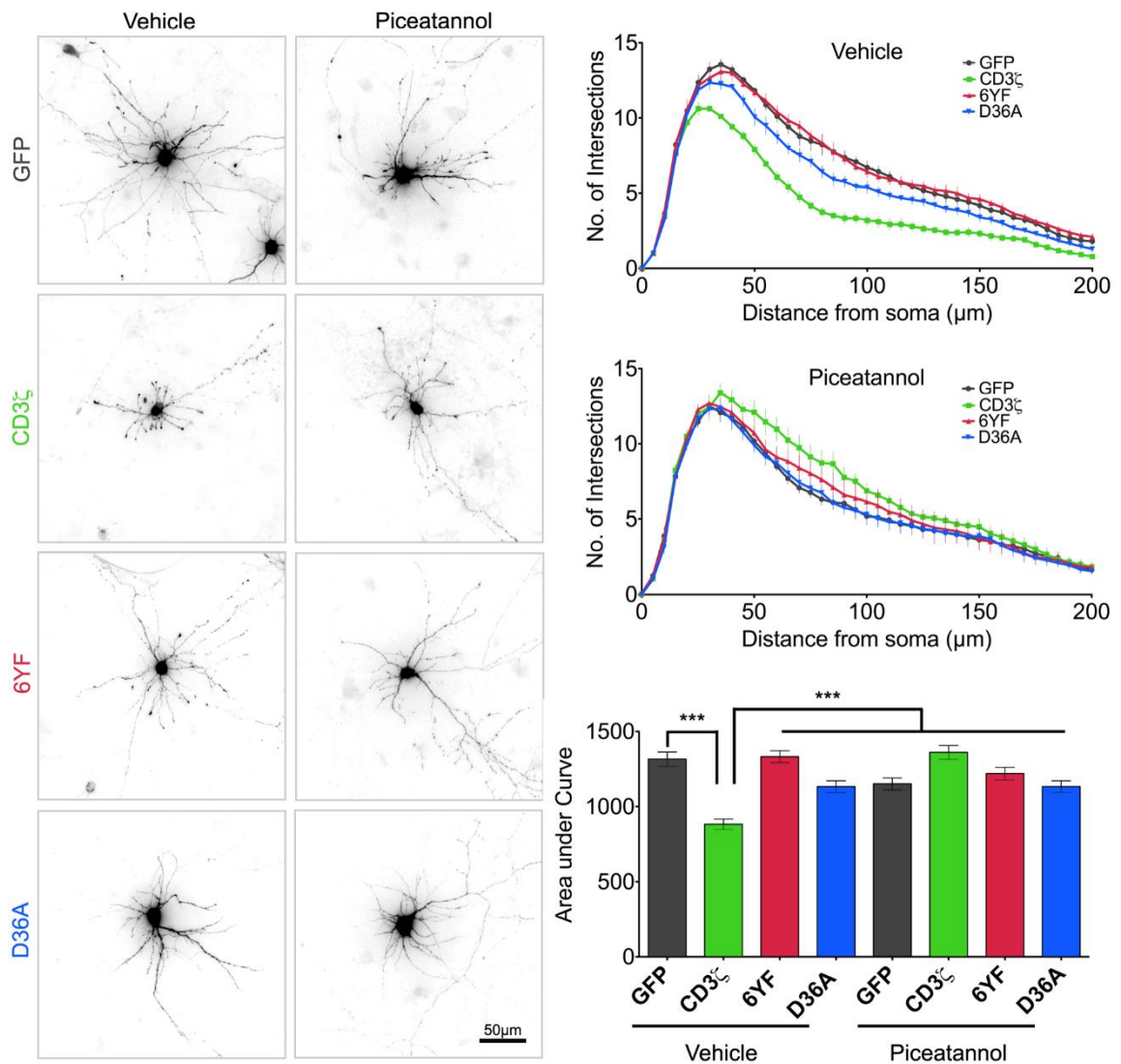


Figure 38: ZAP70 inhibitor piceatannol reverses CD3ζ effect on dendrite complexity. DIV8 cultured hippocampal neurons were transfected with CD3ζGFP, GFP or either one of the mutants. 5 hours prior to fixing, 10 μM piceatannol was applied. Image analysis was performed using Adobe PhotoShop and ImageJ Sholl analysis. The two upper graphs plot the number (No.) of dendritic intersections with concentric circles of the Sholl analysis against the distance from the soma. The area under the curves is shown in the column graph below. Data of four independent experiments are expressed as mean ± SEM (one-way ANOVA, ***p < 0.001)

With the involvement of ZAP70 and PI3K established, there were a number of possible pathways to close the gap towards actin remodeling of which the RhoA/ROCK pathway is well described in neurons (Da Silva et al., 2003; Govek et al., 2005). If this pathway were involved, application of the ROCK inhibitor Y-27632 would abolish the negative effect of CD3ζ overexpression in neurons. Indeed, this was the case. As can be seen in figure 39, Y-27632 prevents the negative regulation of

CD3 ζ overexpression on dendrite complexity. There was no observable effect on neurons expressing GFP or either one of the mutants.

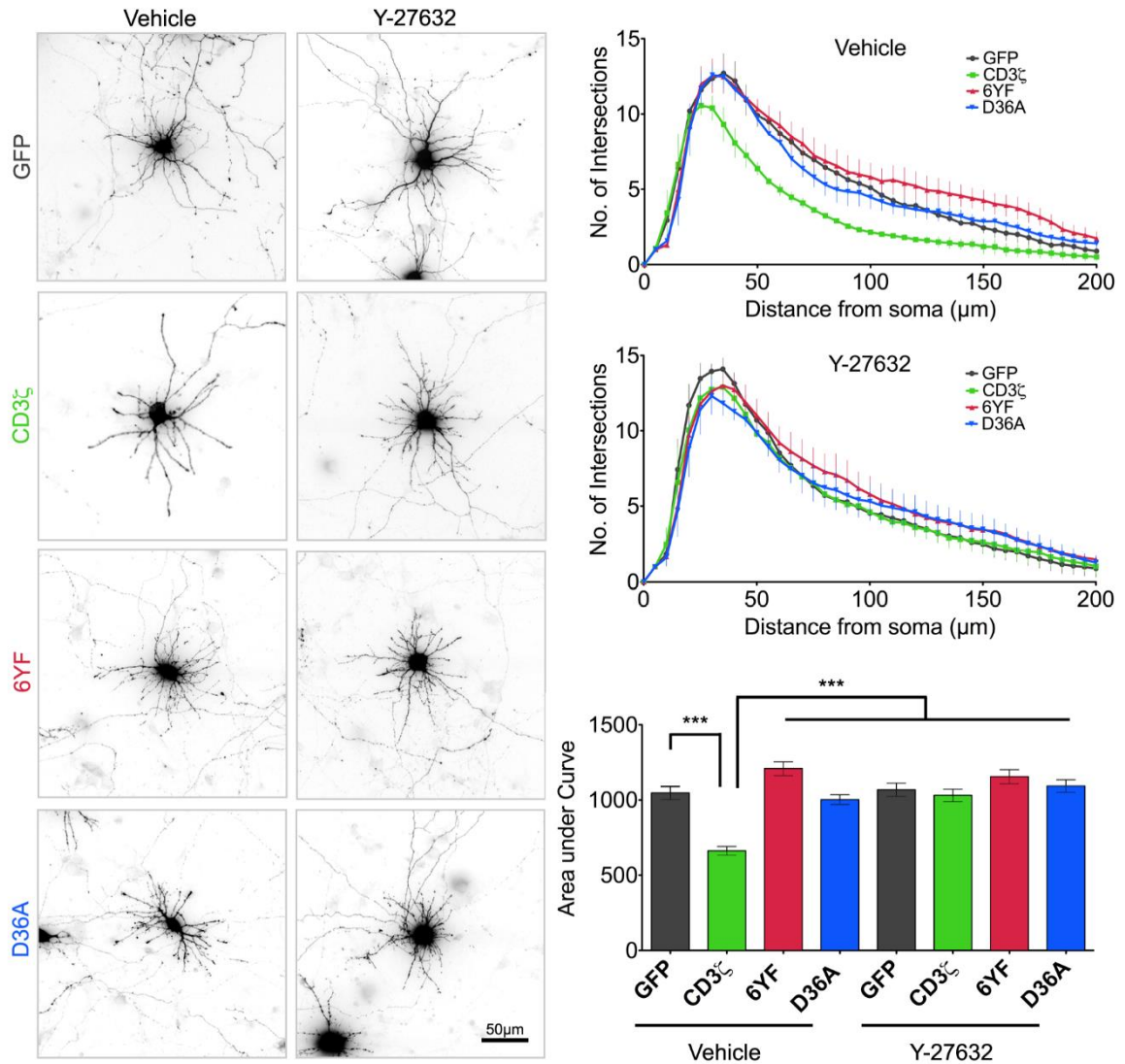


Figure 39: ROCK inhibitor Y-27632 reverses CD3 ζ effect on dendrite complexity. DIV8 cultured hippocampal neurons were transfected with CD3 ζ GFP, GFP or either one of the mutants. 5 hours prior to fixing, 10 μ M Y-27632 was applied. Image analysis was performed using Adobe PhotoShop and ImageJ Sholl analysis. The two upper graphs plot the number (No.) of dendritic intersections with concentric circles of the Sholl analysis against the distance from the soma. The area under the curves is shown in the column graph below. Data of three independent experiments are expressed as mean \pm SEM (one-way ANOVA, ***p<0.001)

4 Discussion

The formerly prevalent concept of an immune-privileged brain had to be revised over the past few decades (Steinman, 2004; Marin and Kipnis, 2013). For one thing, it was shown that the immune and the central nervous system communicate with each other using chemical transmitters that find their corresponding receptors in cells of both systems (Mousa and Bakhiet, 2013; Marin and Kipnis, 2013). But even more astonishing was the fact to find proteins in neurons thought to be exclusively expressed by immune cells (Fourgeaud and Boulanger, 2010).

The present work gives an overview about TCR signaling molecules expressed in neurons of the rat, mouse or human brain. The underlying data were collected using several databases and screening published literature. 84 out of 95 proteins belonging to the immune signaling network were found to be expressed in neurons of the CNS. Among these molecules, we discovered the crucial signaling subunit of the TCR complex CD3 ζ , but not the T-cell receptor itself. As CD3 ζ only comprises a very short ectodomain unable to bind ligands, it needs an associated receptor to receive extracellular information. This thesis, therefore, evolved around the questions of the receptor-dependency of CD3 ζ in neurons and of its neuronal functions.

Our experiments show that CD3 ζ negatively regulates dendrite outgrowth in DIV8 hippocampal neurons through the RhoA/ROCK pathway. The reorganization of the actin cytoskeleton by CD3 ζ depends on NR2B-containing NMDA receptors implying a novel function for NR2B in hippocampal neurons prior to synaptogenesis.

4.1 A Comparative Study of Immune and Neuronal Signaling

The first part of this thesis is concerned with the comparison of TCR signaling with neuronal signaling. An extended model of the one published by Saez-Rodriguez *et al.* (2007) was used as a basis. Researching published literature as well as the databases Allen Brain Atlas, Human Protein Atlas and SynProt, we found that 82 out of 94 proteins are expressed in neurons. The evidence for 77 proteins could be found in peer-reviewed publications. The neuronal expression of seven further proteins was published in either one of the databases. However, they are limited by the use of an appropriate hybridization probe (Allen Brain Atlas) or a specific antibody (Human

Protein Atlas). Therefore, a negative result may still be overturned by the use of better working tools. This can be seen with NF-kappa-B essential modulator (IKKG) whose neuronal expression was negated by the databases, but was published in peer-reviewed journals (Shen *et al.*, 2003).

The postsynaptic density (PSD) is one of the best-characterized signaling platforms in neurons (Sheng and Kim, 2011). The database SynProt (Pielot *et al.*, 2011) provides an overview over proteins found in the fraction of synaptic junctions which includes the PSD. 36 out of 84 neuronal expressed proteins could be detected in these biochemical preparations. As a metastudy, SynProt relies on published works whose limitations are just the ones described above. Therefore, the present comparative study is not exclusive, but rather the beginning of ongoing work. While it may take a lot of time to be completed, especially considering the possibility of including more proteins, it serves as an insightful basis for understanding the signaling in neuronal models.

As our neuronal model was the hippocampal CA3 synapse on CA1 pyramidal neurons, we were particularly interested in the expression of the proteins in these cells. Indeed, the presence of 69 proteins has been shown in principal cells of the hippocampus. Among them are several very well-characterized proteins such as the src kinase Fyn (Xu *et al.*, 2006), proteins of the MAPK signaling pathway (Sweatt, 2001; Derkinderen *et al.*, 2003) or Calmodulin and its related kinases (Maletic-Savatic *et al.*, 1998; Palfi *et al.*, 2002). Their functions have been implied in the regulation of LTP and LTD, transcription regulation as well as in neuronal receptor signaling such as the NMDAR, AMPAR and TrkB to only name a few (Salter and Kalia, 2004; Appleby *et al.*, 2011;). However, we know very little of the neuronal function of other proteins such as ZAP70.

Zap70 kinase is a major signaling hub in TCR signal transduction (Wange and Samelson, 1996). It phosphorylates tyrosine residues of many regulatory proteins that further diverge incoming signals (Baniyash, 2004). Some of these proteins are also expressed in hippocampal neurons including phospholipase C γ (PLCG) (Minichiello *et al.*, 2002), diacylglycerol kinase (DGK) (Kim *et al.*, 2010) or son of sevenless (SOS) (Tian *et al.*, 2004). ZAP70 activation requires its conformational change triggered by the binding of so-called immunoreceptor tyrosine-based activation motifs (ITAM) (Wang *et al.*, 2010) that despite the name can also be found

in cells outside the immune system. The ITAM-containing proteins Jedi-1 and MEGF10 are both expressed in glial precursor cells in the peripheral nervous system. They regulate the phagocytosis of neuronal cell debris after apoptosis occurring during development (Wu *et al.*, 2009). Their signals are transduced via the ZAP70-related kinase Syk (Scheib *et al.*, 2012). Both proteins share 73% sequence homology including the tandem SH2 domain responsible for binding ITAMs (Béné, 2006), and their functions might be partially overlapping (Kong *et al.*, 1995).

Another ITAM-bearing protein expressed in both T-cells and neurons is CD3 ζ , the crucial signaling subunit of the TCR. Immunological CD3 ζ signal transduction occurs through the interaction with ZAP70 (Wange and Samelson, 1996). However, its neuronal implications are poorly understood. The main objective of this thesis was the further characterization of CD3 ζ functions in neurons, and the outcome will be discussed in the next chapters.

4.2 Characterization of CD3 ζ in the Rat Brain

First evidence for the presence of CD3 ζ mRNA in the brain came from Corriveau *et al.* (1998) probing young and adult feline lateral geniculate nuclei and Huh *et al.* (2000) examining the same brain area in young mice. Baudouin *et al.* (2008) then showed CD3 ζ mRNA expression in adult rat brain after synthesizing cDNA from a total RNA extract. They claimed that CD3 ζ mRNA levels are lower in brain compared to a spleen positive control. Our data generated using cDNA from rat hippocampus and cortex do not confirm this impression. CD3 ζ mRNA levels in adult rat brain and spleen are rather the same. The difference might be that Baudouin and colleagues have used total rat brain RNA which might have included areas with little or no CD3 ζ mRNA, whereas we concentrated our studies on hippocampal and cortical areas. However, we observed lower levels in young rats compared to adult rats. To confirm this result, further experiments need to be performed. Moreover, *in situ* hybridization of rat or mouse brain at different developmental stages will give deeper insights in the area specific expression of CD3 ζ mRNA.

The protein CD3 ζ has mostly been studied in hippocampal neurons which led to our decision to use these cells as our model system. Immunofluorescent labeling of CD3 ζ in cultured hippocampal neurons at different developmental stages revealed a

remarkable localization of the protein at sites of ongoing structural changes. At DIV2, CD3 ζ can be detected at the growth cones of neurites colocalizing with actin, and its presence at dendritic tips can still be observed at DIV7 confirming previously published results (Baudouin *et al.*, 2008). While neurons mature, their dendritic arbor stabilizes and its structural plasticity decreases (Koleske 2013). However, at this time synaptogenesis is at its peak. In cultured neurons, this can be observed at around DIV11 which is also the time point when CD3 ζ starts colocalizing with the postsynaptic protein homer. The presence of CD3 ζ in postsynaptic spines in mature neurons and neurite tips of developing neurites implies a possible role in structural reorganization or stabilization.

Another interesting observation is that the colocalization of CD3 ζ with homer is only partial leading to the conclusion that CD3 ζ might not be integrated into the PSD, but rather is a part of the surrounding environment. Some images even imply the presence of CD3 ζ in the spine neck. If CD3 ζ translocates to the PSD under certain conditions, e.g. receptor stimulation, can be the objective of further studies.

Immunoblot analysis of fractions obtained through differential centrifugation of total rat forebrain shows CD3 ζ in detergent resistant membranes (DRM) derived from P2 membrane fraction. This fraction includes lipid rafts and the PSD giving a hint that CD3 ζ might be enriched in particular signaling platforms of cellular membranes. Interestingly, CD3 ζ cannot only be detected in membrane fractions, but also in the S2 fraction comprising the cytosol and intracellular membranes. Compared to P2, the cytosolic fraction contains even more CD3 ζ possibly included in microsomes. There might be a protein pool in the endoplasmic reticulum or vesicles ready for surface membrane integration upon certain stimuli as shown for other proteins such as the TrkB receptor surfacing upon BDNF stimulation (Huang *et al.*, 2013) or the AMPA receptor that is introduced into the synaptic membrane during LTP (Hanley 2008)

The multitude of immunoreactive bands in brain samples imposed new questions. The CD3 ζ monomer runs at approximately 25kDa and can also be found in spleen membrane fraction. All brain fractions show a band of 50kDa implying the existence of a dimer complex resistant to β -mercaptoethanol lysis. A trimer explaining the band at 75kDa has never been reported though. Therefore, the cause for this band as well for the weak staining at 30kDa remains rather elusive and might be due to unspecific

antibody binding. Therefore, we generated antisera against CD3 ζ that would allow us to elucidate CD3 ζ function in hippocampal neurons. Some of these antisera showed high affinity toward CD3 ζ fusion proteins in immunoblot analysis and immunofluorescent stainings. However, they were not able to recognize endogenous CD3 ζ . Attempts to increase the affinity toward the endogenous proteins by purification did not prove successful. Consequently, we decided to take a different approach by designing CD3 ζ mutants.

4.3 Characterization of Two CD3 ζ Loss-of-Function Mutants

To further assess CD3 ζ function in neurons, we generated two loss-of-functions mutants as GFP-tagged fusion proteins. For the 6YF mutant, all six tyrosine residues of the ITAMs were replaced by phenylalanine to prevent phosphorylation of CD3 ζ and phosphorylation-dependent downstream signaling. For the second mutant, the aspartate residue within in the transmembrane domain was replaced by alanine. Both mutants have been published, but lacked proper characterization in neurons (Rutledge *et al.*, 1992; Call *et al.*, 2002; Baudouin *et al.*, 2008). They were examined regarding certain properties crucial for proper CD3 ζ functioning: dimerization, tyrosine phosphorylation as well as their localization and surface expression in neurons.

CD3 ζ GFP mutants are indeed able to form dimers with a wildtype TAP-tagged CD3 ζ fusion protein in about the same extent as CD3 ζ GFP wildtype. Double bands again point to the existence of phosphorylated and unphosphorylated protein. Remarkably, the CD3 ζ -D36A-GFP/CD3 ζ TAP dimers seem to be partially resistant to β -mercaptoethanol treatment as indicated by an additional double band at 50-60kDa. Rutledge *et al.* (1992) reported that the aspartic acid residue is crucial for dimer formation which occurs at a cysteine residue lying only four amino acids N-terminal from D36. However, they only tested dimer formation of two D36A mutants and not of a mutant with the wildtype protein. It seems that in this case dimer formation can still occur as shown here. Nevertheless, complex formation might also be due to third factors in an immunoprecipitation experiment that was performed with total cell lysates and not purified proteins.

As CD3 ζ signaling in T-cells depends on its ability to be phosphorylated and subsequently bound by ZAP70 (Wange and Samelson, 1996), we tested the effect of the tyrosine kinase inhibitor pervanadate on the phosphorylation status of both CD3 ζ wildtype and mutant fusion proteins in neurons. As expected wildtype CD3 ζ is phosphorylated whereas the 6YF mutant shows no phosphorylations. The phosphorylation of the D36A mutant is clearly reduced compared to the wildtype protein. While the anti-phospho-tyrosine antibody produces a double band in the CD3 ζ wildtype sample, only the lower band of these two can be seen in the D36A mutant lane indicating the phosphorylation of only some of the six possible tyrosine residues. This suggests a smaller signaling capacity compared to wildtype CD3 ζ , but does not necessarily mean that signal transduction is largely impaired.

The only moderate phosphorylation suggests an impaired functionality of the D36A mutant which might be due to its reduced surface expression in hippocampal neurons. It is clearly decreased compared to CD3 ζ wildtype. Whether this is caused by an impaired plasma membrane integration of the protein or by fast degradation owing to the lack of functionality is not clear. Both phenomena would explain the inclusion of CD3 ζ -D36A-GFP in vesicles as can be observed after overexpression in COS7 cells. These vesicles might either be structures of the Golgi apparatus or the proteasome degradation machinery. The neuronal surface expression of the 6YF mutant is only slightly and not significantly reduced leading to fewer and smaller vesicles in COS7 cells. Nevertheless, both mutants fail to reach their destined localization in developing neurons. While CD3 ζ wildtype fusion protein is present at dendritic tips in DIV7 hippocampal neurons, comparable with the endogenous protein, both mutants show a more equal distribution throughout the dendritic branch. After all these experiments, it still remained unclear whether CD3 ζ -D36A is a true loss-of-function mutant.

Therefore, we decided to test all mutants in a previously published functional paradigm. Baudouin *et al.* (2008) reported that transient CD3 ζ GFP overexpression led to reduced dendrite complexity in developing neurons while the 6YF mutant had the opposite effect when performing Sholl analysis two days after transfection. We transfected DIV8 hippocampal neurons with CD3 ζ wildtype, both mutants and GFP control and analyzed the dendritic arbor nine hours later. Overexpression CD3 ζ GFP

indeed resulted in decreased dendrite complexity. Both mutants have no effect within the nine-hour overexpression period.

The influence of CD3 ζ wildtype and mutant overexpression in mature neurons is very different though. While viral overexpression of the wildtype has no effect on dendrite complexity, both mutants lead to increased dendritic arborization at DIV16. This apparent contradiction might be explained by the different overexpression modes. In DIV8 neurons, overexpression was achieved by classical transient transfection with a eukaryotic pEGFP vector resulting in high protein expression levels within a short amount of time. Older neurons were infected with a CD3 ζ wildtype or mutant virus at DIV10 and fixed at DIV16. This approach yields much more subtle and physiological expression levels that can explain the normal dendrite complexity in CD3 ζ wildtype overexpressing neurons. Furthermore, at DIV11 endogenous CD3 ζ is found at postsynaptic sites suggesting that it has little effect on dendrite outgrowth from this time point on.

On the other hand, this would suggest an influence on synaptic structures. Analogously to its effect on dendrite complexity, the 6YF mutant increases the area of post- and presynaptic puncta without altering their numbers. The enlargement of the postsynapse can be explained by an influence on the actin-based spinoskeleton. The increase in presynaptic area might then just be a cellular response to this.

Why the overexpression of the D36A mutant also results in larger presynapses remains elusive and hard to explain. As the observed effect is rather small, it might just be a statistical artifact, especially since the number of postsynaptic sites under these conditions is clearly reduced. Contrarily, CD3 ζ wildtype overexpression decreases the amount of presynaptic sites. In both cases, the logical consequence is the presence of fewer synapses. For the better understanding of synaptic CD3 ζ functions, it is advisable to conduct a 3D-analysis of high-resolution confocal images yielding much more precise results.

Concluding the characterization of the mutants, one can state that the impaired functioning of CD3 ζ -6YF is clearly explained by the lack of phosphorylation sites. However, the operation mode of the D36A mutant remains speculative. It is perceivable that the mutant sequesters endogenous CD3 ζ in vesicles through dimerization and thereby keeps it from exerting its proper function analogous to the

effect of a knock-down. Another possibility is that the mutations impairs the interaction with a putative receptor whose signaling is pivotal for CD3 ζ functioning.

4.4 Linking CD3 ζ to the NR2B Subunit of the NMDAR

Studies have connected CD3 ζ to the NMDAR before. For example, CD3 $\zeta^{-/-}$ mice show enhanced hippocampal LTP that can be abolished by the application of the general NMDAR receptor inhibitor D-APV (Huh *et al.*, 2000). These mice also display impaired glutamate receptor dependent synaptogenesis in retinal ganglion cells (Xu *et al.*, 2010). In 2013, Louveau *et al.* presented a first evidence of an immediate molecular association between the NMDAR and CD3 ζ . The subunit NR2A could be co-immunoprecipitated with CD3 ζ from adult mouse brain lysate.

In our study, we are able to coimmunoprecipitate NR2B with CD3 ζ from synaptosomes lysate from adult rat forebrain. Both proteins also show colocalization at homer-positive postsynaptic sites in DIV21 hippocampal neurons. On a functional level, CD3 ζ influences NR2B expression levels after stimulation with NMDA in DIV16 hippocampal neurons. In this paradigm, NR2B levels in GFP control and CD3 ζ wildtype overexpressing neurons decrease after treatment in agreement with published data (Nong *et al.*, 2013). NR2B in mutant transfected cells remains at pre-treatment levels which are slightly, albeit not significantly lower than in the other two groups. Louveau *et al.* (2013) have shown that adult CD3 $\zeta^{-/-}$ mice display reduced NR2A levels, but no significant alteration in NR2B levels in synaptosome fractions. Nevertheless, it proves that CD3 ζ influences NMDAR expression.

We asked whether this also applies to NR2B surface expression. Overexpression of CD3 ζ wildtype and D36A mutant reduces intensity of NR2B immunofluorescence compared to GFP control and the 6YF mutant whereas the area of surface NR2B positive puncta remains the same under all conditions. This gives a first hint of an altered surface expression. Here again, 3D-analysis of high-resolution confocal images would help to verify the results.

While the assessment of CD3 ζ influence on NMDARs is rather complex, the reciprocal effect is easier to observe by testing the phosphorylation levels of CD3 ζ . The experiment clearly shows the dependency of CD3 ζ phosphorylation on NMDAR, but

not on AMPAR activation. As the NR2B-specific inhibitor only yielded a minor and not significant decrease of CD3 ζ phosphorylation, we can conclude that in mature neurons, CD3 ζ functionality might depend more on NR2A-containing than on NR2B-containing receptors. But what about developing neurons?

Assessing NR2B expression levels in DIV8 neurons overexpressing CD3 ζ or its mutants resulted in reduced levels in all conditions compared to GFP control. Apparently, NR2B is very sensitive to any strong changes in CD3 ζ . Indeed, it has been described that NR2B and CD3 ζ work together to regulate the cytoskeleton (Baudouin *et al.*, 2008; Bustos *et al.*, 2014), thus we decided to assess their association employing Sholl analysis in DIV8 CD3 ζ wildtype or mutant overexpressing neurons under the influence of selected inhibitors putative upstream and downstream signaling partners.

4.5 CD3 ζ Mediates NR2B-dependent Regulation of the Neuronal Cytoskeleton

NMDARs have long been implicated in the reorganization of the neuronal actin cytoskeleton (Rajan *et al.*, 1998; McAllister, 2000; Sin *et al.*, 2002; Ruthazer *et al.*, 2003). Most published studies examine the function of NMDARs in spines, where they have been shown to regulate cofilin activity after induction of LTP or LTD leading to spine growth or shrinkage respectively (Fukazawa *et al.*, 2003; Zhou *et al.*, 2004). Postsynaptic NMDARs have been linked to late dendritic development and outgrowth in *Xenopus laevis* tadpoles (Rajan *et al.*, 1998; Sin *et al.*, 2002). However, there is only one study addressing NMDAR involvement in cytoskeletal dynamics during initial formation of dendrites prior to synapse formation corresponding to a prenatal neuronal state *in vivo* equivalent to several days *in vitro* (Dotti *et al.*, 1988). Due to the presence of NR2B-containing NMDARs during early developmental stages, it is likely that the NR2B subunit plays a crucial role in these early phases. Only very recently, Bustos *et al.* (2014) reported that overexpression of NR2B in DIV7 hippocampal neurons results in a more complex dendrite arbor. They argue that high levels of endogenous NR2B correlate with high dendrite complexity which peaks around DIV7 in hippocampal neurons. As neurons mature, the NMDAR ratio shifts toward NR2A-containing receptors coinciding with the deceleration of the dendritic arborization.

However, the study by Bustos et al. (2014) lacks a mechanism linking NR2B to the cytoskeleton.

As an important and novel finding, our experiments show that actin regulation through CD3 ζ depends on NMDAR activation. As ifenprodil also abolished the dendrite complexity reducing effect of CD3 ζ , we conclude that NR2B is the crucial subunit in this mechanism. This view is confirmed by the fact that both APV and ifenprodil inhibition reduces CD3 ζ phosphorylation needed for its activation in cultured hippocampal neurons. In contrast, CNQX blockage of AMPAR does not rescue the CD3 ζ overexpression phenotype. This is consistent with my experiments showing that neither the GluR1 nor the GluR2 subunit of the receptor can be coimmunoprecipitated with CD3 ζ . Interestingly, blocking AMPAR activity leads to reduced CD3 ζ phosphorylation allowing us to speculate about a second functional CD3 ζ pool involved in additional and different signaling pathways involved in other cell function.

As described in the introductory section, CD3 ζ can be phosphorylated by two Src kinase family members in T-cells – Fyn and Lck (Wange and Samelson, 1996). These non-receptor type tyrosine kinases are also expressed in neurons. Whereas there's little known about Lck function in the brain, Fyn and Src kinase have been studied extensively. Both kinases seem to have redundant functions to a certain degree (Stein *et al.*, 1994), and both have been implied in the regulation of dendritic and axonal outgrowth. Brouns *et al.* (2001) observed defects in axonal outgrowth in Src $^{-/-}$ and Fyn $^{-/-}$ mice. The latter also display shorter apical dendrites of pyramidal neurons in the CA1 region of the hippocampus (Kojima *et al.*, 1997).

Consistent with the literature, applying PP2, a general src-kinase family inhibitor with an affinity for all three above-mentioned kinases (Hanke *et al.*, 1996), resulted in reduced dendrite complexity in GFP-overexpressing control neurons in our experiment. More importantly, PP2 was also able to rescue the CD3 ζ overexpression phenotype indicating the involvement of src kinases in the pathway. By using the Lck inhibitor damnacanthal (Faltynek *et al.*, 1995), we aimed at clarifying if Lck or rather Fyn and Src were the responsible kinases. Indeed, damnacanthal treatment resulted in higher complexity of dendrites in CD3 ζ GFP overexpressing cells similar to control and loss-of-function mutant levels. Again, the inhibitor had the reverse effect on GFP

control neurons. However, while damnacanthal had previously been reported to be a specific inhibitor of Lck (Faltynek *et al.*, 1995), more recent studies have shown a much higher affinity for the kinase LIMK (Ohashi *et al.*, 2014). LIMK phosphorylates cofilin and thereby regulates actin dynamics (Yang *et al.*, 1998). Therefore, the effect on dendrite outgrowth cannot be clearly related to Lck. This is supported by the fact that damnacanthal does not affect CD3 ζ phosphorylation levels in neurons. If Lck was inhibited, a decrease of phosphorylation as seen with PP2 would be expected. The current evidence points to the involvement of Fyn and/or Src in the activation of CD3 ζ and the subsequent negative regulation of dendrite outgrowth.

Another kinase shown to participate in CD3 ζ signaling in T-cells (Koyasu, 2003) and in the regulation of the neuronal cytoskeleton (Jacinto *et al.*, 2004) is PI3K. Application of the PI3K inhibitor wortmannin (Wymann *et al.*, 1996) abolishes the effect of CD3 ζ GFP overexpression on dendrite complexity, but does not impair CD3 ζ phosphorylation. This leads to the conclusion that PI3K acts downstream of CD3 ζ . At the same time this might associate CD3 ζ with the mTOR signaling pathway in neurons as it has already been shown in T-cells (Thomson *et al.*, 2009; Chi, 2012; Hamilton *et al.*, 2014). Conducting experiments using the mTOR inhibitor rapamycin might be able verify this hypothesis.

Nevertheless, the most prominent kinase associated with CD3 ζ in T-cells is ZAP70 (Wang *et al.*, 2010). As an immediate downstream actor of the TCR complex, it is the central signaling hub where most signals involved in T-cell activation diverge from (Chan *et al.*, 1994). The ZAP70 inhibitor piceatannol (Geahlen *et al.*, 1989; Oliver *et al.* 1994) can block the effect of CD3 ζ and leads to control levels of dendrite complexity in CD3 ζ GFP overexpressing neurons. This implies a direct involvement of ZAP70 in CD3 ζ -dependent remodeling of the actin cytoskeleton, but also opens up possibilities for yet unknown neuronal signaling pathways. One of these pathways seems to regulate CD3 ζ localization at dendritic tips of developing hippocampal neurons (Baudouin *et al.*, 2008). Here, short application of piceatannol leads to the dispersion of CD3 ζ clusters throughout the dendrite away from the dendritic tip.

Both PI3K and ZAP70 have been implied in the regulation of small GTPases of the Rho subfamily (Jacinto *et al.*, 2004; Piragyte and Jun, 2012; Kumari *et al.*, 2013). In neurons, negative regulation of dendrite outgrowth is mediated by the GTPase RhoA

and its effector kinase ROCK (McAllister, 2000; Luo, 2002; Koleske, 2013). Inhibition of ROCK with Y-27632 (Uehata *et al.*, 1997) abolishes the CD3 ζ GFP overexpression phenotype suggesting that the CD3 ζ -dependent regulation of actin cytoskeleton remodeling is mediated by the RhoA/ROCK pathway. This pathway leads to the phosphorylation and subsequent inactivation of cofilin resulting in higher actin polymer stability. However, at the same time, ROCK can inactivate profilin which has the opposite effect (Okamoto *et al.*, 2009). The final outcome is the result of a well-balanced process to enable a precise regulation of actin dynamics.

4.6 Conclusion and Outlook

Taking all data together, there is strong evidence for the activation of ZAP70 and PI3K downstream of CD3 ζ in hippocampal neurons that leads to a negative regulation of dendritic outgrowth by activating the RhoA/ROCK pathway. Furthermore, this is NMDAR-, but not AMPAR-dependent. To our knowledge, this is the first study showing a mechanism between NR2B-containing NMDARs and the regulation of the actin cytoskeleton in developing hippocampal neurons prior to synaptogenesis. Figure 40 shows a possible signal transduction model including suggestions for further downstream signaling events that are partially inferred by the TCR signaling network and can be objects of future studies. It is perceivable that similar processes take place at postsynapses of mature neurons, although here, NR2A-containing NMDARs may play a bigger role.

Nevertheless, the questions of how NMDARs influence CD3 ζ remains. There is no evidence for a direct interaction between both proteins. One possibility is that Ca²⁺ influx through NMDARs activates yet unknown mediators. If the CD3 ζ -receptor interaction follows the same rules as in T-cell, we are looking for a transmembrane protein with a positively charged amino acid residue with its transmembrane domain. In this case, the CD3 ζ -D36A mutant may prove as a useful tool. However, there is also the possibility that the interaction follows other rules. Studies show that CD3 ζ associates with Fc γ receptor III (Lanier *et al.*, 1989; Arase *et al.*, 2001) that does not possess a positively charged amino acid in its transmembrane domain.

In either case, electrophysiological studies of CD3 ζ -dependent NMDAR behavior will give a more complete picture on their apparent interdependence. Here, not only the

mutants, but also the shRNA constructs introduced in this work may be helpful – especially when introduced into lentiviral expression vectors allowing for a longer observation period of CD3 ζ deficiency.

With the tools presented in this thesis, further experiments regarding neuronal CD3 ζ signaling can be conducted. It will be worthwhile to take a look at the immunological side when deciphering signaling pathways in neurons. This study among others (for review see Boulanger, 2009; Fourgeaud and Boulanger, 2010; Steinman, 2012) shows that they have much more in common than obvious at first sight, and immunologists and neurobiologists may learn a lot from each other.

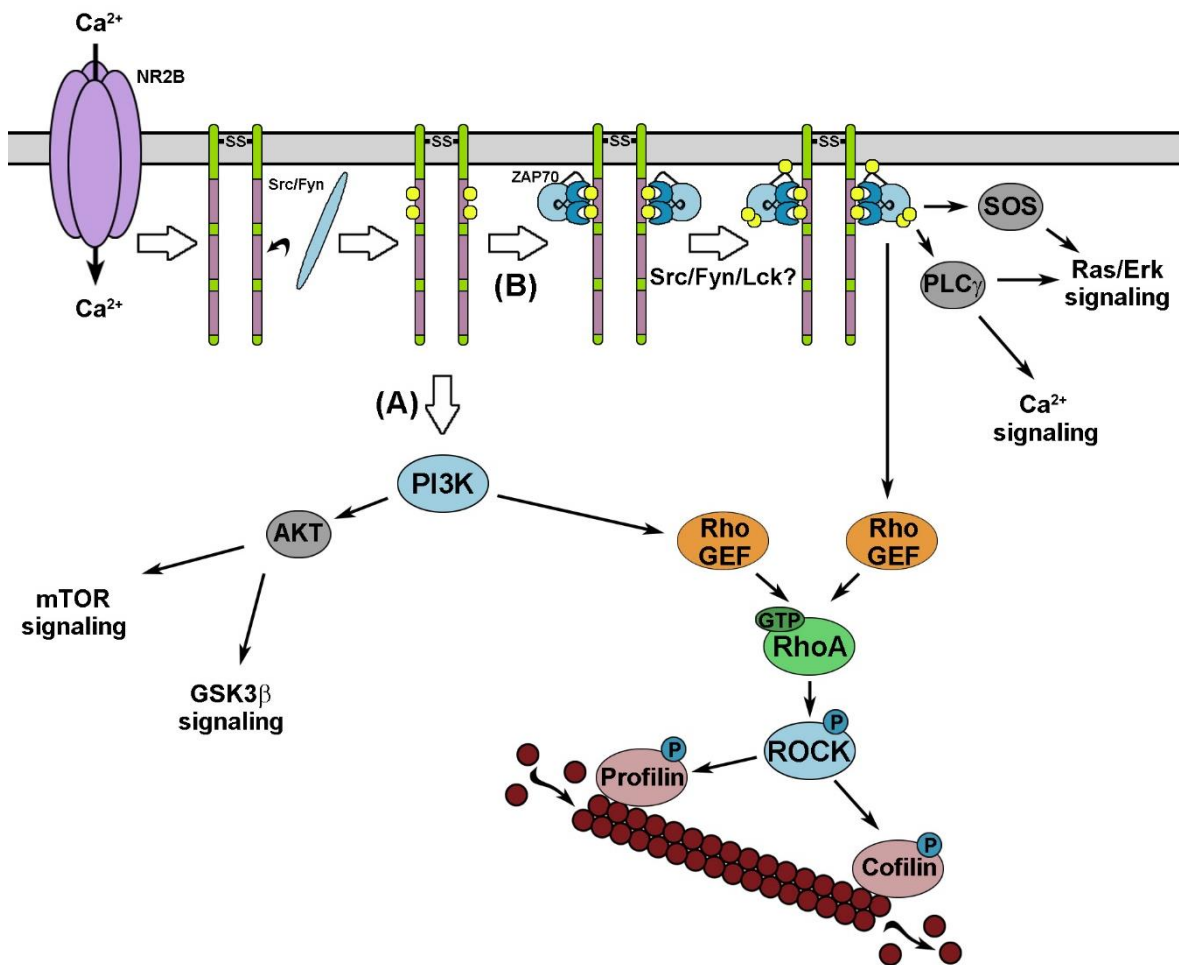


Figure 40: Proposed model of CD3 ζ signaling in developing hippocampal neurons. The activation of NR2B-containing NMDARs leads to the activation of CD3 ζ by Src/Fyn. Then our data suggest two probably independent scenarios. **(A)** Phosphorylated CD3 ζ leads to the activation of PI3K and its subsequent regulation of RhoA through a yet unidentified RhoGEF. **(B)** ZAP70 binds phosphorylated CD3 ζ and is itself activated by a src family kinase. ZAP70 then triggers the activation of RhoA. The GTPase activates ROCK and thereby regulates the actin-binding proteins cofilin and profilin. This way a finely balanced adjustment of the actin cytoskeleton can be achieved that in this specific case leads to a negative regulation of dendrite outgrowth. The association of CD3 ζ with ZAP70 and PI3K also opens further putative pathways indicated in grey.

5 Literature

Angibaud J, Baudouin SJ, Louveau A, Nerriere-Daguin V, Bonnamain V, Csaba Z, Dournaud P, Naveilhan P, Noraz N, Pellier-Monnin V, Boudin H (2012) Ectopic expression of the immune adaptor protein CD3zeta in neural stem/progenitor cells disrupts cell-fate specification. *Journal of molecular neuroscience : MN* **46**: 431-441

Angibaud J, Louveau A, Baudouin SJ, Nerriere-Daguin V, Evain S, Bonnamain V, Hulin P, Csaba Z, Dournaud P, Thinarth R, Naveilhan P, Noraz N, Pellier-Monnin V, Boudin H (2011) The immune molecule CD3zeta and its downstream effectors ZAP-70/Syk mediate ephrin signaling in neurons to regulate early neurogenesis. *Journal of neurochemistry* **119**: 708-722

Appleby VJ, Correa SA, Duckworth JK, Nash JE, Noel J, Fitzjohn SM, Collingridge GL, Molnar E (2011) LTP in hippocampal neurons is associated with a CaMKII-mediated increase in GluA1 surface expression. *Journal of neurochemistry* **116**: 530-543

Arase H, Suenaga T, Arase N, Kimura Y, Ito K, Shiina R, Ohno H, Saito T (2001) Negative regulation of expression and function of Fc gamma RIII by CD3 zeta in murine NK cells. *Journal of immunology* **166**: 21-25

Bach TL, Kerr WT, Wang Y, Bauman EM, Kine P, Whiteman EL, Morgan RS, Williamson EK, Ostap EM, Burkhardt JK, Koretzky GA, Birnbaum MJ, Abrams CS (2007) PI3K regulates pleckstrin-2 in T-cell cytoskeletal reorganization. *Blood* **109**: 1147-1155

Baniyash M (2004) TCR zeta-chain downregulation: curtailing an excessive inflammatory immune response. *Nature reviews Immunology* **4**: 675-687

Baudouin SJ, Angibaud J, Loussouarn G, Bonnamain V, Matsuura A, Kinebuchi M, Naveilhan P, Boudin H (2008) The signaling adaptor protein CD3zeta is a negative regulator of dendrite development in young neurons. *Molecular biology of the cell* **19**: 2444-2456

Birnboim HC, Doly J (1979) A rapid alkaline extraction procedure for screening recombinant plasmid DNA. *Nucleic Acids Res* **7**: 1513-1523

Boulanger LM (2009) Immune proteins in brain development and synaptic plasticity. *Neuron* **64**: 93-109

Broderick G, Craddock TJ (2013) Systems biology of complex symptom profiles: capturing interactivity across behavior, brain and immune regulation. *Brain, behavior, and immunity* **29**: 1-8

Brouns MR, Matheson SF, Settleman J (2001) p190 RhoGAP is the principal Src substrate in brain and regulates axon outgrowth, guidance and fasciculation. *Nature cell biology* **3**: 361-367

Bustos FJ, Varela-Nallar L, Campos M, Henriquez B, Phillips M, Opazo C, Aguayo LG, Montecino M, Constantine-Paton M, Inestrosa NC, van Zundert B (2014) PSD95 suppresses dendritic arbor development in mature hippocampal neurons by occluding the clustering of NR2B-NMDA receptors. *PLoS One* **9**: e94037

Call ME, Pyrdol J, Wiedmann M, Wucherpfennig KW (2002) The organizing principle in the formation of the T cell receptor-CD3 complex. *Cell* **111**: 967-979

Call ME, Pyrdol J, Wucherpfennig KW (2004) Stoichiometry of the T-cell receptor-CD3 complex and key intermediates assembled in the endoplasmic reticulum. *The EMBO journal* **23**: 2348-2357

Chan AC, Desai DM, Weiss A (1994) The role of protein tyrosine kinases and protein tyrosine phosphatases in T cell antigen receptor signal transduction. *Annual review of immunology* **12**: 555-592

Chen H, Firestein BL (2007) RhoA regulates dendrite branching in hippocampal neurons by decreasing cypin protein levels. *The Journal of neuroscience : the official journal of the Society for Neuroscience* **27**: 8378-8386

Chi H (2012) Regulation and function of mTOR signalling in T cell fate decisions. *Nature reviews Immunology* **12**: 325-338

Cingolani LA, Goda Y (2008) Actin in action: the interplay between the actin cytoskeleton and synaptic efficacy. *Nature reviews Neuroscience* **9**: 344-356

Corriveau RA, Huh GS, Shatz CJ (1998) Regulation of class I MHC gene expression in the developing and mature CNS by neural activity. *Neuron* **21**: 505-520

Cull-Candy SG, Leszkiewicz DN (2004) Role of distinct NMDA receptor subtypes at central synapses. *Science's STKE : signal transduction knowledge environment* **2004**: re16

Da Silva JS, Medina M, Zuliani C, Di Nardo A, Witke W, Dotti CG (2003) RhoA/ROCK regulation of neuriteogenesis via profilin IIa-mediated control of actin stability. *The Journal of cell biology* **162**: 1267-1279

Datwani A, McConnell MJ, Kanold PO, Micheva KD, Busse B, Shamloo M, Smith SJ, Shatz CJ (2009) Classical MHCI molecules regulate retinogeniculate refinement and limit ocular dominance plasticity. *Neuron* **64**: 463-470

Derkinderen P, Valjent E, Toutant M, Corvol JC, Enslen H, Ledent C, Trzaskos J, Caboche J, Girault JA (2003) Regulation of extracellular signal-regulated kinase by cannabinoids in hippocampus. *The Journal of neuroscience : the official journal of the Society for Neuroscience* **23**: 2371-2382

Diamond B (2010) Antibodies and the Brain: Lessons from Lupus. *Journal of immunology* **185**: 2637-2640

Dittgen T, Nimmerjahn A, Komai S, Licznanski P, Waters J, Margrie TW, Helmchen F, Denk W, Brecht M, Osten P (2004) Lentivirus-based genetic manipulations of cortical neurons and their optical and electrophysiological monitoring in vivo. *Proceedings of the National Academy of Sciences of the United States of America* **101**: 18206-18211

Dotti CG, Sullivan CA, Banker GA (1988) The establishment of polarity by hippocampal neurons in culture. *The Journal of neuroscience : the official journal of the Society for Neuroscience* **8**: 1454-1468

Dustin ML, Colman DR (2002) Neural and immunological synaptic relations. *Science* **298**: 785-789

Dustin ML, Cooper JA (2000) The immunological synapse and the actin cytoskeleton: molecular hardware for T cell signaling. *Nature immunology* **1**: 23-29

Faltynek CR, Schroeder J, Mauvais P, Miller D, Wang S, Murphy D, Lehr R, Kelley M, Maycock A, Michne W, et al. (1995) Damnacanthal is a highly potent, selective inhibitor of p56lck tyrosine kinase activity. *Biochemistry* **34**: 12404-12410

Fourgeaud L, Boulanger LM (2010) Role of immune molecules in the establishment and plasticity of glutamatergic synapses. *The European journal of neuroscience* **32**: 207-217

Fukazawa Y, Saitoh Y, Ozawa F, Ohta Y, Mizuno K, Inokuchi K (2003) Hippocampal LTP is accompanied by enhanced F-actin content within the dendritic spine that is essential for late LTP maintenance in vivo. *Neuron* **38**: 447-460

Geahlen RL, McLaughlin JL (1989) Piceatannol (3,4,3',5'-tetrahydroxy-trans-stilbene) is a naturally occurring protein-tyrosine kinase inhibitor. *Biochemical and biophysical research communications* **165**: 241-245

Gladding CM, Raymond LA (2011) Mechanisms underlying NMDA receptor synaptic/extrasynaptic distribution and function. *Molecular and cellular neurosciences* **48**: 308-320

Glantz LA, Gilmore JH, Hamer RM, Lieberman JA, Jarskog LF (2007) Synaptophysin and postsynaptic density protein 95 in the human prefrontal cortex from mid-gestation into early adulthood. *Neuroscience* **149**: 582-591

Gloeckner CJ, Boldt K, Schumacher A, Roepman R, Ueffing M (2007) A novel tandem affinity purification strategy for the efficient isolation and characterisation of native protein complexes. *Proteomics* **7**: 4228-4234

Goddard CA, Butts DA, Shatz CJ (2007) Regulation of CNS synapses by neuronal MHC class I. *Proceedings of the National Academy of Sciences of the United States of America* **104**: 6828-6833

Gornall AG, Bardawill CJ, David MM (1949) Determination of serum proteins by means of the biuret reaction. *The Journal of biological chemistry* **177**: 751-766

Govek EE, Newey SE, Van Aelst L (2005) The role of the Rho GTPases in neuronal development. *Genes & development* **19**: 1-49

Green, MR and Sambrook J (2012) Molecular Cloning – A Laboratory Manual (Fourth Edition). *Cold Spring Harbor Laboratory Press*

Groc L, Heine M, Cousins SL, Stephenson FA, Lounis B, Cognet L, Choquet D (2006) NMDA receptor surface mobility depends on NR2A-2B subunits. *Proceedings of the National Academy of Sciences of the United States of America* **103**: 18769-18774

Gunning PW, Hardeman EC, Lappalainen P, Mulvihill DP (2015) Tropomyosin - master regulator of actin filament function in the cytoskeleton. *Journal of cell science* **128**: 2965-2974

Hamilton KS, Phong B, Corey C, Cheng J, Gorentla B, Zhong X, Shiva S, Kane LP (2014) T cell receptor-dependent activation of mTOR signaling in T cells is mediated by Carma1 and MALT1, but not Bcl10. *Science signaling* **7**: ra55

Hanisch UK, Kettenmann H (2007) Microglia: active sensor and versatile effector cells in the normal and pathologic brain. *Nature neuroscience* **10**: 1387-1394

Hanke JH, Gardner JP, Dow RL, Changelian PS, Brissette WH, Weringer EJ, Pollok BA, Connelly PA (1996) Discovery of a novel, potent, and Src family-selective tyrosine kinase inhibitor. Study of Lck- and FynT-dependent T cell activation. *The Journal of biological chemistry* **271**: 695-701

Hanley JG (2008) AMPA receptor trafficking pathways and links to dendritic spine morphogenesis. *Cell adhesion & migration* **2**: 276-282

Hardingham GE, Bading H (2010) Synaptic versus extrasynaptic NMDA receptor signalling: implications for neurodegenerative disorders. *Nature reviews Neuroscience* **11**: 682-696

Hatterer E, Benon A, Chounlamountri N, Watrin C, Angibaud J, Jouanneau E, Boudin H, Honnorat J, Pellier-Monnin V, Noraz N (2011) Syk kinase is phosphorylated in specific areas of the developing nervous system. *Neurosci Res* **70**: 172-182

Herrera-Molina R, Sarto-Jackson I, Montenegro-Venegas C, Heine M, Smalla KH, Seidenbecher CI, Beesley PW, Gundelfinger ED, Montag D (2014) Structure of excitatory synapses and GABAA receptor localization at inhibitory synapses are regulated by neuroplastin-65. *The Journal of biological chemistry* **289**: 8973-8988

Herrmann H, Bar H, Kreplak L, Strelkov SV, Aebi U (2007) Intermediate filaments: from cell architecture to nanomechanics. *Nature reviews Molecular cell biology* **8**: 562-573

Honore T, Davies SN, Drejer J, Fletcher EJ, Jacobsen P, Lodge D, Nielsen FE (1988) Quinoxalinediones: potent competitive non-NMDA glutamate receptor antagonists. *Science* **241**: 701-703

Horak M, Petralia RS, Kaniakova M, Sans N (2014) ER to synapse trafficking of NMDA receptors. *Frontiers in cellular neuroscience* **8**: 394

Hotulainen P, Hoogenraad CC (2010) Actin in dendritic spines: connecting dynamics to function. *The Journal of cell biology* **189**: 619-629

Huang SH, Wang J, Sui WH, Chen B, Zhang XY, Yan J, Geng Z, Chen ZY (2013) BDNF-dependent recycling facilitates TrkB translocation to postsynaptic density during LTP via a Rab11-dependent pathway. *The Journal of neuroscience : the official journal of the Society for Neuroscience* **33**: 9214-9230

Huh GS, Boulanger LM, Du H, Riquelme PA, Brotz TM, Shatz CJ (2000) Functional requirement for class I MHC in CNS development and plasticity. *Science* **290**: 2155-2159

Huyer G, Liu S, Kelly J, Moffat J, Payette P, Kennedy B, Tsaprailis G, Gresser MJ, Ramachandran C (1997) Mechanism of inhibition of protein-tyrosine phosphatases by vanadate and pervanadate. *The Journal of biological chemistry* **272**: 843-851

Ippolito DM, Eroglu C (2010) Quantifying synapses: an immunocytochemistry-based assay to quantify synapse number. *Journal of visualized experiments : JoVE*

Jacinto E, Loewith R, Schmidt A, Lin S, Ruegg MA, Hall A, Hall MN (2004) Mammalian TOR complex 2 controls the actin cytoskeleton and is rapamycin insensitive. *Nature cell biology* **6**: 1122-1128

Jan YN, Jan LY (2010) Branching out: mechanisms of dendritic arborization. *Nature reviews Neuroscience* **11**: 316-328

Jones AR, Overly CC, Sunkin SM (2009) The Allen Brain Atlas: 5 years and beyond. *Nature reviews Neuroscience* **10**: 821-828

Kaech S, Banker G (2006) Culturing hippocampal neurons. *Nat Protoc* **1**: 2406-2415

Kapitein LC, Hoogenraad CC (2011) Which way to go? Cytoskeletal organization and polarized transport in neurons. *Molecular and cellular neurosciences* **46**: 9-20

Kim DY, Kovacs DM (2011) Surface trafficking of sodium channels in cells and in hippocampal slices. *Methods in molecular biology* **793**: 351-361

Kim K, Yang J, Kim E (2010) Diacylglycerol kinases in the regulation of dendritic spines. *Journal of neurochemistry* **112**: 577-587

Kojima N, Wang J, Mansuy IM, Grant SG, Mayford M, Kandel ER (1997) Rescuing impairment of long-term potentiation in fyn-deficient mice by introducing Fyn transgene. *Proceedings of the National Academy of Sciences of the United States of America* **94**: 4761-4765

Koleske AJ (2013) Molecular mechanisms of dendrite stability. *Nature reviews Neuroscience* **14**: 536-550

Koyasu S (2003) The role of PI3K in immune cells. *Nature immunology* **4**: 313-319

Kumari S, Curado S, Mayya V, Dustin ML (2014) T cell antigen receptor activation and actin cytoskeleton remodeling. *Biochimica et biophysica acta* **1838**: 546-556

Laemmli UK (1970) Cleavage of structural proteins during the assembly of the head of bacteriophage T4. *Nature* **227**: 680-685

Lanier LL, Yu G, Phillips JH (1989) Co-association of CD3 zeta with a receptor (CD16) for IgG Fc on human natural killer cells. *Nature* **342**: 803-805

Lee MK, Cleveland DW (1996) Neuronal intermediate filaments. *Annual review of neuroscience* **19**: 187-217

Leemhuis J, Boutillier S, Barth H, Feuerstein TJ, Brock C, Nurnberg B, Aktories K, Meyer DK (2004) Rho GTPases and phosphoinositide 3-kinase organize formation of branched dendrites. *The Journal of biological chemistry* **279**: 585-596

Lein ES, Hawrylycz MJ, Ao N, Ayres M, Bensinger A, Bernard A, Boe AF, Boguski MS, Brockway KS, Byrnes EJ, Chen L, Chen TM, Chin MC, Chong J, Crook BE, Czaplinska A, Dang CN, Datta S, Dee NR, Desaki AL, Desta T, Diep E, Dolbeare TA, Donelan MJ, Dong HW, Dougherty JG, Duncan BJ, Ebbert AJ, Eichele G, Estin LK, Faber C, Facer BA, Fields R, Fischer SR, Fliss TP, Frensley C, Gates SN, Glattfelder KJ, Halverson KR, Hart MR, Hohmann JG, Howell MP, Jeung DP, Johnson RA, Karr PT, Kawal R, Kidney JM, Knapik RH, Kuan CL, Lake JH, Laramée AR, Larsen KD, Lau C, Lemon TA, Liang AJ, Liu Y, Luong LT, Michaels J, Morgan JJ, Morgan RJ, Mortrud MT, Mosqueda NF, Ng LL, Ng R, Orta GJ, Overly CC, Pak TH, Parry SE, Pathak SD, Pearson OC, Puchalski RB, Riley ZL, Rockett HR, Rowland SA, Royall JJ, Ruiz MJ, Sarno NR, Schaffnit K, Shapovalova NV, Sivisay T, Slaughterbeck CR, Smith SC, Smith KA, Smith BI, Sott AJ, Stewart NN, Stumpf KR, Sunkin SM, Sutram M, Tam A, Teemer CD, Thaller C, Thompson CL, Varnam LR, Visel A, Whitlock RM, Wohnoutka PE, Wolkey CK, Wong VY, Wood M, Yaylaoglu MB, Young RC, Youngstrom BL, Yuan XF, Zhang B, Zwingman TA, Jones AR (2007) Genome-wide atlas of gene expression in the adult mouse brain. *Nature* **445**: 168-176

Levite M (2008) Neurotransmitters activate T-cells and elicit crucial functions via neurotransmitter receptors. *Current opinion in pharmacology* **8**: 460-471

Li GH, Jackson MF, Orser BA, Macdonald JF (2009) Reciprocal and activity-dependent regulation of surface AMPA and NMDA receptors in cultured neurons. *International journal of physiology, pathophysiology and pharmacology* **2**: 47-56

Lois C, Hong EJ, Pease S, Brown EJ, Baltimore D (2002) Germline transmission and tissue-specific expression of transgenes delivered by lentiviral vectors. *Science* **295**: 868-872

Long SK, Smith DA, Siarey RJ, Evans RH (1990) Effect of 6-cyano-2,3-dihydroxy-7-nitro-quinoline (CNQX) on dorsal root-, NMDA-, kainate- and quisqualate-mediated depolarization of rat motoneurons in vitro. *British journal of pharmacology* **100**: 850-854

Louveau A, Angibaud J, Haspot F, Opazo MC, Thinard R, Thepenier V, Baudouin SJ, Lescaudron L, Hulin P, Riedel CA, Boudin H (2013) Impaired spatial memory in mice lacking CD3zeta is associated with altered NMDA and AMPA receptors signaling independent of T-cell deficiency. *The Journal of neuroscience : the official journal of the Society for Neuroscience* **33**: 18672-18685

Lucin KM, Wyss-Coray T (2009) Immune activation in brain aging and neurodegeneration: too much or too little? *Neuron* **64**: 110-122

Luo L (2002) Actin cytoskeleton regulation in neuronal morphogenesis and structural plasticity. *Annual review of cell and developmental biology* **18**: 601-635

Luscher C, Malenka RC (2012) NMDA receptor-dependent long-term potentiation and long-term depression (LTP/LTD). *Cold Spring Harbor perspectives in biology* **4**

Luscher C, Xia H, Beattie EC, Carroll RC, von Zastrow M, Malenka RC, Nicoll RA (1999) Role of AMPA receptor cycling in synaptic transmission and plasticity. *Neuron* **24**: 649-658

Maletic-Savatic M, Koothan T, Malinow R (1998) Calcium-evoked dendritic exocytosis in cultured hippocampal neurons. Part II: mediation by calcium/calmodulin-dependent protein kinase II. *The Journal of neuroscience : the official journal of the Society for Neuroscience* **18**: 6814-6821

Marin I, Kipnis J (2013) Learning and memory ... and the immune system. *Learning & memory* **20**: 601-606

Martel MA, Wyllie DJ, Hardingham GE (2009) In developing hippocampal neurons, NR2B-containing N-methyl-D-aspartate receptors (NMDARs) can mediate signaling to neuronal survival and synaptic potentiation, as well as neuronal death. *Neuroscience* **158**: 334-343

Matus A (2000) Actin-based plasticity in dendritic spines. *Science* **290**: 754-758

McAllister AK (2000) Cellular and molecular mechanisms of dendrite growth. *Cerebral cortex* **10**: 963-973

Minichiello L, Calella AM, Medina DL, Bonhoeffer T, Klein R, Korte M (2002) Mechanism of TrkB-mediated hippocampal long-term potentiation. *Neuron* **36**: 121-137

Monyer H, Burnashev N, Laurie DJ, Sakmann B, Seeburg PH (1994) Developmental and regional expression in the rat brain and functional properties of four NMDA receptors. *Neuron* **12**: 529-540

Morris RG (1989) Synaptic plasticity and learning: selective impairment of learning rats and blockade of long-term potentiation in vivo by the N-methyl-D-aspartate receptor antagonist AP5. *The Journal of neuroscience : the official journal of the Society for Neuroscience* **9**: 3040-3057

Mousa A, Bakhiet M (2013) Role of cytokine signaling during nervous system development. *International journal of molecular sciences* **14**: 13931-13957

Nakamura K, Hirai H, Torashima T, Miyazaki T, Tsurui H, Xiu Y, Ohtsuji M, Lin QS, Tsukamoto K, Nishimura H, Ono M, Watanabe M, Hirose S (2007) CD3 and immunoglobulin G Fc receptor regulate cerebellar functions. *Molecular and cellular biology* **27**: 5128-5134

Nance DM, Sanders VM (2007) Autonomic innervation and regulation of the immune system (1987-2007). *Brain, behavior, and immunity* **21**: 736-745

Needleman LA, Liu XB, El-Sabeawy F, Jones EG, McAllister AK (2010) MHC class I molecules are present both pre- and postsynaptically in the visual cortex during postnatal development and in adulthood. *Proceedings of the National Academy of Sciences of the United States of America* **107**: 16999-17004

Newton CR and Graham A (1997) PCR in *Labor im Fokus, Spektrum Akademischer Verlag*.

Nishiyori A, Hanno Y, Saito M, Yoshihara Y (2004) Aberrant transcription of unrearranged T-cell receptor beta gene in mouse brain. *The Journal of comparative neurology* **469**: 214-226

Nong Y, Huang YQ, Ju W, Kalia LV, Ahmadian G, Wang YT, Salter MW (2003) Glycine binding primes NMDA receptor internalization. *Nature* **422**: 302-307

Ohashi K, Sampei K, Nakagawa M, Uchiumi N, Amanuma T, Aiba S, Oikawa M, Mizuno K (2014) Damnacanthal, an effective inhibitor of LIM-kinase, inhibits cell migration and invasion. *Molecular biology of the cell* **25**: 828-840

Okamoto K, Bosch M, Hayashi Y (2009) The roles of CaMKII and F-actin in the structural plasticity of dendritic spines: a potential molecular identity of a synaptic tag? *Physiology* **24**: 357-366

Oliver JM, Burg DL, Wilson BS, McLaughlin JL, Geahlen RL (1994) Inhibition of mast cell Fc epsilon R1-mediated signaling and effector function by the Syk-selective inhibitor, piceatannol. *The Journal of biological chemistry* **269**: 29697-29703

Pak CW, Flynn KC, Bamburg JR (2008) Actin-binding proteins take the reins in growth cones. *Nature reviews Neuroscience* **9**: 136-147

Palfi A, Kortvely E, Fekete E, Kovacs B, Varszegi S, Gulya K (2002) Differential calmodulin gene expression in the rodent brain. *Life sciences* **70**: 2829-2855

Paoletti P (2011) Molecular basis of NMDA receptor functional diversity. *The European journal of neuroscience* **33**: 1351-1365

Paoletti P, Bellone C, Zhou Q (2013) NMDA receptor subunit diversity: impact on receptor properties, synaptic plasticity and disease. *Nature reviews Neuroscience* **14**: 383-400

Penzes P, Cahill ME (2012) Deconstructing signal transduction pathways that regulate the actin cytoskeleton in dendritic spines. *Cytoskeleton (Hoboken)* **69**: 426-441

Penzes P, Rafalovich I (2012) Regulation of the actin cytoskeleton in dendritic spines. *Adv Exp Med Biol* **970**: 81-95

Petralia RS (2012) Distribution of extrasynaptic NMDA receptors on neurons. *TheScientificWorldJournal* **2012**: 267120

Pielot R, Smalla KH, Muller A, Landgraf P, Lehmann AC, Eisenschmidt E, Haus UU, Weismantel R, Gundelfinger ED, Dieterich DC (2012) SynProt: A Database for Proteins of Detergent-Resistant Synaptic Protein Preparations. *Front Synaptic Neurosci* **4**: 1

Piragyte I, Jun CD (2012) Actin engine in immunological synapse. *Immune network* **12**: 71-83

Pollard TD, Cooper JA (2009) Actin, a central player in cell shape and movement. *Science* **326**: 1208-1212

Popov N, Schmitt M, Schulzeck S, Matthies H (1975) [Reliable micromethod for determination of the protein content in tissue homogenates]. *Acta biologica et medica Germanica* **34**: 1441-1446

Racz B, Weinberg RJ (2013) Microdomains in forebrain spines: an ultrastructural perspective. *Molecular neurobiology* **47**: 77-89

Rajan I, Witte S, Cline HT (1999) NMDA receptor activity stabilizes presynaptic retinotectal axons and postsynaptic optic tectal cell dendrites in vivo. *Journal of neurobiology* **38**: 357-368

Ritter AT, Angus KL, Griffiths GM (2013) The role of the cytoskeleton at the immunological synapse. *Immunological reviews* **256**: 107-117

Rohn JL, Baum B (2010) Actin and cellular architecture at a glance. *Journal of cell science* **123**: 155-158

Ruthazer ES, Akerman CJ, Cline HT (2003) Control of axon branch dynamics by correlated activity in vivo. *Science* **301**: 66-70

Rutledge T, Cosson P, Manolios N, Bonifacino JS, Klausner RD (1992) Transmembrane helical interactions: zeta chain dimerization and functional association with the T cell antigen receptor. *The EMBO journal* **11**: 3245-3254

Saez-Rodriguez J, Simeoni L, Lindquist JA, Hemenway R, Bommhardt U, Arndt B, Haus UU, Weismantel R, Gilles ED, Klamt S, Schraven B (2007) A logical model provides insights into T cell receptor signaling. *PLoS Comput Biol* **3**: e163

Sakaguchi N, Takahashi T, Hata H, Nomura T, Tagami T, Yamazaki S, Sakihama T, Matsutani T, Negishi I, Nakatsuru S, Sakaguchi S (2003) Altered thymic T-cell selection due to a mutation of the ZAP-70 gene causes autoimmune arthritis in mice. *Nature* **426**: 454-460

Salter MW, Kalia LV (2004) Src kinases: a hub for NMDA receptor regulation. *Nature reviews Neuroscience* **5**: 317-328

Sanz-Clemente A, Nicoll RA, Roche KW (2013) Diversity in NMDA receptor composition: many regulators, many consequences. *The Neuroscientist : a review journal bringing neurobiology, neurology and psychiatry* **19**: 62-75

Scott EK, Reuter JE, Luo L (2003) Small GTPase Cdc42 is required for multiple aspects of dendritic morphogenesis. *The Journal of neuroscience : the official journal of the Society for Neuroscience* **23**: 3118-3123

Shen WH, Zhang CY, Zhang GY (2003) Modulation of I κ B kinase autophosphorylation and activity following brain ischemia. *Acta pharmacologica Sinica* **24**: 311-315

Sheng M, Cummings J, Roldan LA, Jan YN, Jan LY (1994) Changing subunit composition of heteromeric NMDA receptors during development of rat cortex. *Nature* **368**: 144-147

Sheng M, Kim E (2011) The postsynaptic organization of synapses. *Cold Spring Harbor perspectives in biology* **3**

Sin WC, Haas K, Ruthazer ES, Cline HT (2002) Dendrite growth increased by visual activity requires NMDA receptor and Rho GTPases. *Nature* **419**: 475-480

Singh P, Rathinasamy K, Mohan R, Panda D (2008) Microtubule assembly dynamics: an attractive target for anticancer drugs. *IUBMB life* **60**: 368-375

Snyder EM, Nong Y, Almeida CG, Paul S, Moran T, Choi EY, Nairn AC, Salter MW, Lombroso PJ, Gouras GK, Greengard P (2005) Regulation of NMDA receptor trafficking by amyloid-beta. *Nature neuroscience* **8**: 1051-1058

Sole L, Roura-Ferrer M, Perez-Verdaguer M, Oliveras A, Calvo M, Fernandez-Fernandez JM, Felipe A (2009) KCNE4 suppresses Kv1.3 currents by modulating trafficking, surface expression and channel gating. *Journal of cell science* **122**: 3738-3748

Sprengel R, Suchanek B, Amico C, Brusa R, Burnashev N, Rozov A, Hvalby O, Jensen V, Paulsen O, Andersen P, Kim JJ, Thompson RF, Sun W, Webster LC, Grant SG, Eilers J, Konnerth A, Li J, McNamara JO, Seeburg PH (1998) Importance of the intracellular domain of NR2 subunits for NMDA receptor function in vivo. *Cell* **92**: 279-289

Stein PL, Vogel H, Soriano P (1994) Combined deficiencies of Src, Fyn, and Yes tyrosine kinases in mutant mice. *Genes & development* **8**: 1999-2007

Steinman L (2004) Elaborate interactions between the immune and nervous systems. *Nature immunology* **5**: 575-581

Steinman L (2012) Lessons learned at the intersection of immunology and neuroscience. *The Journal of clinical investigation* **122**: 1146-1148

Sweatt JD (2001) The neuronal MAP kinase cascade: a biochemical signal integration system subserving synaptic plasticity and memory. *Journal of neurochemistry* **76**: 1-10

Syken J, Shatz CJ (2003) Expression of T cell receptor beta locus in central nervous system neurons. *Proceedings of the National Academy of Sciences of the United States of America* **100**: 13048-13053

Tada T, Sheng M (2006) Molecular mechanisms of dendritic spine morphogenesis. *Current opinion in neurobiology* **16**: 95-101

Thomas CG, Miller AJ, Westbrook GL (2006) Synaptic and extrasynaptic NMDA receptor NR2 subunits in cultured hippocampal neurons. *J Neurophysiol* **95**: 1727-1734

Thomson AW, Turnquist HR, Raimondi G (2009) Immunoregulatory functions of mTOR inhibition. *Nature reviews Immunology* **9**: 324-337

Tian X, Gotoh T, Tsuji K, Lo EH, Huang S, Feig LA (2004) Developmentally regulated role for Ras-GRFs in coupling NMDA glutamate receptors to Ras, Erk and CREB. *The EMBO journal* **23**: 1567-1575

Towbin H, Staehelin T, Gordon J (1979) Electrophoretic transfer of proteins from polyacrylamide gels to nitrocellulose sheets: procedure and some applications. *Proceedings of the National Academy of Sciences of the United States of America* **76**: 4350-4354

Traynelis SF, Wollmuth LP, McBain CJ, Menniti FS, Vance KM, Ogden KK, Hansen KB, Yuan H, Myers SJ, Dingledine R (2010) Glutamate receptor ion channels: structure, regulation, and function. *Pharmacological reviews* **62**: 405-496

Uehata M, Ishizaki T, Satoh H, Ono T, Kawahara T, Morishita T, Tamakawa H, Yamagami K, Inui J, Maekawa M, Narumiya S (1997) Calcium sensitization of smooth muscle mediated by a Rho-associated protein kinase in hypertension. *Nature* **389**: 990-994

Uhlen M, Fagerberg L, Hallstrom BM, Lindskog C, Oksvold P, Mardinoglu A, Sivertsson A, Kampf C, Sjostedt E, Asplund A, Olsson I, Edlund K, Lundberg E, Navani S, Szigartyo CA, Odeberg J, Djureinovic D, Takanen JO, Hober S, Alm T, Edqvist PH, Berling H, Tegel H, Mulder J, Rockberg J, Nilsson P, Schwenk JM, Hamsten M, von Feilitzen K, Forsberg M, Persson L, Johansson F, Zwahlen M, von Heijne G, Nielsen J, Ponten F (2015) Proteomics. Tissue-based map of the human proteome. *Science* **347**: 1260419

- Vale RD (2003) The molecular motor toolbox for intracellular transport. *Cell* **112**: 467-480
- Van Aelst L, D'Souza-Schorey C (1997) Rho GTPases and signaling networks. *Genes & development* **11**: 2295-2322
- von Willebrand M, Williams S, Saxena M, Gilman J, Tailor P, Jascur T, Amarante-Mendes GP, Green DR, Mustelin T (1998) Modification of phosphatidylinositol 3-kinase SH2 domain binding properties by Abl- or Lck-mediated tyrosine phosphorylation at Tyr-688. *The Journal of biological chemistry* **273**: 3994-4000
- Wang H, Kadlecck TA, Au-Yeung BB, Goodfellow HE, Hsu LY, Freedman TS, Weiss A (2010) ZAP-70: an essential kinase in T-cell signaling. *Cold Spring Harbor perspectives in biology* **2**: a002279
- Wang P, Bouwman FG, Mariman EC (2009) Generally detected proteins in comparative proteomics--a matter of cellular stress response? *Proteomics* **9**: 2955-2966
- Wange RL, Samelson LE (1996) Complex complexes: signaling at the TCR. *Immunity* **5**: 197-205
- Watanabe M, Inoue Y, Sakimura K, Mishina M (1992) Developmental changes in distribution of NMDA receptor channel subunit mRNAs. *Neuroreport* **3**: 1138-1140
- Wickstead B, Gull K (2011) The evolution of the cytoskeleton. *The Journal of cell biology* **194**: 513-525
- Wu HH, Bellmunt E, Scheib JL, Venegas V, Burkert C, Reichardt LF, Zhou Z, Farinas I, Carter BD (2009) Glial precursors clear sensory neuron corpses during development via Jedi-1, an engulfment receptor. *Nature neuroscience* **12**: 1534-1541
- Wucherpennig KW, Gagnon E, Call MJ, Huseby ES, Call ME (2010) Structural biology of the T-cell receptor: insights into receptor assembly, ligand recognition, and initiation of signaling. *Cold Spring Harbor perspectives in biology* **2**: a005140
- Wymann MP, Bulgarelli-Leva G, Zvelebil MJ, Pirola L, Vanhaesebroeck B, Waterfield MD, Panayotou G (1996) Wortmannin inactivates phosphoinositide 3-kinase by covalent modification of Lys-802, a residue involved in the phosphate transfer reaction. *Molecular and cellular biology* **16**: 1722-1733
- Xu HP, Chen H, Ding Q, Xie ZH, Chen L, Diao L, Wang P, Gan L, Crair MC, Tian N (2010) The immune protein CD3zeta is required for normal development of neural circuits in the retina. *Neuron* **65**: 503-515
- Xu J, Cheng Y, Lai A, Lv Z, Campbell RA, Yu H, Luo C, Shan B, Xu L, Xu X (2015) Autoantibodies Affect Brain Density Reduction in Nonneuropsychiatric Systemic Lupus Erythematosus Patients. *Journal of immunology research* **2015**: 920718
- Yamada S, Nelson WJ (2007) Synapses: sites of cell recognition, adhesion, and functional specification. *Annual review of biochemistry* **76**: 267-294

Yang N, Higuchi O, Ohashi K, Nagata K, Wada A, Kangawa K, Nishida E, Mizuno K (1998) Cofilin phosphorylation by LIM-kinase 1 and its role in Rac-mediated actin reorganization. *Nature* **393**: 809-812

Yirmiya R, Goshen I (2011) Immune modulation of learning, memory, neural plasticity and neurogenesis. *Brain, behavior, and immunity* **25**: 181-213

Zhou Q, Homma KJ, Poo MM (2004) Shrinkage of dendritic spines associated with long-term depression of hippocampal synapses. *Neuron* **44**: 749-757

Ziv NE, Smith SJ (1996) Evidence for a role of dendritic filopodia in synaptogenesis and spine formation. *Neuron* **17**: 91-102

6 Appendix

6.1 Abbreviations

A	alanine
AMPA	α -amino-3-hydroxy-5-methyl-4-isoxazolepropionic acid receptor
ANOVA	analysis of variance
APV	(2R)-amino-5-phosphonovaleric acid
BBB	blood-brain barrier
BDNF	brain-derived neurotrophic factor
bp	base pairs
BSA	bovine serum albumin
C	Celsius
Ca	calcium
CD	cluster of differentiation
cDNA	complementary DNA
CNQX	6-cyano-7-nitroquinoxaline-2,3-dione
ddH ₂ O	bidistilled water
CNS	central nervous system
Cx	Cortex
D	aspartate
DAG	diacylglycerol
DIV	days <i>in vitro</i>
DNA	deoxyribonucleic acid
DRM	detergent resistant membranes
ECL	enhanced chemiluminescence
EDTA	ethylenediaminetetraacetic acid
<i>E.coli</i>	<i>Escherichia coli</i>
e.g.	exempli gratia
<i>et al.</i>	<i>et alias</i>
F	phenylalanine
fig.	Figure
GAPDH	glyceraldehyde 3-phosphate dehydrogenase
GDP	guanosine diphosphate
GFP	green fluorescent protein
gp	guinea pig
GTP	guanosine triphosphate
h	hour
HBSS	Hank's balanced salt solution
Hc	hippocampus
H ₂ O	water
HRP	horse radish peroxidase
IgG	Immunoglobulin G
ITAM	immunoreceptor tyrosine-based activation motif
kDa	kilo Dalton

Lck	lymphocyte-specific protein tyrosine kinase
LGN	lateral geniculate nucleus
LTD	Long-term depression
LTP	Long-term potentiation
M	molar
mEPSC	miniature excitatory postsynaptic current
Mg	magnesium
MHC I	major histocompatibility complex I
min	minutes
mRNA	messenger RNA
mTOR	mechanistic target of rapamycin
ms	mouse
NaOH	sodium hydroxide
NMDA	N-methyl-D-aspartate
NMDAR	N-methyl-D-aspartate receptor
NR2A	N-methyl-D-aspartate receptor subunit A
NR2B	N-methyl-D-aspartate receptor subunit B
NR2C	N-methyl-D-aspartate receptor subunit C
NR2D	N-methyl-D-aspartate receptor subunit D
n.s.	not significant
p	p-value (statistics)
P	pellet
PBS	phosphate-buffered saline
PCR	polymerase chain reaction
PFA	paraformaldehyde
PI3K	phosphoinositide 3-kinase
PSD	postsynaptic density
pTyr	phosphorylated tyrosine
Rb	rabbit
RGC	retinal ganglion cell
RNA	ribonucleic acid
ROCK	Rho-associated protein kinase
S	supernatant
SDS	sodium dodecyl sulfate
SEM	standard error of the mean
SH2	src homology 2 (domain)
TAE	Tris-acetate-EDTA-buffer
TAP	tandem affinity purification tag
TCR	T-cell receptor
T _m	annealing temperature
TRIS	Tris(hydroxymethyl)aminomethane
USA	United States of America
wt	wildtype
Y	tyrosine
ZAP70	zeta-chain-associated protein kinase 70

6.2 Vectors and cDNA Expression Constructs

Table 4: Applied expression vectors.

Vector	System	Company
pEGFP-N1	Living Colors™ Fluorescent Proteins	Clontech
N-SF-TAP-pcDNA3	Mammalian expression construct	Gloeckner <i>et al.</i> (2007)
pCMV-VSV-G	Lentiviral expression construct	Addgene
pSPAX2	Lentiviral expression construct	Addgene
pFUGW	Lentiviral expression construct	Lois <i>et al.</i> (2002)

Information regarding the base pair (bp) positions refer to the cDNA sequence BC097933.1 of CD247 rat.

Table 5: Applied cDNA expression constructs.

Name	Insert	Vector	Restriction Sites	Application
CD3 ζ TAP	bp 63-554 Primers 5,6	N-SF-TAP- pcDNA3	HindIII / EcoRI	Expression
CD3 ζ GFP	bp 63-554 Primers 1,2	pEGFP-N1	AgeI / EcoRI	Expression
CD3 ζ -6YF-GFP	bp 63-554 Mutagenesis Primers 7-18	pEGFP-N1	AgeI / EcoRI	Expression
CD3 ζ -D36A- GFP	bp 63-554 Mutagenesis Primers 19,20	pEGFP-N1	AgeI / EcoRI	Expression
CD3 ζ FUGW	bp 63-554 Primers 3,4	pFUGW		Expression
CD3 ζ -6YF- FUGW	bp 63-554 Mutagenesis Primers 7-18	pFUGW		Expression
CD3 ζ -D36A- FUGW	bp 63-554 Mutagenesis Primers 19,20	pFUGW		Expression

6.3 Applied Primers

Primers were used for subcloning, mutagenesis, or PCR from cDNA. The annealing temperature (T_m) for each primer and the primer pair is given in the table below among other information.

Table 6: Applied primers.

No.	Name	Sequence (5' → 3')	Restriction site	T_m (°C)	T_m (°C) PCR	Experiment
1	CD3z fw	TCGAGGAATTCCCACGAAGT GGACGGCATCAGTC	EcoRI	78	63	Subcloning PCR
2	CD3z rev	TGACGACCGGTGCGCGAGGG GGCAGGGTCT	BamHI	83		Subcloning PCR
3	CD3zFUGW fw	CAAGCTTCTGATCACCATGA AG	BclI	52	63 (with No. 2)	Subcloning
4	CD3zTAP fw	CTTCAAGCTTCCACCATGAA GTGGACG	HindIII	65	67	Subcloning
5	CD3zTAP rev	CGACGAATTCGCGAGGGGGC AGGGT	EcoRI	73		Subcloning
6	CD3zY72F fw	CAGCTCTTTAACGAGCTCAA TCTAG	-	53	53	Mutagenesis
7	CD3zY72F rev	CTAGATTGAGCTCGTTAAAG AGCTG	-	53		Mutagenesis
8	CD3zY83F fw	GAGGAATTTGATGTTTTGGA CAAG	-	54	54	Mutagenesis
9	CD3zY83F rev	CTTGTCCAAAACATCAAATT CCTC	-	54		Mutagenesis
10	CD3zY111F fw	GAAGGCGTGTTC AATGCACT GCAG	-	63	63	Mutagenesis
11	CD3zY111F rev	CTGCAGTGCATTGAACACGC CTTC	-	63		Mutagenesis
12	CD3zY123F fw	GAGGCC TTCAGTGAGATTGG CATG	-	61	61	Mutagenesis
13	CD3zY123F rev	CATGCCAATCTCACTGAAGG CCTC	-	61		Mutagenesis
14	CD3zY142F fw	GACGGCCTTTTCCAGGGTCT CAGC	-	65	65	Mutagenesis
15	CD3zY142F rev	GCTGAGACCCTGAAAAAGGC CGTC	-	65		Mutagenesis
16	CD3zY153F fw	GACACCTTTGACGCCCTGCA TATG	-	61	61	Mutagenesis
17	CD3zY153F rev	CATATGCAGGGCGTCAAAGG TGTC	-	61		Mutagenesis
18	CD3zD36A fw	CTATATGCTAGCTGGAATCC TCTTC	-	52	52	Mutagenesis
19	CD3zD36A rev	GAAGAGGATTCAGCTAGCA TATAG	-	52		Mutagenesis
20	GAPDH fw	ACCACAGTCCATGCCATCAC	-	53	54	PCR
21	GAPDH rev	TCCACCACCCTGTTGCTGTA	-	54		PCR

6.4 Proteins of the TCR Signaling Network

The table on the following pages shows all the proteins of the aforementioned TCR signaling network (fig. 5) with their full name, gene name and accession number as stated by the database Uniprot. Note that for certain proteins, several genes and their expression were considered. Furthermore, the table contains information concerning the classification and Ca²⁺-binding properties of the protein. Most importantly, the expression of the protein in rat, mouse or human brain (neurons and glia) according to published literature, the Allen Brain Atlas or the Human Protein Atlas is presented. The latter even showed quantitative measurements of protein expression (high, medium, low) in neurons and glia. Using the database SynProt, the postsynaptic localization of the proteins was assessed. Literature used for the screening process is listed in section 6.5 of the appendix. Symbols and abbreviations of the table are explain in the legend below. Proteins whose search did not yield any data are marked in red.

a	astroglia
b	Bergmann-glia
cb	cerebellum
cx	cortex
hc	hippocampus
m	microglia
med	medium
Neu	neurons
No.	number
o	oligodendrocytes
✓	expressed
•	data not available
✗	not expressed

No.	Network	Name (Uniprot)
1	A20	Tumor necrosis factor alpha-induced protein 3
2	ABL	tyrosine-protein kinase ABL1
3	AKAP79	A-Kinase Anchor protein 5
4	AP1	Transcription factor AP-1
5	BAD	Bcl2-associated agonist of cell death
6	BCAT	Catenin beta-1
7	BCL10	B-cell lymphoma/leukemia 10
8	BCLXL	B-cell lymphoma-extra large / Bcl-2-like protein 1 isoform XL
9	c-FLIP	CASP8 and FADD-like apoptosis regulator
10	CABIN1	Calcineurin-binding protein cabin-1
11	CALCIN	Calcineurin Subunit B type 1
		Calcineurin subunit B type 2
12	CALPR1	Calciressin-1
13	CAM	Calmodulin
14	CAMK2	Calcium/calmodulin-dependent protein kinase type II subunit alpha
		Calcium/calmodulin-dependent protein kinase type II subunit beta
		Calcium/calmodulin-dependent protein kinase type II subunit delta
		Calcium/calmodulin-dependent protein kinase type II subunit gamma
15	CAMK4	Calcium/calmodulin-dependent protein kinase type IV
16	CARD11	Caspase recruitment domain-containing protein 11
17	Caspase 8	Caspase-8
18	CBLB	E3 ubiquitin-protein ligase CBL-B
19	CCBLP1	E3 ubiquitin-protein ligase CBL
20	CD28	T-cell-specific surface glycoprotein CD28
21	CD4	T-cell surface glycoprotein CD4
22	CD45	Receptor-type tyrosine-protein phosphatase C
23	CDC42	Cell division control protein 42 homolog
24	CREB	Cyclic AMP-responsive element-binding protein 1
		Cyclic AMP-responsive element-binding protein 5
25	CSK	Tyrosine-protein kinase CSK
26	CYC1	Cytochrome c1, heme protein, mitochondrial
27	DGK	Diacylglycerol kinase alpha
28	ERK2	Mitogen-activated protein kinase 1
29	ERK1	Mitogen-activated protein kinase 3
30	FKHR	Forkhead box protein O1
31	FOS	Proto-oncogene protein c-fos
32	FYN	Proto-oncogene tyrosine-protein kinase Fyn
33	GAB2	GRB2-associated-binding protein 2
34	GADD45	Growth arrest and DNA-damage-inducible protein GADD45 alpha
		Growth arrest and DNA-damage-inducible protein GADD45 beta
		Growth arrest and DNA-damage-inducible protein GADD45 gamma
35	GADS	GRB2-related adapter protein 2
36	GRB2	Growth factor receptor-bound protein 2
37	GSK3	Glycogen synthase kinase-3 alpha
		Glycogen synthase kinase-3 beta
38	HPK1	Mitogen-activated protein kinase kinase kinase kinase 1
39	IKB	NF-kappa-B inhibitor beta
		NF-kappa-B inhibitor epsilon
40	IKKAB	Inhibitor of nuclear factor kappa-B kinase subunit alpha
		Inhibitor of nuclear factor kappa-B kinase subunit beta
41	IKKG	NF-kappa-B essential modulator
42a	IP3	Inositol-trisphosphate 3-kinase A
		Inositol-trisphosphate 3-kinase B
42b		Inositol 1,4,5-trisphosphate receptor type 1
43	ITK	Tyrosine-protein kinase ITK/TSK

No.	Network	Name (Uniprot)
44	JNK	Mitogen-activated protein kinase 8
45	JUN	Transcription factor jun-B
		Transcription factor jun-D
46	LAT	Linker for activation of T-cells family member 1
47	LCKR	Proto-oncogene tyrosine-protein kinase LCK
48	MALT1	Mucosa-associated lymphoid tissue lymphoma translocation protein 1
49	MEK	Dual specificity mitogen-activated protein kinase kinase 1
50	MEKK1	Mitogen-activated protein kinase kinase kinase 1
51	MKK4	Dual specificity mitogen-activated protein kinase kinase 4
52	MLK3	Mitogen-activated protein kinase kinase kinase 11
53	NFAT	Nuclear factor of activated T-cells, cytoplasmic 1
		Nuclear factor of activated T-cells, cytoplasmic 2
		Nuclear factor of activated T-cells, cytoplasmic 3
54	NFKB	Nuclear factor NF-kappa-B p105 subunit
		Nuclear factor NF-kappa-B p100 subunit
55	P21C	Cyclin-dependent kinase inhibitor 1
56	P27K	Cyclin-dependent kinase inhibitor 1B
57	p38	Mitogen-activated protein kinase 14
58	P70S	Ribosomal protein S6 kinase beta-1
59	PAG	Phosphoprotein associated with glycosphingolipid-enriched microdomains 1
60	PKD1	3-phosphoinositide-dependent protein kinase 1
61	PI3K	Phosphatidylinositol-4,5-bisphosphate 3-kinase catalytic subunit alpha isoform
62	PKB	RAC-alpha serine/threonine-protein kinase
63	PKCTH	Protein kinase C theta type
64	PLCGA	1-phosphatidylinositol-4,5-bisphosphate phosphodiesterase gamma-1
65	PTEN	Phosphatidylinositol-3,4,5-trisphosphate 3-phosphatase and dual-specificity protein phosphatase PTEN
66	RAC1R	Ras-related C3 botulinum toxin substrate 1
67	RAF	RAF proto-oncogene serine/threonine-protein kinase
68	RAS	GTPase HRas
69	RASGRP	RAS guanyl-releasing protein 1
70	RIP1	Receptor-interacting serine/threonine-protein kinase 1
71	RIP2	Receptor-interacting serine/threonine-protein kinase 2
72	RLK	TXK tyrosine kinase
73	RSK	Ribosomal protein S6 kinase alpha-1
74	SH3BP2	SH3 Domain Binding Protein
75	SHIP1	Phosphatidylinositol-3,4,5-trisphosphate 5-phosphatase 1
76	SHP1	Tyrosine-protein phosphatase non-receptor type 6
77	SHP2	Tyrosine-protein phosphatase non-receptor type 11
78	SLP76	Lymphocyte cytosolic protein 2
79	SOS	Son of sevenless homolog 1
		Son of sevenless homolog 2
80	CD3G	CD3 gamma
81	CD3D	CD3 delta
82	CD3E	CD3 epsilon
83	CD3Z	CD3 zeta
84	CD3H	CD3 eta
85	TRAF2	TNF receptor-associated factor 2
86	TRAF6	TNF receptor-associated factor 6
87	VAV1	Proto-oncogene vav
88	VAV3	Guanine nucleotide exchange factor VAV3
89	ZAP70	Tyrosine-protein kinase ZAP-70

No.	Network	Gene	Classification	Ca ²⁺ -binding	Uniprot Accession Number		
					Rat	Mouse	Human
1	A20	TNFAIP3	ubiquitination		M0R7V5	Q60769	P21580
2	ABL	ABL1	Kinase		E9PT20	P00520	P00519
3	AKAP79	AKAP5	regulatory		P24587	D3YVF0	P24588
4	AP1	JUN	DNA-binding		P17325	P05627	P05412
5	BAD	BAD	Apoptosis		O35147	Q61337	Q92934
6	BCAT	CTNNB1	DNA-binding		Q9WU82	Q02248	P35222
7	BCL10	BCL10	Apoptosis		Q9QYN5	Q9Z0H7	O95999
8	BCLXL	Bcl2l1	Regulatory		P53563	Q64373	Q07817
9	c-FLIP	CFLAR	Apoptosis		C0H5Y5	O35732	O15519
10	CABIN1	CABIN1	Regulatory		O88480	Q6PFH4	Q9Y6J0
11	CALCIN	PPP3R1	Phosphatase	✓	P63100	Q63810	P63098
		PPP3R2			P28470	Q63811	Q96LZ3
12	CALPR1	RCAN1	Regulatory	✓	Q6IN33	Q9JHG6	P53805
13	CAM	CALM1	Regulatory	✓	P62161	P62204	P62158
14	CAMK2	CAMK2A	Kinase		P11275	P11798	Q9UQM7
		CAMK2B		P08413	P28652	Q13554	
		CAMK2D		P15791	Q6PHZ2	Q13557	
		CAMK2G		P11730	Q923T9	Q13555	
15	CAMK4	CAMK4	Kinase		P13234	P08414	Q16566
16	CARD11	CARD11	Regulatory		F1M1I1	Q8CIS0	Q9BXL7
17	Caspase 8	CASP8	Apoptosis		Q9JHX4	O89110	Q14790
18	CBLB	CBLB	ubiquitination	✓	Q8K4S7	Q3TTA7	Q13191
19	CCBLP1	CBLC	ubiquitination	✓	G3V8H4	Q80XL1	Q9ULV8
20	CD28	CD28	Adaptor		P31042	P31041	P10747
21	CD4	CD4	Regulatory		P05540	P06332	P01730
22	CD45	PTPRC	Phosphatase		P04157	P06800	P08575
23	CDC42	CDC42	Regulatory		Q8CFN2	P60766	P60953
24	CREB	CREB1	DNA-biding		P15337	Q01147	P16220
		CREB5		D3ZBH0	Q8K1L0	Q02930	
25	CSK	CSK	Kinase		P32577	P41241	P41240
26	CYC1	CYC1	mitochondrial		D3ZFQ8	Q9D0M3	P08574
27	DGK	DGKA	Kinase	✓	P51556	O88673	P23743
28	ERK2	MAPK1	Kinase		P63086	P63085	P28482
29	ERK1	MAPK3	Kinase		P21708	Q63844	P27361
30	FKHR	FOXO1	DNA-binding		G3V7R4	Q9R1E0	Q12778
31	FOS	FOS	DNA-binding		P12841	P01101	P01100
32	FYN	FYN	Kinase		Q62844	P39688	P06241
33	GAB2	GAB2	Adaptor		Q9EQH1	Q9Z1S8	Q9UQC2
34	GADD45	GADD45A	Regulatory		P48317	P48316	P24522
		GADD45B		Q5U3Z2	P22339	O75293	
		GADD45G		Q9WTQ7	Q9Z111	O95257	
35	GADS	GRAP2	Adaptor		Q3KR57	O89100	O75791
36	GRB2	GRB2	Adaptor		P62994	Q60631	P62993
37	GSK3	GSK3A	Kinase		P18265	Q2NL51	P49840
		GSK3B		P18266	Q9WV60	P49841	
38	HPK1	MAP4K1	Kinase		D3Z8I4	P70218	Q92918
39	IKB	NFKBIB	Regulatory		Q9JIA3	Q60778	Q15653
		NFKBIE		Q6P780	O54910	O00221	
40	IKKAB	CHUK	Kinase		B5DF32	Q60680	O15111
		IKKBK		Q9QY78	O88351	O14920	
41	IKKG	IKBKG	Kinase		Q6TMG5	O88522	Q9Y6K9
42a	IP3	ITPKA	Kinase		P17105	Q8R071	P23677
		ITPKB		P42335	B2RXC2	P27987	

No.	Network	Gene	Classification	Ca ²⁺ -binding	Uniprot Accession Number		
					Rat	Mouse	Human
42b	IP3	ITPR1	Regulatory		P29994	P11881	Q14643
43	ITK	ITK	Kinase		D4A7W7	Q03526	Q08881
44	JNK	MAPK8	Kinase		P49185	Q91Y86	P45983
45	JUN	JUNB	DNA-binding		P24898	P09450	P17275
		JUND			P52909	P15066	P17535
46	LAT	LAT	Adaptor		O70601	O54957	O43561
47	LCKR	LCK	Kinase		Q01621	P06240	P06239
48	MALT1	MALT1	ubiquitination		D4A980	Q2TBA3	Q9UDY8
49	MEK	MAP2K1	Kinase		Q01986	P31938	Q02750
50	MEKK1	MAP3K1	Kinase		Q62925	P53349	Q13233
51	MKK4	MAP2K4	Kinase		Q4KSH6	P47809	P45985
52	MLK3	MAP3K11	Kinase		Q66HA1	Q80XI6	Q16584
53	NFAT	NFATC1	DNA-binding		D3ZE20	O88942	O95644
		NFATC2			D4A0I8	Q60591	Q13469
		NFATC3			D3ZU59	P97305	Q12968
54	NFKB	NFKB1	DNA-binding		Q63369	P25799	P19838
		NFKB2			Q5U2Z4	Q9WTK5	Q00653
55	P21C	CDKN1A	Regulatory		Q64315	P39689	P38936
56	P27K	CDKN1B	Regulatory		O08769	P46414	P46527
57	p38	MAPK14	Kinase		P70618	P47811	Q16539
58	P70S	RPS6KB1	Kinase		P67999	Q8BSK8	P23443
59	PAG	PAG1	Adaptor		Q9JM80	A6H659	Q9NWQ8
60	PDK1	PDPK1	Kinase		O55173	Q9Z2A0	O15530
61	PI3K	PIK3CA	Kinase		Q91XL6	P42337	P42336
62	PKB	AKT1	Kinase		P47196	P31750	P31749
63	PKCTH	PRKCQ	Kinase		Q9WTQ0	Q02111	Q04759
64	PLCGA	PLCG1	Regulatory	✓	P10686	Q62077	P19174
65	PTEN	PTEN	phosphatase		O54857	O08586	P60484
66	RAC1R	RAC1	Regulatory		Q6RUV5	P63001	P63000
67	RAF	RAF1	Kinase		P11345	Q99N57	P04049
68	RAS	HRAS	Regulatory		P20171	Q61411	P01112
69	RASGRP	RASGRP1	Regulatory	✓	Q9R1K8	Q9Z1S3	O95267
70	RIP1	RIPK1	Kinase		D3ZYL0	Q60855	Q13546
71	RIP2	RIPK2	Kinase		G3V783	P58801	O43353
72	RLK	TXK	Kinase		Q501W1	P42682	P42681
73	RSK	RPS6KA1	Kinase		Q63531	P18653	Q15418
74	SH3BP2	SH3BP2	Adaptor		F1LS93	Q06649	P78314
75	SHIP1	INPP5D	phosphatase		P97573	Q9ES52	Q92835
76	SHP1	PTPN6	phosphatase		P81718	P29351	P29350
77	SHP2	PTPN11	phosphatase		P41499	P35235	Q06124
78	SLP76	LCP2	Adaptor		Q920L0	Q60787	Q13094
79	SOS	SOS1	Regulatory		Q497A5	Q62245	Q07889
		SOS2			F1MAI3	Q02384	Q07890
80	CD3G	CD3G	Regulatory		Q64159	P11942	P09693
81	CD3D	CD3D	Regulatory		P19377	P04235	P04234
82	CD3E	CD3E	Regulatory		D4A5M2	P22646	P07766
83	CD3Z	CD247	Regulatory		Q4V7G0	P24161	P20963
84	CD3H	CD3H	Regulatory		-	P29020	-
85	TRAF2	TRAF2	ubiquitination		B5DFH7	P39429	Q12933
86	TRAF6	TRAF6	ubiquitination		B5DF45	P70196	Q9Y4K3
87	VAV1	VAV1	Regulatory		P54100	P27870	P15498
88	VAV3	VAV3	Regulatory		F1LWB1	Q9R0C8	Q9UKW4
89	ZAP70	ZAP70	kinase		Q5FVN9	P43404	P43403

No.	Gene	Publications											
		Rat				Mouse				Human			
		Neu	Hc	Cx	Glia	Neu	Hc	Cx	Glia	Neu	Hc	Cx	Glia
1	TNFAIP3	•	•	•	•	✓	•	✓	•	•	•	•	•
2	ABL1	✓	•	✓	•	✓	•	•	•	✓	•	✓	•
3	AKAP5	✓	✓	✓	•	✓	✓	✓	•	✓	✓	✓	•
4	JUN	✓	✓	✓	a	✓	✓	✓	•	✓	•	✓	•
5	BAD	✓	•	✓	•	✓	✓	✓	•	•	•	•	•
6	CTNNB1	✓	•	✓	a	✓	✓	✓	a	•	•	•	a
7	BCL10	•	•	(yes)	a	•	•	•	•	•	•	•	•
8	Bcl211	✓	mRNA	✓	•	•	•	•	•	✓	•	✓	•
9	CFLAR	•	•	•	•	✓	✓	✓	a	•	•	•	•
10	CABIN1	✓	✓	✓	a	•	•	•	•	•	•	•	•
11	PPP3R1	✓	✓	✓	a	•	•	•	•	✓	•	•	•
	PPP3R2	✓	✓	✓	a	•	•	•	•	•	•	•	•
12	RCAN1	✓	✓	✓	•	✓	✓	✓	•	✓	✓	✓	•
13	CALM1	✓	✓	✓	a	✓	✓	✓	•	✓	✓	•	•
14	CAMK2A	✓	✓	✓	•	✓	•	✓	•	•	•	•	•
	CAMK2B	✓	✓	✓	•	✓	•	✓	•	•	•	•	•
	CAMK2D	•	•	•	•	•	•	•	•	•	•	•	•
	CAMK2G	•	•	•	•	•	•	•	•	•	•	•	•
15	CAMK4	✓	✓	✓	•	✓	✓	✓	•	•	•	•	•
16	CARD11	•	•	•	•	•	•	•	•	•	•	•	•
17	CASP8	✓	✓	✓	a/o	✓	✓	✓	•	✓	•	•	•
18	CBLB	✓	✓	•	•	✓	•	✓	•	•	•	•	•
19	CBLC	✓	✓	•	•	•	•	•	•	•	•	•	•
20	CD28	•	•	•	•	•	•	•	•	•	•	•	•
21	CD4	•	•	•	m	✓	✓	✓	•	•	•	•	•
22	PTPRC	•	•	•	m	•	•	•	•	•	•	•	•
23	CDC42	✓	✓	✓	a	✓	✓	✓	m/a	✓	•	•	•
24	CREB1	✓	✓	✓	a	✓	•	✓	•	✓	•	✓	•
	CREB5	•	•	•	•	✓	•	✓	•	•	•	•	•
25	CSK	✓	✓	✓	•	✓	•	•	•	•	•	•	•
26	CYC1	✓	✓	✓	a	•	•	•	•	•	•	•	•
27	DGKA	✓	✓	✓	•	✓	✓	✓	•	✓	✓	✓	•
28	MAPK1	✓	✓	✓	a	✓	✓	✓	•	✓	✓	✓	•
29	MAPK3	✓	✓	✓	a	✓	✓	✓	•	✓	✓	✓	•
30	FOXO1	✓	✓	✓	m/a	✓	✓	✓	•	✓	✓	✓	•
31	FOS	✓	✓	✓	a	✓	✓	✓	•	✓	•	✓	•
32	FYN	✓	✓	✓	a	✓	✓	✓	o	✓	✓	•	•
33	GAB2	•	•	•	•	brain	•	•	•	✓	✓	✓	•
34	GADD45A	✓	✓	✓	•	✓	✓	✓	•	•	•	•	•
	GADD45B	✓	✓	✓	•	✓	✓	✓	•	•	•	•	•
	GADD45G	✓	✓	✓	•	✓	✓	✓	•	•	•	•	•
35	GRAP2	•	•	•	•	•	•	•	•	•	•	•	•
36	GRB2	✓	•	✓	•	✓	✓	✓	•	•	•	•	•
37	GSK3A	✓	✓	✓	•	✓	✓	✓	•	•	•	•	•
	GSK3B	✓	✓	✓	•	✓	✓	✓	•	✓	✓	✓	•
38	MAP4K1	•	•	•	•	•	•	•	•	•	•	•	•
39	NFKBIB	Cb	•	•	•	•	•	•	•	•	•	•	•
	NFKBIE	•	•	•	•	•	•	•	•	•	•	•	•
40	CHUK	✓	✓	✓	•	✓	✓	✓	a	•	•	•	•
	IKBKB	✓	✓	✓	•	✓	✓	✓	a	•	•	•	•
41	IKBKG	✓	✓	✓	•	✓	✓	✓	a	•	•	•	•
42a	ITPKA	✓	✓	✓	✗	✓	✓	✓	•	•	•	•	•
	ITPKB	✓	✓	✓	✓	✓	✓	✓	•	•	•	•	•

No.	Gene	Publiccations											
		Rat				Mouse				Human			
		Neu	Hc	Cx	Glia	Neu	Hc	Cx	Glia	Neu	Hc	Cx	Glia
42b	ITPR1	✓	✓	✓	a	✓	✓	✓	•	•	•	•	•
43	ITK	•	•	•	•	•	•	•	•	•	•	•	•
44	MAPK8	✓	✓	✓	a	✓	✓	✓	a	✓	✓	✓	•
45	JUNB	✓	✓	✓	a	✓	✓	✓	•	✓	•	✓	•
	JUND	✓	✓	✓	a	✓	✓	✓	•	✓	•	✓	•
46	LAT	•	•	•	•	•	•	•	•	•	•	•	•
47	LCK	✓	✓	✓	•	✓	✓	✓	•	•	•	•	•
48	MALT1	•	•	•	•	•	•	•	•	•	•	•	•
49	MAP2K1	✓	✓	✓	•	✓	✓	✓	a/o	•	•	•	•
50	MAP3K1	✓	•	•	•	✓	✓	•	•	•	•	•	•
51	MAP2K4	✓	✓	✓	•	✓	✓	✓	•	•	•	•	•
52	MAP3K11	✓	✓	✓	•	•	•	•	•	•	•	•	•
53	NFATC1	✓	✓	✓	•	✓	✓	✓	•	✓	•	✓	•
	NFATC2	✓	✓	✓	•	✓	✓	✓	•	✓	•	✓	•
	NFATC3	✓	✓	✓	•	✓	✓	✓	•	✓	•	✓	•
54	NFKB1	✓	✓	✓	•	✓	✓	✓	a	✓	✓	•	•
	NFKB2	✓	✓	✓	•	✓	✓	✓	a	✓	✓	•	•
55	CDKN1A	✓	✓	✓	a	✓	✓	✓	•	•	•	•	a
56	CDKN1B	✓	✓	✓	a	✓	✓	✓	a	✓	•	✓	•
57	MAPK14	✓	✓	✓	a	✓	✓	✓	•	✓	✓	✓	•
58	RPS6KB1	✓	✓	✓	•	✓	✓	✓	•	✓	✓	✓	•
59	PAG1	•	•	•	•	✓	✓	✓	•	•	•	•	•
60	PDPK1	✓	✓	✓	a	✓	✓	✓	a	•	•	•	•
61	PIK3CA	✓	✓	✓	a	•	•	•	•	•	•	•	•
62	AKT1	✓	✓	✓	a	✓	✓	✓	•	✓	✓	✓	•
63	PRKCQ	✓	•	•	•	✓	•	•	•	•	•	•	•
64	PLCG1	✓	✓	✓	•	✓	•	✓	•	•	•	•	•
65	PTEN	✓	✓	✓	•	✓	✓	✓	a	•	•	•	•
66	RAC1	✓	✓	✓	•	✓	✓	✓	•	•	•	•	•
67	RAF1	✓	✓	✓	•	✓	✓	✓	•	•	•	•	•
68	HRAS	✓	✓	✓	a	✓	✓	✓	•	•	•	•	•
69	RASGRP1	✓	✓	✓	•	✓	•	✓	•	•	•	•	•
70	RIPK1	✓	•	✓	•	✓	✓	•	•	•	•	•	•
71	RIPK2	•	•	•	•	✓	•	✓	a	•	•	•	•
72	TXK	•	•	•	•	•	•	•	•	•	•	•	•
73	RPS6KA1	✓	✓	✓	•	✓	✓	✓	a	✓	•	•	•
74	SH3BP2	•	•	•	•	•	•	•	•	•	•	•	•
75	INPP5D	•	•	•	•	•	•	•	•	•	•	•	•
76	PTPN6	✓	•	✓	a	✓	✓	•	•	•	•	•	•
77	PTPN11	✓	✓	•	•	✓	✓	✓	a	•	•	•	•
78	LCP2	•	•	•	•	•	•	•	•	•	•	•	•
79	SOS1	✓	✓	✓	•	✓	✓	✓	•	✓	✓	✓	•
	SOS2	✓	✓	✓	•	✓	✓	✓	•	✓	✓	✓	•
80	CD3G	•	•	•	•	Cb	•	•	•	•	•	•	•
81	CD3D	•	•	•	•	Cb	•	•	•	•	•	•	•
82	CD3E	•	•	•	•	Cb	•	•	b	•	•	•	•
83	CD247	✓	✓	✓	a/o	✓	✓	•	•	•	•	•	•
84	CD3H	•	•	•	•	•	•	•	•	•	•	•	•
85	TRAF2	•	•	•	•	✓	•	•	•	✓	✓	✓	•
86	TRAF6	•	•	•	•	✓	•	•	•	✓	✓	✓	•
87	VAV1	•	•	•	•	•	•	•	•	•	•	•	•
88	VAV3	✓	✓	•	a	✓	✓	✓	•	•	•	•	•
89	ZAP70	✓	✓	✓	•	✓	✓	✓	•	•	•	•	•

No.	Gene	Allen Brain Atlas			Human Protein Atlas				SynProt
		Mouse			Human				
		Neu	Hc	Cx	Neu	Hc	Cx	Glia	
1	TNFAIP3	*	*	*	✓	low	med	*	*
2	ABL1	✓	✓	✓	✓	low	low	low	*
3	AKAP5	•	•	•	✓	high	high	low (Cx)	✓
4	JUN	✓	✓	✓	✓	*	low	*	*
5	BAD	✓	✓	✓	✓	med	med	med	✓
6	CTNNB1	✓	✓	✓	✓	low	low	low	✓
7	BCL10	*	*	*	✓	med	med	low	*
8	Bcl2l1	✓	✓	✓	*	*	*	*	*
9	CFLAR	✓	✓	✓	✓	med	med	med	*
10	CABIN1	✓	✓	✓	✓	high	med	low (Cx)	*
11	PPP3R1	✓	✓	✓	✓	med	high	*	✓
	PPP3R2	*	*	*	✓	med	high	*	*
12	RCAN1	✓	✓	✓	✓	high	high	med	*
13	CALM1	✓	✓	✓	✓	med	med	low (Cx) med (hc)	✓
14	CAMK2A	✓	✓	✓	✓	high	high	*	✓
	CAMK2B	✓	✓	✓	✓	high	med	*	✓
	CAMK2D	✓	✓	✓	✓	med	med	low (Cx)	✓
	CAMK2G	✓	✓	✓	✓	high	high	low (Cx)	✓
15	CAMK4	✓	✓	✓	✓	high	high	low	✓
16	CARD11	*	*	*	✓	low	low	*	*
17	CASP8	*	*	*	✓	low	low	*	*
18	CBLB	✓	✓	✓	✓	med	med	*	*
19	CBLC	*	*	*	✓	low	low	low (Cx)	*
20	CD28	*	*	*	•	•	•	•	*
21	CD4	✓	✓	✓	*	*	*	*	*
22	PTPRC	*	*	*	*	*	*	*	*
23	CDC42	✓	✓	✓	•	•	•	•	✓
24	CREB1	*	*	*	✓	high	low	high	*
	CREB5	*	*	*	•	•	•	•	*
25	CSK	✓	✓	✓	✓	high	high	low	*
26	CYC1	✓	✓	✓	✓	med	med	low	✓
27	DGKA	*	*	*	✓	low	med	low (Cx)	*
28	MAPK1	✓	✓	✓	✓	high	high	med (Cx) high (Hc)	✓
29	MAPK3	✓	✓	✓	✓	high	high	med	✓
30	FOXO1	*	*	*	✓	low	low	*	*
31	FOS	✓	✓	✓	✓	low	low	low(Cx)	*
32	FYN	✓	✓	✓	*	*	*	*	✓
33	GAB2	*	*	*	✓	low	med	high	*
34	GADD45A	✓	✓	✓	•	•	•	•	*
	GADD45B	*	*	*	✓	med	low	med (Cx) low (Hc)	*
	GADD45G	✓	✓	✓	✓	high	high	low (Cx)	*
35	GRAP2	*	*	*	✓	low	low	*	*
36	GRB2	✓	✓	✓	✓	med	med	low	✓
37	GSK3A	✓	✓	✓	✓	high	high	med (Cx) low (Hc)	✓
	GSK3B	✓	✓	✓	✓	med	med	*	✓
38	MAP4K1	*	*	*	*	*	*	*	*
39	NFKBIB	*	*	*	✓	med	med	*	*
	NFKBIE	✓	✓	✓	✓	med	med	med (Cx) low (Hc)	✓
40	CHUK	✓	✓	✓	✓	high	med	med	*
	IKBKB	✓	✓	✓	✓	med	med	med (Cx) low (Hc)	✓
41	IKBKG	*	*	*	*	*	*	*	*
42a	ITPKA	✓	✓	✓	*	*	*	med (Cx)	✓
	ITPKB	*	*	*	*	*	*	med	*

No.	Gene	Allen Brain Atlas			Human Protein Atlas				SynProt
		Mouse			Human				
		Neu	Hc	Cx	Neu	Hc	Cx	Glia	
42b	ITPR1	✓	✓	✓	✓	✗	med	✗	✓
43	ITK	✗	✗	✗	•	•	•	•	✗
44	MAPK8	✓	✓	✓	✓	med	med	low (Hc)	✗
45	JUNB	✓	✓	✓	✓	high	high	high	✗
	JUND	✓	✓	✓	✓	med	nd	med (Cx)	✗
46	LAT	✗	✗	✗	✗	✗	✗	✗	✗
47	LCK	✗	✗	✗	✗	✗	✗	✗	✓
48	MALT1	✓	✓	✓	✗	✗	✗	✗	✗
49	MAP2K1	✓	✓	✓	✓	med	med	low	✓
50	MAP3K1	✗	✗	✗	✓	med	med	low	✗
51	MAP2K4	✓	✓	✓	✓	high	med	✗	✗
52	MAP3K11	✓	✓	✓	✓	high	med	low	✗
53	NFATC1	✓	✓	✓	✓	low	✗	✗	✗
	NFATC2	✓	✓	✓	✓	low	low	✗	✗
	NFATC3	✗	✗	✗	✓	med	med	low	✗
54	NFKB1	✓	✓	✓	✗	✗	✗	✗	✓
	NFKB2	✗	✗	✗	✓	low	low	✗	✗
55	CDKN1A	✓	✓	✓	✗	✗	✗	✗	✗
56	CDKN1B	✓	✓	✓	✓	med	high	med	✗
57	MAPK14	✗	✗	✗	✓	med	low	✗	✗
58	RPS6KB1	✗	✗	✗	✓	high	med	low	✓
59	PAG1	✓	✓	✗	✓	low	low	✗	✗
60	PDPK1	✓	✓	✓	✓	high	med	low	✓
61	PIK3CA	✓	✓	✓	✓	med	med	low (Cx)	✓
62	AKT1	✓	✓	✓	✓	high	high	med	✓
63	PRKCQ	✓	✓	✗	•	•	•	•	✗
64	PLCG1	✓	✓	✓	✓	high	high	low	✓
65	PTEN	✓	✓	✓	✓	med	low	✗	✗
66	RAC1	✓	✓	✓	✗	✗	✗	✗	✓
67	RAF1	✗	✗	✗	✓	low	med	low	✓
68	HRAS	✓	✓	✓	✓	high	high	high	✓
69	RASGRP1	✓	✓	✓	•	•	•	•	✗
70	RIPK1	✓	✓	✓	✓	low	med	low (Cx)	✗
71	RIPK2	✗	✗	✗	✓	low	med	low (Cx)	✗
72	TXK	✗	✗	✗	✗	✗	✗	✗	✗
73	RPS6KA1	✓	✓	✓	✓	med	med	med (Cx)	✗
74	SH3BP2	✗	✗	✗	✓	high	med	low	✗
75	INPP5D	✗	✗	✗	✗	✗	✗	low	✗
76	PTPN6	✓	✓	✗	✗	✗	✗	✗	✗
77	PTPN11	✗	✗	✗	✓	high	high	high	✓
78	LCP2	✗	✗	✗	✗	✗	✗	✗	✗
79	SOS1	✓	✓	✓	✗	✗	✗	✗	✓
	SOS2	✓	✓	✓	✓	high	high	med	✗
80	CD3G	✗	✗	✗	✗	✗	✗	✗	✗
81	CD3D	✗	✗	✗	yes	✗	✗	✗	✗
82	CD3E	✗	✗	✗	✗	✗	✗	✗	✗
83	CD247	✓	✓	✗	✗	✗	✗	✗	✗
84	CD3H	•	•	•	•	•	•	•	✗
85	TRAF2	✓	✓	✓	✓	low	low	low	✗
86	TRAF6	yes	✗	✗	✗	✗	✗	✗	✗
87	VAV1	✗	✗	✗	✓	high	high	med (Cx) low (Hc)	✓
88	VAV3	✓	✓	✓	✓	low	med	low (Cx) med (Hc)	✗
89	ZAP70	✓	✗	✓	✗	✗	✗	✗	✗

6.5 Literature TCR Signaling Network

Alavian KN, Li H, Collis L, Bonanni L, Zeng L, Sacchetti S, Lazrove E, Nabili P, Flaherty B, Graham M, Chen Y, Messerli SM, Mariggio MA, Rahner C, McNay E, Shore GC, Smith PJ, Hardwick JM, Jonas EA (2011) Bcl-xL regulates metabolic efficiency of neurons through interaction with the mitochondrial F1FO ATP synthase. *Nat Cell Biol* **13**: 1224-1233

Almolda B, Costa M, Montoya M, Gonzalez B, Castellano B (2009) CD4 microglial expression correlates with spontaneous clinical improvement in the acute Lewis rat EAE model. *J Neuroimmunol* **209**: 65-80

Alonso D, Encinas JM, Uttenthal LO, Bosca L, Serrano J, Fernandez AP, Castro-Blanco S, Santacana M, Bentura ML, Richart A, Fernandez-Vizarra P, Rodrigo J (2002) Coexistence of translocated cytochrome c and nitrated protein in neurons of the rat cerebral cortex after oxygen and glucose deprivation. *Neuroscience* **111**: 47-56

An WL, Cowburn RF, Li L, Braak H, Alafuzoff I, Iqbal K, Iqbal IG, Winblad B, Pei JJ (2003) Up-regulation of phosphorylated/activated p70 S6 kinase and its relationship to neurofibrillary pathology in Alzheimer's disease. *Am J Pathol* **163**: 591-607

Angibaud J, Baudouin SJ, Louveau A, Nerriere-Daguin V, Bonnamain V, Csaba Z, Dournaud P, Naveilhan P, Noraz N, Pellier-Monnin V, Boudin H (2012) Ectopic expression of the immune adaptor protein CD3zeta in neural stem/progenitor cells disrupts cell-fate specification. *J Mol Neurosci* **46**: 431-441

Angibaud J, Louveau A, Baudouin SJ, Nerriere-Daguin V, Evain S, Bonnamain V, Hulin P, Csaba Z, Dournaud P, Thinard R, Naveilhan P, Noraz N, Pellier-Monnin V, Boudin H (2011) The immune molecule CD3zeta and its downstream effectors ZAP-70/Syk mediate ephrin signaling in neurons to regulate early neurogenesis. *J Neurochem* **119**: 708-722

Appleby VJ, Correa SA, Duckworth JK, Nash JE, Noel J, Fitzjohn SM, Collingridge GL, Molnar E (2011) LTP in hippocampal neurons is associated with a CaMKII-mediated increase in GluA1 surface expression. *J Neurochem* **116**: 530-543

Arai K, Lee SR, Lo EH (2003) Essential role for ERK mitogen-activated protein kinase in matrix metalloproteinase-9 regulation in rat cortical astrocytes. *Glia* **43**: 254-264

Arrazola MS, Varela-Nallar L, Colombres M, Toledo EM, Cruzat F, Pavez L, Assar R, Aravena A, Gonzalez M, Montecino M, Maass A, Martinez S, Inestrosa NC (2009) Calcium/calmodulin-dependent protein kinase type IV is a target gene of the Wnt/beta-catenin signaling pathway. *J Cell Physiol* **221**: 658-667

Arthur JS, Fong AL, Dwyer JM, Davare M, Reese E, Obrietan K, Impey S (2004) Mitogen- and stress-activated protein kinase 1 mediates cAMP response element-binding protein phosphorylation and activation by neurotrophins. *J Neurosci* **24**: 4324-4332

Bae ON, Rajanikant K, Min J, Smith J, Baek SH, Serfozo K, Hejabian S, Lee KY, Kassab M, Majid A (2012) Lymphocyte cell kinase activation mediates neuroprotection during ischemic preconditioning. *J Neurosci* **32**: 7278-7286

Barcia C, Ros CM, Annese V, Carrillo-de Sauvage MA, Ros-Bernal F, Gomez A, Yuste JE, Campuzano CM, de Pablos V, Fernandez-Villalba E, Herrero MT (2012) ROCK/Cdc42-mediated microglial motility and gliapse formation lead to phagocytosis of degenerating dopaminergic neurons in vivo. *Sci Rep* **2**: 809

Baudouin SJ, Angibaud J, Loussouarn G, Bonnamain V, Matsuura A, Kinebuchi M, Naveilhan P, Boudin H (2008) The signaling adaptor protein CD3zeta is a negative regulator of dendrite development in young neurons. *Mol Biol Cell* **19**: 2444-2456

Baumgartel K, Mansuy IM (2012) Neural functions of calcineurin in synaptic plasticity and memory. *Learn Mem* **19**: 375-384

Beazely MA, Weerapura M, MacDonald JF (2008) Abelson tyrosine kinase links PDGFbeta receptor activation to cytoskeletal regulation of NMDA receptors in CA1 hippocampal neurons. *Mol Brain* **1**: 20

Beer R, Franz G, Krajewski S, Pike BR, Hayes RL, Reed JC, Wang KK, Klimmer C, Schmutzhard E, Poewe W, Kampfl A (2001) Temporal and spatial profile of caspase 8 expression and proteolysis after experimental traumatic brain injury. *J Neurochem* **78**: 862-873

Benes FM, Lim B, Subburaju S (2009) Site-specific regulation of cell cycle and DNA repair in post-mitotic GABA cells in schizophrenic versus bipolars. *Proc Natl Acad Sci U S A* **106**: 11731-11736

Berninger B, Marty S, Zafra F, da Penha Berzaghi M, Thoenen H, Lindholm D (1995) GABAergic stimulation switches from enhancing to repressing BDNF expression in rat hippocampal neurons during maturation in vitro. *Development* **121**: 2327-2335

Bernstein HG, Dobrowolny H, Schott BH, Gorny X, Becker V, Steiner J, Seidenbecher CI, Bogerts B (2013) Increased density of AKAP5-expressing neurons in the anterior cingulate cortex of subjects with bipolar disorder. *J Psychiatr Res* **47**: 699-705

Betz R, Sandhoff K, Fischer KD, van Echten-Deckert G (2003) Detection and identification of Vav1 protein in primary cultured murine cerebellar neurons and in neuroblastoma cells (SH-SY5Y and Neuro-2a). *Neurosci Lett* **339**: 37-40

Brunet A, Datta SR, Greenberg ME (2001) Transcription-dependent and -independent control of neuronal survival by the PI3K-Akt signaling pathway. *Curr Opin Neurobiol* **11**: 297-305

Camarero G, Tyrsin OY, Xiang C, Pfeiffer V, Pleiser S, Wiese S, Gotz R, Rapp UR (2006) Cortical migration defects in mice expressing A-RAF from the B-RAF locus. *Mol Cell Biol* **26**: 7103-7115

Carrero I, Gonzalo MR, Martin B, Sanz-Anquela JM, Arevalo-Serrano J, Gonzalo-Ruiz A (2012) Oligomers of beta-amyloid protein (Abeta1-42) induce the activation of cyclooxygenase-2 in astrocytes via an interaction with interleukin-1beta, tumour necrosis factor-alpha, and a nuclear factor kappa-B mechanism in the rat brain. *Exp Neurol* **236**: 215-227

Chen CH, Zhou W, Liu S, Deng Y, Cai F, Tone M, Tone Y, Tong Y, Song W (2012a) Increased NF-kappaB signalling up-regulates BACE1 expression and its therapeutic potential in Alzheimer's disease. *Int J Neuropsychopharmacol* **15**: 77-90

Chen CY, Weng YH, Chien KY, Lin KJ, Yeh TH, Cheng YP, Lu CS, Wang HL (2012b) (G2019S) LRRK2 activates MKK4-JNK pathway and causes degeneration of SN dopaminergic neurons in a transgenic mouse model of PD. *Cell Death Differ* **19**: 1623-1633

Chen J, Graham SH, Nakayama M, Zhu RL, Jin K, Stetler RA, Simon RP (1997) Apoptosis repressor genes Bcl-2 and Bcl-x-long are expressed in the rat brain following global ischemia. *J Cereb Blood Flow Metab* **17**: 2-10

Chen J, Uchimura K, Stetler RA, Zhu RL, Nakayama M, Jin K, Graham SH, Simon RP (1998) Transient global ischemia triggers expression of the DNA damage-inducible gene GADD45 in the rat brain. *J Cereb Blood Flow Metab* **18**: 646-657

Chen L, Liao G, Yang L, Campbell K, Nakafuku M, Kuan CY, Zheng Y (2006) Cdc42 deficiency causes Sonic hedgehog-independent holoprosencephaly. *Proc Natl Acad Sci U S A* **103**: 16520-16525

Chen WW, Yu H, Fan HB, Zhang CC, Zhang M, Zhang C, Cheng Y, Kong J, Liu CF, Geng D, Xu X (2012c) RIP1 mediates the protection of geldanamycin on neuronal injury induced by oxygen-glucose deprivation combined with zVAD in primary cortical neurons. *J Neurochem* **120**: 70-77

Chun JT, Crispino M, Tocco G (2004) The dual response of protein kinase Fyn to neural trauma: early induction in neurons and delayed induction in reactive astrocytes. *Exp Neurol* **185**: 109-119

Chung JY, Park HR, Lee SJ, Lee SH, Kim JS, Jung YS, Hwang SH, Ha NC, Seol WG, Lee J, Park BJ (2013) Elevated TRAF2/6 expression in Parkinson's disease is caused by the loss of Parkin E3 ligase activity. *Lab Invest* **93**: 663-676

Clark CJ, McDade DM, O'Shaughnessy CT, Morris BJ (2007) Contrasting roles of neuronal Msk1 and Rsk2 in Bad phosphorylation and feedback regulation of Erk signalling. *J Neurochem* **102**: 1024-1034

Coffey ET (2014) Nuclear and cytosolic JNK signalling in neurons. *Nat Rev Neurosci* **15**: 285-299

Cosenza-Nashat MA, Kim MO, Zhao ML, Suh HS, Lee SC (2006) CD45 isoform expression in microglia and inflammatory cells in HIV-1 encephalitis. *Brain Pathol* **16**: 256-265

Crespel A, Rigau V, Coubes P, Rousset MC, de Bock F, Okano H, Baldy-Moulinier M, Bockaert J, Lerner-Natoli M (2005) Increased number of neural progenitors in human temporal lobe epilepsy. *Neurobiol Dis* **19**: 436-450

Culpan D, Cram D, Chalmers K, Cornish A, Palmer L, Palmer J, Hughes A, Passmore P, Craig D, Wilcock GK, Kehoe PG, Love S (2009) TNFR-associated factor-2 (TRAF-2) in Alzheimer's disease. *Neurobiol Aging* **30**: 1052-1060

Damjanac M, Rioux Bilan A, Paccalin M, Pontcharraud R, Fauconneau B, Hugon J, Page G (2008) Dissociation of Akt/PKB and ribosomal S6 kinase signaling markers in a transgenic mouse model of Alzheimer's disease. *Neurobiol Dis* **29**: 354-367

de la Torre-Ubieta L, Gaudilliere B, Yang Y, Ikeuchi Y, Yamada T, DiBacco S, Stegmuller J, Schuller U, Salih DA, Rowitch D, Brunet A, Bonni A (2010) A FOXO-Pak1 transcriptional pathway controls neuronal polarity. *Genes Dev* **24**: 799-813

- Dell'Acqua ML, Faux MC, Thorburn J, Thorburn A, Scott JD (1998) Membrane-targeting sequences on AKAP79 bind phosphatidylinositol-4, 5-bisphosphate. *EMBO J* **17**: 2246-2260
- Derijard B, Raingeaud J, Barrett T, Wu IH, Han J, Ulevitch RJ, Davis RJ (1995) Independent human MAP-kinase signal transduction pathways defined by MEK and MKK isoforms. *Science* **267**: 682-685
- Derkinderen P, Valjent E, Toutant M, Corvol JC, Enslin H, Ledent C, Trzaskos J, Caboche J, Girault JA (2003) Regulation of extracellular signal-regulated kinase by cannabinoids in hippocampus. *J Neurosci* **23**: 2371-2382
- Dewaste V, Roymans D, Moreau C, Erneux C (2002) Cloning and expression of a full-length cDNA encoding human inositol 1,4,5-trisphosphate 3-kinase B. *Biochem Biophys Res Commun* **291**: 400-405
- Ding L, McIntyre TM, Zimmerman GA, Prescott SM (1998a) The cloning and developmental regulation of murine diacylglycerol kinase zeta. *FEBS Lett* **429**: 109-114
- Ding L, Traer E, McIntyre TM, Zimmerman GA, Prescott SM (1998b) The cloning and characterization of a novel human diacylglycerol kinase, DGK ι . *J Biol Chem* **273**: 32746-32752
- Dittmer PJ, Dell'Acqua ML, Sather WA (2014) Ca $^{2+}$ /calcineurin-dependent inactivation of neuronal L-type Ca $^{2+}$ channels requires priming by AKAP-anchored protein kinase A. *Cell Rep* **7**: 1410-1416
- Dong H, Zhang X, Dai X, Lu S, Gui B, Jin W, Zhang S, Qian Y (2014) Lithium ameliorates lipopolysaccharide-induced microglial activation via inhibition of toll-like receptor 4 expression by activating the PI3K/Akt/FoxO1 pathway. *J Neuroinflammation* **11**: 140
- Dumitriu A, Latourelle JC, Hadzi TC, Pankratz N, Garza D, Miller JP, Vance JM, Foroud T, Beach TG, Myers RH (2012) Gene expression profiles in Parkinson disease prefrontal cortex implicate FOXO1 and genes under its transcriptional regulation. *PLoS Genet* **8**: e1002794
- Emeterio EP, Tramullas M, Hurle MA (2006) Modulation of apoptosis in the mouse brain after morphine treatments and morphine withdrawal. *J Neurosci Res* **83**: 1352-1361
- Etienne-Manneville S, Hall A (2001) Integrin-mediated activation of Cdc42 controls cell polarity in migrating astrocytes through PKC ζ . *Cell* **106**: 489-498
- Exil V, Ping L, Yu Y, Chakraborty S, Caito SW, Wells KS, Karki P, Lee E, Aschner M (2014) Activation of MAPK and FoxO by manganese (Mn) in rat neonatal primary astrocyte cultures. *PLoS One* **9**: e94753
- Farnsworth CL, Freshney NW, Rosen LB, Ghosh A, Greenberg ME, Feig LA (1995) Calcium activation of Ras mediated by neuronal exchange factor Ras-GRF. *Nature* **376**: 524-527
- Fernandez AM, Fernandez S, Carrero P, Garcia-Garcia M, Torres-Aleman I (2007) Calcineurin in reactive astrocytes plays a key role in the interplay between proinflammatory and anti-inflammatory signals. *J Neurosci* **27**: 8745-8756
- Fraser MM, Zhu X, Kwon CH, Uhlmann EJ, Gutmann DH, Baker SJ (2004) Pten loss causes hypertrophy and increased proliferation of astrocytes in vivo. *Cancer Res* **64**: 7773-7779

Fukushima H, Maeda R, Suzuki R, Suzuki A, Nomoto M, Toyoda H, Wu LJ, Xu H, Zhao MG, Ueda K, Kitamoto A, Mamiya N, Yoshida T, Homma S, Masushige S, Zhuo M, Kida S (2008) Upregulation of calcium/calmodulin-dependent protein kinase IV improves memory formation and rescues memory loss with aging. *J Neurosci* **28**: 9910-9919

Gao WL, Tian F, Zhang SQ, Zhang H, Yin ZS (2014) Epidermal growth factor increases the expression of Nestin in rat reactive astrocytes through the Ras-Raf-ERK pathway. *Neurosci Lett* **562**: 54-59

Gardner LA, Tavalin SJ, Goehring AS, Scott JD, Bahouth SW (2006) AKAP79-mediated targeting of the cyclic AMP-dependent protein kinase to the beta1-adrenergic receptor promotes recycling and functional resensitization of the receptor. *J Biol Chem* **281**: 33537-33553

Gary DS, Mattson MP (2002) PTEN regulates Akt kinase activity in hippocampal neurons and increases their sensitivity to glutamate and apoptosis. *Neuromolecular Med* **2**: 261-269

Gonzalez-Zuniga M, Contreras PS, Estrada LD, Chamorro D, Villagra A, Zanlungo S, Seto E, Alvarez AR (2014) c-Abl stabilizes HDAC2 levels by tyrosine phosphorylation repressing neuronal gene expression in Alzheimer's disease. *Mol Cell* **56**: 163-173

Graef IA, Mermelstein PG, Stankunas K, Neilson JR, Deisseroth K, Tsien RW, Crabtree GR (1999) L-type calcium channels and GSK-3 regulate the activity of NF-ATc4 in hippocampal neurons. *Nature* **401**: 703-708

Graef IA, Wang F, Charron F, Chen L, Neilson J, Tessier-Lavigne M, Crabtree GR (2003) Neurotrophins and netrins require calcineurin/NFAT signaling to stimulate outgrowth of embryonic axons. *Cell* **113**: 657-670

Grewal SS, York RD, Stork PJ (1999) Extracellular-signal-regulated kinase signalling in neurons. *Curr Opin Neurobiol* **9**: 544-553

Griffin RJ, Moloney A, Kelliher M, Johnston JA, Ravid R, Dockery P, O'Connor R, O'Neill C (2005) Activation of Akt/PKB, increased phosphorylation of Akt substrates and loss and altered distribution of Akt and PTEN are features of Alzheimer's disease pathology. *J Neurochem* **93**: 105-117

Haglund K, Ivankovic-Dikic I, Shimokawa N, Kruh GD, Dikic I (2004) Recruitment of Pyk2 and Cbl to lipid rafts mediates signals important for actin reorganization in growing neurites. *J Cell Sci* **117**: 2557-2568

Hainsworth AH, Bermpohl D, Webb TE, Darwish R, Fiskum G, Qiu J, McCarthy D, Moskowitz MA, Whalen MJ (2005) Expression of cellular FLICE inhibitory proteins (cFLIP) in normal and traumatic murine and human cerebral cortex. *J Cereb Blood Flow Metab* **25**: 1030-1040

Hale CF, Dietz KC, Varela JA, Wood CB, Zirlin BC, Leverich LS, Greene RW, Cowan CW (2011) Essential role for vav Guanine nucleotide exchange factors in brain-derived neurotrophic factor-induced dendritic spine growth and synapse plasticity. *J Neurosci* **31**: 12426-12436

Harper SJ, LoGrasso P (2001) Signalling for survival and death in neurones: the role of stress-activated kinases, JNK and p38. *Cell Signal* **13**: 299-310

Harris CD, Ermak G, Davies KJ (2007) RCAN1-1L is overexpressed in neurons of Alzheimer's disease patients. *FEBS J* **274**: 1715-1724

Hatterer E, Benon A, Chounlamountri N, Watrin C, Angibaud J, Jouanneau E, Boudin H, Honnorat J, Pellier-Monnin V, Noraz N (2011) Syk kinase is phosphorylated in specific areas of the developing nervous system. *Neurosci Res* **70**: 172-182

Heine VM, Maslam S, Joels M, Lucassen PJ (2004) Increased P27KIP1 protein expression in the dentate gyrus of chronically stressed rats indicates G1 arrest involvement. *Neuroscience* **129**: 593-601

Henshall DC, Araki T, Schindler CK, Lan JQ, Tiekoter KL, Taki W, Simon RP (2002) Activation of Bcl-2-associated death protein and counter-response of Akt within cell populations during seizure-induced neuronal death. *J Neurosci* **22**: 8458-8465

Henshall DC, Sinclair J, Simon RP (1999) Relationship between seizure-induced transcription of the DNA damage-inducible gene GADD45, DNA fragmentation, and neuronal death in focally evoked limbic epilepsy. *J Neurochem* **73**: 1573-1583

Herrmann O, Baumann B, de Lorenzi R, Muhammad S, Zhang W, Kleesiek J, Malfertheiner M, Kohrmann M, Potrovita I, Maegele I, Beyer C, Burke JR, Hasan MT, Bujard H, Wirth T, Pasparakis M, Schwaninger M (2005) IKK mediates ischemia-induced neuronal death. *Nat Med* **11**: 1322-1329

Hoekman MF, Jacobs FM, Smidt MP, Burbach JP (2006) Spatial and temporal expression of FoxO transcription factors in the developing and adult murine brain. *Gene Expr Patterns* **6**: 134-140

Horvat A, Schwaiger F, Hager G, Brocker F, Streif R, Knyazev P, Ullrich A, Kreutzberg GW (2001) A novel role for protein tyrosine phosphatase shp1 in controlling glial activation in the normal and injured nervous system. *J Neurosci* **21**: 865-874

Hozumi Y, Ito T, Nakano T, Nakagawa T, Aoyagi M, Kondo H, Goto K (2003) Nuclear localization of diacylglycerol kinase zeta in neurons. *Eur J Neurosci* **18**: 1448-1457

Hu MC, Wang Y, Qiu WR, Mikhail A, Meyer CF, Tan TH (1999) Hematopoietic progenitor kinase-1 (HPK1) stress response signaling pathway activates I κ B kinases (IKK- α / β) and IKK- β is a developmentally regulated protein kinase. *Oncogene* **18**: 5514-5524

Huh GS, Boulanger LM, Du H, Riquelme PA, Brotz TM, Shatz CJ (2000) Functional requirement for class I MHC in CNS development and plasticity. *Science* **290**: 2155-2159

Hurley MJ, Brandon B, Gentleman SM, Dexter DT (2013) Parkinson's disease is associated with altered expression of CaV1 channels and calcium-binding proteins. *Brain* **136**: 2077-2097

Imamoto A, Soriano P (1993) Disruption of the csk gene, encoding a negative regulator of Src family tyrosine kinases, leads to neural tube defects and embryonic lethality in mice. *Cell* **73**: 1117-1124

Impey S, Obrietan K, Storm DR (1999) Making new connections: role of ERK/MAP kinase signaling in neuronal plasticity. *Neuron* **23**: 11-14

- Inomata M, Takayama Y, Kiyama H, Nada S, Okada M, Nakagawa H (1994) Regulation of Src family kinases in the developing rat brain: correlation with their regulator kinase, Csk. *J Biochem* **116**: 386-392
- Irani BG, Donato J, Jr., Olson DP, Lowell BB, Sacktor TC, Reyland ME, Tolson KP, Zinn AR, Ueta Y, Sakata I, Zigman JM, Elias CF, Clegg DJ (2010) Distribution and neurochemical characterization of protein kinase C-theta and -delta in the rodent hypothalamus. *Neuroscience* **170**: 1065-1079
- Irving EA, Barone FC, Reith AD, Hadingham SJ, Parsons AA (2000) Differential activation of MAPK/ERK and p38/SAPK in neurones and glia following focal cerebral ischaemia in the rat. *Brain Res Mol Brain Res* **77**: 65-75
- Ishijima SA, Zeng YX, Kurashima C, Utsuyama M, Shirasawa T, Sakamoto K, Hirokawa K (1995) Expression of ZAP-70 gene in the developing thymus and various nonlymphoid tissues of embryonic and adult mice. *Cell Immunol* **165**: 278-283
- Jaworski J, Spangler S, Seeburg DP, Hoogenraad CC, Sheng M (2005) Control of dendritic arborization by the phosphoinositide-3'-kinase-Akt-mammalian target of rapamycin pathway. *J Neurosci* **25**: 11300-11312
- Jing Z, Caltagarone J, Bowser R (2009) Altered subcellular distribution of c-Abl in Alzheimer's disease. *J Alzheimers Dis* **17**: 409-422
- Jones KJ, Korb E, Kundel MA, Kochanek AR, Kabraji S, McEvoy M, Shin CY, Wells DG (2008) CPEB1 regulates beta-catenin mRNA translation and cell migration in astrocytes. *Glia* **56**: 1401-1413
- Kaltschmidt C, Kaltschmidt B, Baeuerle PA (1995) Stimulation of ionotropic glutamate receptors activates transcription factor NF-kappa B in primary neurons. *Proc Natl Acad Sci U S A* **92**: 9618-9622
- Kaltschmidt C, Kaltschmidt B, Neumann H, Wekerle H, Baeuerle PA (1994) Constitutive NF-kappa B activity in neurons. *Mol Cell Biol* **14**: 3981-3992
- Kawauchi T, Chihama K, Nabeshima Y, Hoshino M (2006) Cdk5 phosphorylates and stabilizes p27kip1 contributing to actin organization and cortical neuronal migration. *Nat Cell Biol* **8**: 17-26
- Kharebava G, Makonchuk D, Kalita KB, Zheng JJ, Hetman M (2008) Requirement of 3-phosphoinositide-dependent protein kinase-1 for BDNF-mediated neuronal survival. *J Neurosci* **28**: 11409-11420
- Kim IH, Park SK, Hong ST, Jo YS, Kim EJ, Park EH, Han SB, Shin HS, Sun W, Kim HT, Soderling SH, Kim H (2009) Inositol 1,4,5-trisphosphate 3-kinase a functions as a scaffold for synaptic Rac signaling. *J Neurosci* **29**: 14039-14049
- Kim IH, Wang H, Soderling SH, Yasuda R (2014) Loss of Cdc42 leads to defects in synaptic plasticity and remote memory recall. *Elife* **3**
- Kim K, Yang J, Kim E (2010) Diacylglycerol kinases in the regulation of dendritic spines. *J Neurochem* **112**: 577-587

Kitagawa H, Warita H, Sasaki C, Zhang WR, Sakai K, Shiro Y, Mitsumoto Y, Mori T, Abe K (1999) Immunoreactive Akt, PI3-K and ERK protein kinase expression in ischemic rat brain. *Neurosci Lett* **274**: 45-48

Kortvely E, Palfi A, Bakota L, Gulya K (2002) Ontogeny of calmodulin gene expression in rat brain. *Neuroscience* **114**: 301-316

Kosten TA, Galloway MP, Duman RS, Russell DS, D'Sa C (2008) Repeated unpredictable stress and antidepressants differentially regulate expression of the bcl-2 family of apoptotic genes in rat cortical, hippocampal, and limbic brain structures. *Neuropsychopharmacology* **33**: 1545-1558

Kreutz MR, Bockers TM, Sabel BA, Hulser E, Stricker R, Reiser G (1997) Expression and subcellular localization of p42IP4/centaurin-alpha, a brain-specific, high-affinity receptor for inositol 1,3,4,5-tetrakisphosphate and phosphatidylinositol 3,4,5-trisphosphate in rat brain. *Eur J Neurosci* **9**: 2110-2124

Kuzniewska B, Rejmak E, Malik AR, Jaworski J, Kaczmarek L, Kalita K (2013) Brain-derived neurotrophic factor induces matrix metalloproteinase 9 expression in neurons via the serum response factor/c-Fos pathway. *Mol Cell Biol* **33**: 2149-2162

Lai MM, Burnett PE, Wolosker H, Blackshaw S, Snyder SH (1998) Cain, a novel physiologic protein inhibitor of calcineurin. *J Biol Chem* **273**: 18325-18331

Le HT, Maksumova L, Wang J, Pallen CJ (2006) Reduced NMDA receptor tyrosine phosphorylation in PTPalpha-deficient mouse synaptosomes is accompanied by inhibition of four src family kinases and Pyk2: an upstream role for PTPalpha in NMDA receptor regulation. *J Neurochem* **98**: 1798-1809

Leach PT, Poplawski SG, Kenney JW, Hoffman B, Liebermann DA, Abel T, Gould TJ (2012) Gadd45b knockout mice exhibit selective deficits in hippocampus-dependent long-term memory. *Learn Mem* **19**: 319-324

Lenz G, Avruch J (2005) Glutamatergic regulation of the p70S6 kinase in primary mouse neurons. *J Biol Chem* **280**: 38121-38124

Leroy K, Yilmaz Z, Brion JP (2007) Increased level of active GSK-3beta in Alzheimer's disease and accumulation in argyrophilic grains and in neurones at different stages of neurofibrillary degeneration. *Neuropathol Appl Neurobiol* **33**: 43-55

Lesuisse C, Martin LJ (2002) Immature and mature cortical neurons engage different apoptotic mechanisms involving caspase-3 and the mitogen-activated protein kinase pathway. *J Cereb Blood Flow Metab* **22**: 935-950

Li MY, Zhu M, Zhu B, Wang ZQ (2013) Cholera toxin suppresses expression of ubiquitin editing enzyme A20 and enhances transcytosis. *Cell Physiol Biochem* **31**: 495-504

Li T, Yu XJ, Zhang GY (2008) Tyrosine phosphorylation of HPK1 by activated Src promotes ischemic brain injury in rat hippocampal CA1 region. *FEBS Lett* **582**: 1894-1900

Li X, Newbern JM, Wu Y, Morgan-Smith M, Zhong J, Charron J, Snider WD (2012) MEK Is a Key Regulator of Gliogenesis in the Developing Brain. *Neuron* **75**: 1035-1050

Liang MH, Chuang DM (2007) Regulation and function of glycogen synthase kinase-3 isoforms in neuronal survival. *J Biol Chem* **282**: 3904-3917

Lindquist S, Karitkina D, Langnaese K, Posevitz-Fejfar A, Schraven B, Xavier R, Seed B, Lindquist JA (2011) Phosphoprotein associated with glycosphingolipid-enriched microdomains differentially modulates SRC kinase activity in brain maturation. *PLoS One* **6**: e23978

Liu J, Estes ML, Drazba JA, Liu H, Prayson R, Kondo S, Jacobs BS, Barnett GH, Barna BP (2000) Anti-sense oligonucleotide of p21(waf1/cip1) prevents interleukin 4-mediated elevation of p27(kip1) in low grade astrocytoma cells. *Oncogene* **19**: 661-669

Louveau A, Angibaud J, Haspot F, Opazo MC, Thinard R, Thepenier V, Baudouin SJ, Lescaudron L, Hulin P, Riedel CA, Boudin H (2013) Impaired spatial memory in mice lacking CD3zeta is associated with altered NMDA and AMPA receptors signaling independent of T-cell deficiency. *J Neurosci* **33**: 18672-18685

Ma DK, Jang MH, Guo JU, Kitabatake Y, Chang ML, Pow-Anpongkul N, Flavell RA, Lu B, Ming GL, Song H (2009) Neuronal activity-induced Gadd45b promotes epigenetic DNA demethylation and adult neurogenesis. *Science* **323**: 1074-1077

Mabuchi T, Kitagawa K, Kuwabara K, Takasawa K, Ohtsuki T, Xia Z, Storm D, Yanagihara T, Hori M, Matsumoto M (2001) Phosphorylation of cAMP response element-binding protein in hippocampal neurons as a protective response after exposure to glutamate in vitro and ischemia in vivo. *J Neurosci* **21**: 9204-9213

Machon O, van den Bout CJ, Backman M, Kemler R, Krauss S (2003) Role of beta-catenin in the developing cortical and hippocampal neuroepithelium. *Neuroscience* **122**: 129-143

Maletic-Savatic M, Koothan T, Malinow R (1998) Calcium-evoked dendritic exocytosis in cultured hippocampal neurons. Part II: mediation by calcium/calmodulin-dependent protein kinase II. *J Neurosci* **18**: 6814-6821

Manns M, Leske O, Gottfried S, Bichler Z, Lafenetre P, Wahle P, Heumann R (2011) Role of neuronal ras activity in adult hippocampal neurogenesis and cognition. *Front Neurosci* **5**: 18

Marcus DL, Strafaci JA, Miller DC, Masia S, Thomas CG, Rosman J, Hussain S, Freedman ML (1998) Quantitative neuronal c-fos and c-jun expression in Alzheimer's disease. *Neurobiol Aging* **19**: 393-400

Martin KR, Corlett A, Dubach D, Mustafa T, Coleman HA, Parkington HC, Merson TD, Bourne JA, Porta S, Arbones ML, Finkelstein DI, Pritchard MA (2012) Over-expression of RCAN1 causes Down syndrome-like hippocampal deficits that alter learning and memory. *Hum Mol Genet* **21**: 3025-3041

Matsunaga E, Nambu S, Oka M, Iriki A (2015) Comparative analysis of developmentally regulated expressions of Gadd45a, Gadd45b, and Gadd45g in the mouse and marmoset cerebral cortex. *Neuroscience* **284**: 566-580

Mattson MP, Camandola S (2001) NF-kappaB in neuronal plasticity and neurodegenerative disorders. *J Clin Invest* **107**: 247-254

Mc Guire C, Rahman M, Schwaninger M, Beyaert R, van Loo G (2013) The ubiquitin editing enzyme A20 (TNFAIP3) is upregulated during permanent middle cerebral artery occlusion but does not influence disease outcome. *Cell Death Dis* **4**: e531

Mei XP, Zhang H, Wang W, Wei YY, Zhai MZ, Xu LX, Li YQ (2011) Inhibition of spinal astrocytic c-Jun N-terminal kinase (JNK) activation correlates with the analgesic effects of ketamine in neuropathic pain. *J Neuroinflammation* **8**: 6

Mergenthaler P, Muselmann C, Sunwoldt J, Isaev NK, Wieloch T, Dirnagl U, Meisel A, Ruscher K (2013) A functional role of the cyclin-dependent kinase inhibitor 1 (p21(WAF1/CIP1)) for neuronal preconditioning. *J Cereb Blood Flow Metab* **33**: 351-355

Meyer MA (2014) Highly Expressed Genes within Hippocampal Sector CA1: Implications for the Physiology of Memory. *Neurol Int* **6**: 5388

Mihaly A, Endresz V, Oravec T, Rapp UR, Kuhnt U (1993) Immunohistochemical detection of raf protein kinase in cerebral cortical areas of adult guinea pigs and rats. *Brain Res* **627**: 225-238

Mikoshiha K (2006) Inositol 1,4,5-trisphosphate IP(3) receptors and their role in neuronal cell function. *J Neurochem* **97**: 1627-1633

Minichiello L, Calella AM, Medina DL, Bonhoeffer T, Klein R, Korte M (2002) Mechanism of TrkB-mediated hippocampal long-term potentiation. *Neuron* **36**: 121-137

Miyazaki I, Asanuma M, Diaz-Corrales FJ, Miyoshi K, Ogawa N (2004) Direct evidence for expression of dopamine receptors in astrocytes from basal ganglia. *Brain Res* **1029**: 120-123

Moore AN, Waxham MN, Dash PK (1996) Neuronal activity increases the phosphorylation of the transcription factor cAMP response element-binding protein (CREB) in rat hippocampus and cortex. *J Biol Chem* **271**: 14214-14220

Morales P, Fiedler JL, Andres S, Berrios C, Huaiquin P, Bustamante D, Cardenas S, Parra E, Herrera-Marschitz M (2008) Plasticity of hippocampus following perinatal asphyxia: effects on postnatal apoptosis and neurogenesis. *J Neurosci Res* **86**: 2650-2662

Morice C, Nothias F, Konig S, Vernier P, Baccarini M, Vincent JD, Barnier JV (1999) Raf-1 and B-Raf proteins have similar regional distributions but differential subcellular localization in adult rat brain. *Eur J Neurosci* **11**: 1995-2006

Moser CV, Kynast K, Baatz K, Russe OQ, Ferreiros N, Costiuk H, Lu R, Schmidtko A, Tegeder I, Geisslinger G, Niederberger E (2011) The protein kinase IKKepsilon is a potential target for the treatment of inflammatory hyperalgesia. *J Immunol* **187**: 2617-2625

Movilla N, Bustelo XR (1999) Biological and regulatory properties of Vav-3, a new member of the Vav family of oncoproteins. *Mol Cell Biol* **19**: 7870-7885

Muraille E, Dassesse D, Vanderwinden JM, Cremer H, Rogister B, Erneux C, Schiffmann SN (2001) The SH2 domain-containing 5-phosphatase SHIP2 is expressed in the germinal layers of embryo and adult mouse brain: increased expression in N-CAM-deficient mice. *Neuroscience* **105**: 1019-1030

Murphy JG, Sanderson JL, Gorski JA, Scott JD, Catterall WA, Sather WA, Dell'Acqua ML (2014) AKAP-anchored PKA maintains neuronal L-type calcium channel activity and NFAT transcriptional signaling. *Cell Rep* **7**: 1577-1588

Nakamura K, Hirai H, Torashima T, Miyazaki T, Tsurui H, Xiu Y, Ohtsuji M, Lin QS, Tsukamoto K, Nishimura H, Ono M, Watanabe M, Hirose S (2007) CD3 and immunoglobulin G Fc receptor regulate cerebellar functions. *Mol Cell Biol* **27**: 5128-5134

Nakamura Y, Okuno S, Sato F, Fujisawa H (1995) An immunohistochemical study of Ca²⁺/calmodulin-dependent protein kinase IV in the rat central nervous system: light and electron microscopic observations. *Neuroscience* **68**: 181-194

Narita M, Imai S, Oe K, Kubota C, Yajima Y, Yamazaki M, Suzuki T (2004) Induction of c-fos expression in the mouse brain associated with hyperalgesia induced by intrathecal injection of protein kinase C activator. *Brain Res* **1015**: 189-193

Nguyen L, Besson A, Heng JI, Schuurmans C, Teboul L, Parras C, Philpott A, Roberts JM, Guillemot F (2006) p27kip1 independently promotes neuronal differentiation and migration in the cerebral cortex. *Genes Dev* **20**: 1511-1524

Nguyen T, Di Giovanni S (2008) NFAT signaling in neural development and axon growth. *Int J Dev Neurosci* **26**: 141-145

Nguyen T, Lindner R, Tedeschi A, Forsberg K, Green A, Wuttke A, Gaub P, Di Giovanni S (2009) NFAT-3 is a transcriptional repressor of the growth-associated protein 43 during neuronal maturation. *J Biol Chem* **284**: 18816-18823

Nishida K, Yoshida Y, Itoh M, Fukada T, Ohtani T, Shirogane T, Atsumi T, Takahashi-Tezuka M, Ishihara K, Hibi M, Hirano T (1999) Gab-family adapter proteins act downstream of cytokine and growth factor receptors and T- and B-cell antigen receptors. *Blood* **93**: 1809-1816

Niu YL, Zhang WJ, Wu P, Liu B, Sun GT, Yu DM, Deng JB (2010) Expression of the apoptosis-related proteins caspase-3 and NF-kappaB in the hippocampus of Tg2576 mice. *Neurosci Bull* **26**: 37-46

Nomoto Y, Yamamoto M, Fukushima T, Kimura H, Ohshima K, Tomonaga M (2001) Expression of nuclear factor kappaB and tumor necrosis factor alpha in the mouse brain after experimental thermal ablation injury. *Neurosurgery* **48**: 158-166

O'Kane EM, Stone TW, Morris BJ (2003) Distribution of Rho family GTPases in the adult rat hippocampus and cerebellum. *Brain Res Mol Brain Res* **114**: 1-8

O'Neill LA, Kaltschmidt C (1997) NF-kappa B: a crucial transcription factor for glial and neuronal cell function. *Trends Neurosci* **20**: 252-258

Olenik C, Barth H, Just I, Aktories K, Meyer DK (1997) Gene expression of the small GTP-binding proteins RhoA, RhoB, Rac1, and Cdc42 in adult rat brain. *Brain Res Mol Brain Res* **52**: 263-269

Omri B, Crisanti P, Alliot F, Marty MC, Rutin J, Levallois C, Privat A, Pessac B (1994) CD4 expression in neurons of the central nervous system. *Int Immunol* **6**: 377-385

- Omri B, Crisanti P, Marty MC, Alliot F, Fagard R, Molina T, Pessac B (1996) The Lck tyrosine kinase is expressed in brain neurons. *J Neurochem* **67**: 1360-1364
- Palfi A, Kortvely E, Fekete E, Kovacs B, Varszegi S, Gulya K (2002) Differential calmodulin gene expression in the rodent brain. *Life Sci* **70**: 2829-2855
- Pan J, Zhang QG, Zhang GY (2005) The neuroprotective effects of K252a through inhibiting MLK3/MKK7/JNK3 signaling pathway on ischemic brain injury in rat hippocampal CA1 region. *Neuroscience* **131**: 147-159
- Park J, Kwon K, Kim SH, Yi MH, Zhang E, Kong G, Kim DW (2013) Astrocytic phosphorylation of PDK1 on Tyr9 following an excitotoxic lesion in the mouse hippocampus. *Brain Res* **1533**: 37-43
- Pei JJ, Tanaka T, Tung YC, Braak E, Iqbal K, Grundke-Iqbal I (1997) Distribution, levels, and activity of glycogen synthase kinase-3 in the Alzheimer disease brain. *J Neuropathol Exp Neurol* **56**: 70-78
- Petravicz J, Fiacco TA, McCarthy KD (2008) Loss of IP3 receptor-dependent Ca²⁺ increases in hippocampal astrocytes does not affect baseline CA1 pyramidal neuron synaptic activity. *J Neurosci* **28**: 4967-4973
- Pierret P, Dunn RJ, Djordjevic B, Stone JC, Richardson PM (2000) Distribution of ras guanyl releasing protein (RasGRP) mRNA in the adult rat central nervous system. *J Neurocytol* **29**: 485-497
- Pierret P, Vallee A, Mechawar N, Dower NA, Stone JC, Richardson PM, Dunn RJ (2001) Cellular and subcellular localization of Ras guanyl nucleotide-releasing protein in the rat hippocampus. *Neuroscience* **108**: 381-390
- Pike CJ (1999) Estrogen modulates neuronal Bcl-xL expression and beta-amyloid-induced apoptosis: relevance to Alzheimer's disease. *J Neurochem* **72**: 1552-1563
- Pranski EL, Van Sanford CD, Dalal NV, Orr AL, Karmali D, Cooper DS, Costa N, Heilman CJ, Gearing M, Lah JJ, Levey AI, Betarbet RS (2012) Comparative distribution of protein components of the A20 ubiquitin-editing complex in normal human brain. *Neurosci Lett* **520**: 104-109
- Pugazhenth S, Wang M, Pham S, Sze CI, Eckman CB (2011) Downregulation of CREB expression in Alzheimer's brain and in Aβ-treated rat hippocampal neurons. *Mol Neurodegener* **6**: 60
- Puschmann TB, Turnley AM (2010) Eph receptor tyrosine kinases regulate astrocyte cytoskeletal rearrangement and focal adhesion formation. *J Neurochem* **113**: 881-894
- Raymond CR, Redman SJ, Crouch MF (2002) The phosphoinositide 3-kinase and p70 S6 kinase regulate long-term potentiation in hippocampal neurons. *Neuroscience* **109**: 531-536
- Reiman EM, Webster JA, Myers AJ, Hardy J, Dunckley T, Zismann VL, Joshipura KD, Pearson JV, Hu-Lince D, Huentelman MJ, Craig DW, Coon KD, Liang WS, Herbert RH, Beach T, Rohrer KC, Zhao AS, Leung D, Bryden L, Marlowe L, Kaleem M, Mastroeni D, Grover A, Heward CB, Ravid R, Rogers J, Hutton ML, Melquist S, Petersen RC, Alexander GE, Caselli RJ, Kukull W, Papassotiropoulos A, Stephan DA (2007) GAB2 alleles modify Alzheimer's risk in APOE ε4 carriers. *Neuron* **54**: 713-720

Repici M, Mare L, Colombo A, Ploia C, Scip A, Bonny C, Nicod P, Salmona M, Borsello T (2009) c-Jun N-terminal kinase binding domain-dependent phosphorylation of mitogen-activated protein kinase kinase 4 and mitogen-activated protein kinase kinase 7 and balancing cross-talk between c-Jun N-terminal kinase and extracellular signal-regulated kinase pathways in cortical neurons. *Neuroscience* **159**: 94-103

Ring RH, Valo Z, Gao C, Barish ME, Singer-Sam J (2003) The Cdkn1a gene (p21Waf1/Cip1) is an inflammatory response gene in the mouse central nervous system. *Neurosci Lett* **350**: 73-76

Robel S, Bardehle S, Lepier A, Brakebusch C, Gotz M (2011) Genetic deletion of cdc42 reveals a crucial role for astrocyte recruitment to the injury site in vitro and in vivo. *J Neurosci* **31**: 12471-12482

Rojas JM, Oliva JL, Santos E (2011) Mammalian son of sevenless Guanine nucleotide exchange factors: old concepts and new perspectives. *Genes Cancer* **2**: 298-305

Rui YF, Sun ZH, Gu JP, Shen ZH, He XP, Xie ZP (2006) MEK inhibitor PD98059 acutely inhibits synchronized spontaneous Ca²⁺ oscillations in cultured hippocampal networks. *Acta Pharmacol Sin* **27**: 869-876

Sanchez-Martin FJ, Fan Y, Lindquist DM, Xia Y, Puga A (2013) Lead induces similar gene expression changes in brains of gestationally exposed adult mice and in neurons differentiated from mouse embryonic stem cells. *PLoS One* **8**: e80558

Scales TM, Derkinderen P, Leung KY, Byers HL, Ward MA, Price C, Bird IN, Perera T, Kellie S, Williamson R, Anderton BH, Reynolds CH (2011) Tyrosine phosphorylation of tau by the SRC family kinases lck and fyn. *Mol Neurodegener* **6**: 12

Schell MJ, Erneux C, Irvine RF (2001) Inositol 1,4,5-trisphosphate 3-kinase A associates with F-actin and dendritic spines via its N terminus. *J Biol Chem* **276**: 37537-37546

Schlatterer SD, Suh HS, Conejero-Goldberg C, Chen S, Acker CM, Lee SC, Davies P (2012) Neuronal c-Abl activation leads to induction of cell cycle and interferon signaling pathways. *J Neuroinflammation* **9**: 208

Schmetsdorf S, Gartner U, Arendt T (2005) Expression of cell cycle-related proteins in developing and adult mouse hippocampus. *Int J Dev Neurosci* **23**: 101-112

Schneider A, Mehmood T, Pannetier S, Hanauer A (2011) Altered ERK/MAPK signaling in the hippocampus of the mrsk2_KO mouse model of Coffin-Lowry syndrome. *J Neurochem* **119**: 447-459

Sergent-Tanguy S, Veziers J, Bonnamain V, Boudin H, Neveu I, Naveilhan P (2006) Cell surface antigens on rat neural progenitors and characterization of the CD3 (+)/CD3 (-) cell populations. *Differentiation* **74**: 530-541

Servidei T, Bhide PG, Huang Z, Moskowitz MA, Harsh G, Reeves SA (1998) The protein tyrosine phosphatase SHP-2 is expressed in glial and neuronal progenitor cells, postmitotic neurons and reactive astrocytes. *Neuroscience* **82**: 529-543

Shen WH, Zhang CY, Zhang GY (2003) Modulation of IkappaB kinase autophosphorylation and activity following brain ischemia. *Acta Pharmacol Sin* **24**: 311-315

Shinoda S, Skradski SL, Araki T, Schindler CK, Meller R, Lan JQ, Taki W, Simon RP, Henshall DC (2003) Formation of a tumour necrosis factor receptor 1 molecular scaffolding complex and activation of apoptosis signal-regulating kinase 1 during seizure-induced neuronal death. *Eur J Neurosci* **17**: 2065-2076

Shinoda T, Taya S, Tsuboi D, Hikita T, Matsuzawa R, Kuroda S, Iwamatsu A, Kaibuchi K (2007) DISC1 regulates neurotrophin-induced axon elongation via interaction with Grb2. *J Neurosci* **27**: 4-14

Sik A, Gulacsi A, Lai Y, Doyle WK, Pacia S, Mody I, Freund TF (2000) Localization of the A kinase anchoring protein AKAP79 in the human hippocampus. *Eur J Neurosci* **12**: 1155-1164

Soeda Y, Tsuneki H, Muranaka H, Mori N, Hosoh S, Ichihara Y, Kagawa S, Wang X, Toyooka N, Takamura Y, Uwano T, Nishijo H, Wada T, Sasaoka T (2010) The inositol phosphatase SHIP2 negatively regulates insulin/IGF-I actions implicated in neuroprotection and memory function in mouse brain. *Mol Endocrinol* **24**: 1965-1977

Sola C, Tusell JM, Serratos J (1996) Comparative study of the pattern of expression of calmodulin messenger RNAs in the mouse brain. *Neuroscience* **75**: 245-256

Sola C, Tusell JM, Serratos J (1997) Calmodulin is expressed by reactive microglia in the hippocampus of kainic acid-treated mice. *Neuroscience* **81**: 699-705

Sola C, Tusell JM, Serratos J (1998) Decreased expression of calmodulin kinase II and calcineurin messenger RNAs in the mouse hippocampus after kainic acid-induced seizures. *J Neurochem* **70**: 1600-1608

Song T, Sugimoto K, Ihara H, Mizutani A, Hatano N, Kume K, Kambe T, Yamaguchi F, Tokuda M, Watanabe Y (2007) p90 RSK-1 associates with and inhibits neuronal nitric oxide synthase. *Biochem J* **401**: 391-398

Soriano FX, Papadia S, Hofmann F, Hardingham NR, Bading H, Hardingham GE (2006) Preconditioning doses of NMDA promote neuroprotection by enhancing neuronal excitability. *J Neurosci* **26**: 4509-4518

Sourial-Bassillious N, Eklof AC, Scott L, Aperia A, Zelenin S (2006) Effect of TNF-alpha on CD3-zeta and MHC-I in postnatal rat hippocampus. *Pediatr Res* **60**: 377-381

Sproul AA, Xu Z, Wilhelm M, Gire S, Greene LA (2009) Cbl negatively regulates JNK activation and cell death. *Cell Res* **19**: 950-961

Stein TD, Anders NJ, DeCarli C, Chan SL, Mattson MP, Johnson JA (2004) Neutralization of transthyretin reverses the neuroprotective effects of secreted amyloid precursor protein (APP) in APPSW mice resulting in tau phosphorylation and loss of hippocampal neurons: support for the amyloid hypothesis. *J Neurosci* **24**: 7707-7717

Sterka D, Jr., Rati DM, Marriott I (2006) Functional expression of NOD2, a novel pattern recognition receptor for bacterial motifs, in primary murine astrocytes. *Glia* **53**: 322-330

Suen KL, Bustelo XR, Pawson T, Barbacid M (1993) Molecular cloning of the mouse grb2 gene: differential interaction of the Grb2 adaptor protein with epidermal growth factor and nerve growth factor receptors. *Mol Cell Biol* **13**: 5500-5512

Sugawara T, Fujimura M, Morita-Fujimura Y, Kawase M, Chan PH (1999) Mitochondrial release of cytochrome c corresponds to the selective vulnerability of hippocampal CA1 neurons in rats after transient global cerebral ischemia. *J Neurosci* **19**: RC39

Sun X, Wu Y, Chen B, Zhang Z, Zhou W, Tong Y, Yuan J, Xia K, Gronemeyer H, Flavell RA, Song W (2011) Regulator of calcineurin 1 (RCAN1) facilitates neuronal apoptosis through caspase-3 activation. *J Biol Chem* **286**: 9049-9062

Sweatt JD (2001) The neuronal MAP kinase cascade: a biochemical signal integration system subserving synaptic plasticity and memory. *J Neurochem* **76**: 1-10

Takagi Y, Nozaki K, Sugino T, Hattori I, Hashimoto N (2000) Phosphorylation of c-Jun NH(2)-terminal kinase and p38 mitogen-activated protein kinase after transient forebrain ischemia in mice. *Neurosci Lett* **294**: 117-120

Tan DP, Liu QY, Koshiya N, Gu H, Alkon D (2006) Enhancement of long-term memory retention and short-term synaptic plasticity in cbl-b null mice. *Proc Natl Acad Sci U S A* **103**: 5125-5130

Tanaka T, Fujita Y, Ueno M, Shultz LD, Yamashita T (2013) Suppression of SHP-1 promotes corticospinal tract sprouting and functional recovery after brain injury. *Cell Death Dis* **4**: e567

Tang YP, Murata Y, Nagaya T, Noda Y, Seo H, Nabeshima T (1997) NGFI-B, c-fos, and c-jun mRNA expression in mouse brain after acute carbon monoxide intoxication. *J Cereb Blood Flow Metab* **17**: 771-780

Tejada-Simon MV, Villasana LE, Serrano F, Klann E (2006) NMDA receptor activation induces translocation and activation of Rac in mouse hippocampal area CA1. *Biochem Biophys Res Commun* **343**: 504-512

Tian X, Gotoh T, Tsuji K, Lo EH, Huang S, Feig LA (2004) Developmentally regulated role for Ras-GRFs in coupling NMDA glutamate receptors to Ras, Erk and CREB. *EMBO J* **23**: 1567-1575

Tomasevic G, Kamme F, Stubberod P, Wieloch M, Wieloch T (1999) The tumor suppressor p53 and its response gene p21WAF1/Cip1 are not markers of neuronal death following transient global cerebral ischemia. *Neuroscience* **90**: 781-792

Tomosada Y, Villena J, Murata K, Chiba E, Shimazu T, Aso H, Iwabuchi N, Xiao JZ, Saito T, Kitazawa H (2013) Immunoregulatory effect of bifidobacteria strains in porcine intestinal epithelial cells through modulation of ubiquitin-editing enzyme A20 expression. *PLoS One* **8**: e59259

Uhlmann EJ, Wong M, Baldwin RL, Bajenaru ML, Onda H, Kwiatkowski DJ, Yamada K, Gutmann DH (2002) Astrocyte-specific TSC1 conditional knockout mice exhibit abnormal neuronal organization and seizures. *Ann Neurol* **52**: 285-296

Umemori H, Wanaka A, Kato H, Takeuchi M, Tohyama M, Yamamoto T (1992) Specific expressions of Fyn and Lyn, lymphocyte antigen receptor-associated tyrosine kinases, in the central nervous system. *Brain Res Mol Brain Res* **16**: 303-310

Usuda N, Arai H, Sasaki H, Hanai T, Nagata T, Muramatsu T, Kincaid RL, Higuchi S (1996) Differential subcellular localization of neural isoforms of the catalytic subunit of calmodulin-dependent protein phosphatase (calcineurin) in central nervous system neurons: immunohistochemistry on formalin-fixed paraffin sections employing antigen retrieval by microwave irradiation. *J Histochem Cytochem* **44**: 13-18

Velier JJ, Ellison JA, Kikly KK, Spera PA, Barone FC, Feuerstein GZ (1999) Caspase-8 and caspase-3 are expressed by different populations of cortical neurons undergoing delayed cell death after focal stroke in the rat. *J Neurosci* **19**: 5932-5941

Vieira M, Fernandes J, Carreto L, Anuncibay-Soto B, Santos M, Han J, Fernandez-Lopez A, Duarte CB, Carvalho AL, Santos AE (2014) Ischemic insults induce necroptotic cell death in hippocampal neurons through the up-regulation of endogenous RIP3. *Neurobiol Dis* **68**: 26-36

Vihma H, Pruunsild P, Timmusk T (2008) Alternative splicing and expression of human and mouse NFAT genes. *Genomics* **92**: 279-291

Wang R, Zhang QG, Han D, Xu J, Lu Q, Zhang GY (2006) Inhibition of MLK3-MKK4/7-JNK1/2 pathway by Akt1 in exogenous estrogen-induced neuroprotection against transient global cerebral ischemia by a non-genomic mechanism in male rats. *J Neurochem* **99**: 1543-1554

Wirth A, Chen-Wacker C, Wu YW, Gorinski N, Filippov MA, Pandey G, Ponimaskin E (2013) Dual lipidation of the brain-specific Cdc42 isoform regulates its functional properties. *Biochem J* **456**: 311-322

Wu CL, Yin JH, Hwang CS, Chen SD, Yang DY, Yang DI (2012) c-Jun-dependent sulfiredoxin induction mediates BDNF protection against mitochondrial inhibition in rat cortical neurons. *Neurobiol Dis* **46**: 450-462

Wu HY, Tomizawa K, Oda Y, Wei FY, Lu YF, Matsushita M, Li ST, Moriwaki A, Matsui H (2004) Critical role of calpain-mediated cleavage of calcineurin in excitotoxic neurodegeneration. *J Biol Chem* **279**: 4929-4940

Wu X, Kihara T, Akaike A, Niidome T, Sugimoto H (2010) PI3K/Akt/mTOR signaling regulates glutamate transporter 1 in astrocytes. *Biochem Biophys Res Commun* **393**: 514-518

Xia HJ, Yang G (2005) Inositol 1,4,5-trisphosphate 3-kinases: functions and regulations. *Cell Res* **15**: 83-91

Xia M, Liu J, Wu X, Liu S, Li G, Han C, Song L, Li Z, Wang Q, Wang J, Xu T, Cao X (2013) Histone methyltransferase Ash1l suppresses interleukin-6 production and inflammatory autoimmune diseases by inducing the ubiquitin-editing enzyme A20. *Immunity* **39**: 470-481

Xiong Q, Oviedo HV, Trotman LC, Zador AM (2012) PTEN regulation of local and long-range connections in mouse auditory cortex. *J Neurosci* **32**: 1643-1652

- Xu HP, Chen H, Ding Q, Xie ZH, Chen L, Diao L, Wang P, Gan L, Crair MC, Tian N (2010) The immune protein CD3zeta is required for normal development of neural circuits in the retina. *Neuron* **65**: 503-515
- Xu J, Weerapura M, Ali MK, Jackson MF, Li H, Lei G, Xue S, Kwan CL, Manolson MF, Yang K, Macdonald JF, Yu XM (2008) Control of excitatory synaptic transmission by C-terminal Src kinase. *J Biol Chem* **283**: 17503-17514
- Xu Y, Hou XY, Liu Y, Zong YY (2009) Different protection of K252a and N-acetyl-L-cysteine against amyloid-beta peptide-induced cortical neuron apoptosis involving inhibition of MLK3-MKK7-JNK3 signal cascades. *J Neurosci Res* **87**: 918-927
- Yabuki Y, Nakagawasai O, Moriguchi S, Shioda N, Onogi H, Tan-No K, Tadano T, Fukunaga K (2013) Decreased CaMKII and PKC activities in specific brain regions are associated with cognitive impairment in neonatal ventral hippocampus-lesioned rats. *Neuroscience* **234**: 103-115
- Yamada M, Ohnishi H, Sano S, Araki T, Nakatani A, Ikeuchi T, Hatanaka H (1999) Brain-derived neurotrophic factor stimulates interactions of Shp2 with phosphatidylinositol 3-kinase and Grb2 in cultured cerebral cortical neurons. *J Neurochem* **73**: 41-49
- Yang C, Iyer RR, Yu AC, Yong RL, Park DM, Weil RJ, Ikejiri B, Brady RO, Lonser RR, Zhuang Z (2012) beta-Catenin signaling initiates the activation of astrocytes and its dysregulation contributes to the pathogenesis of astrocytomas. *Proc Natl Acad Sci U S A* **109**: 6963-6968
- Yao HB, Shaw PC, Wong CC, Wan DC (2002) Expression of glycogen synthase kinase-3 isoforms in mouse tissues and their transcription in the brain. *J Chem Neuroanat* **23**: 291-297
- Yoneya H, Yanagi S, Inatome R, Ding J, Hitomi T, Amatsu M, Yamamura H (1998) Antibodies directed against ZAP-70 cross-react with a 66 kDa tyrosine kinase in the rat brain. *Biochem Biophys Res Commun* **245**: 140-143
- Zaman K, Ryu H, Hall D, O'Donovan K, Lin KI, Miller MP, Marquis JC, Baraban JM, Semenza GL, Ratan RR (1999) Protection from oxidative stress-induced apoptosis in cortical neuronal cultures by iron chelators is associated with enhanced DNA binding of hypoxia-inducible factor-1 and ATF-1/CREB and increased expression of glycolytic enzymes, p21(waf1/cip1), and erythropoietin. *J Neurosci* **19**: 9821-9830
- Zhang F, Jiang L (2015) Neuroinflammation in Alzheimer's disease. *Neuropsychiatr Dis Treat* **11**: 243-256
- Zhang M, Patriarchi T, Stein IS, Qian H, Matt L, Nguyen M, Xiang YK, Hell JW (2013) Adenylyl cyclase anchoring by a kinase anchor protein AKAP5 (AKAP79/150) is important for postsynaptic beta-adrenergic signaling. *J Biol Chem* **288**: 17918-17931
- Zhang WH, Wang X, Narayanan M, Zhang Y, Huo C, Reed JC, Friedlander RM (2003a) Fundamental role of the Rip2/caspase-1 pathway in hypoxia and ischemia-induced neuronal cell death. *Proc Natl Acad Sci U S A* **100**: 16012-16017
- Zhang X, Graham SH, Kochanek PM, Marion DW, Nathaniel PD, Watkins SC, Clark RS (2003b) Caspase-8 expression and proteolysis in human brain after severe head injury. *FASEB J* **17**: 1367-1369

Zhang Y, Zhai Q, Luo Y, Dorf ME (2002) RANTES-mediated chemokine transcription in astrocytes involves activation and translocation of p90 ribosomal S6 protein kinase (RSK). *J Biol Chem* **277**: 19042-19048

Zhao J, Qu Y, Wu J, Cao M, Ferriero DM, Zhang L, Mu D (2013) PTEN inhibition prevents rat cortical neuron injury after hypoxia-ischemia. *Neuroscience* **238**: 242-251

Zhu JH, Kulich SM, Oury TD, Chu CT (2002) Cytoplasmic aggregates of phosphorylated extracellular signal-regulated protein kinases in Lewy body diseases. *Am J Pathol* **161**: 2087-2098

Zhu LQ, Wang SH, Liu D, Yin YY, Tian Q, Wang XC, Wang Q, Chen JG, Wang JZ (2007) Activation of glycogen synthase kinase-3 inhibits long-term potentiation with synapse-associated impairments. *J Neurosci* **27**: 12211-12220

Zurashvili T, Cordon-Barris L, Ruiz-Babot G, Zhou X, Lizcano JM, Gomez N, Gimenez-Llort L, Bayascas JR (2013) Interaction of PDK1 with phosphoinositides is essential for neuronal differentiation but dispensable for neuronal survival. *Mol Cell Biol* **33**: 1027-1040

Lebenslauf

Name Anne-Christin Lehmann
Geburtstag 22. November 1983
Geburtsort Burg (b. Magdeburg)
Staatsangehörigkeit deutsch

Bildungsweg:

1990 – 1992 Grundschule in Genthin
1993 – 1994 Grundschule in Parchen
1994 – 2003 Bismarck-Gymnasiums in Genthin
2000 – 2001 Grapevine High School in Grapevine, Texas, USA
28. Juni 2003 Abitur

10/2003 – 09/2006 Studium der Diplom-Biochemie (Vordiplom)
Freie Universität Berlin

10/2006 – 09/2008 Studium der Diplom-Neurowissenschaften
Otto-von-Guericke-Universität Magdeburg

10/2008 – 12/2009 Diplomarbeit am Leibniz-Institut für Neurobiologie
Magdeburg

18. Dezember 2009 Diplom

01/2010 – 10/2015 Anfertigung der Doktorarbeit am Leibniz-Institut für
Neurobiologie Magdeburg

(Ort, Datum)

(Anne-Christin Lehmann)

List of Publications

SynProt: A Database for Proteins of Detergent-Resistant Synaptic Protein Preparations. Pielot R, Smalla KH, Müller A, Landgraf P, Lehmann AC, Eisenschmidt E, Haus UU, Weismantel R, Gundelfinger ED, Dieterich DC. *Front Synaptic Neurosci.* 2012 Jun 25;4:1

Erklärung

Hiermit erkläre ich, dass ich die von mir eingereichte Dissertation zum dem Thema **” Immune Proteins in Neurons – Towards an Understanding of the Neuronal Role of the Immune Protein CD3 ζ in NMDA Receptor Signaling and Cytoskeleton Remodeling”** selbständig verfasst, nicht schon als Dissertation verwendet habe und die benutzten Hilfsmittel und Quellen vollständig angegeben wurden.

Weiterhin erkläre ich, dass ich weder diese noch eine andere Arbeit zur Erlangung des akademischen Grades doctor rerum naturalium (Dr. rer. nat.) an anderen Einrichtungen eingereicht habe.

(Ort, Datum)

(Anne-Christin Lehmann)